Artificial Neural Network Based Maximum Power Point Tracking for Solar Photovoltaics

By

Haider Saif Agha

00000118346

Session 2015-18

Supervised by

Prof. Dr. Muhammad Bilal Khan

A Thesis submitted to the U.S.-Pakistan Center for Advanced Studies in Energy in partial fulfillment of the requirements for the

degree of

MASTERS of SCIENCE in

ENERGY SYSTEMS ENGINEERING

U.S.-Pakistan Center for Advanced Studies in Energy (USPCAS-E)

National University of Sciences and Technology (NUST)

H-12, Islamabad 44000, Pakistan

February 2018

Artificial Neural Network Based Maximum Power Point Tracking for Solar Photovoltaics

By

Haider Saif Agha

00000118346

Session 2015-18

Supervised by

Prof. Dr. Muhammad Bilal Khan

A Thesis submitted to the U.S.-Pakistan Center for Advanced Studies in Energy in partial fulfillment of the requirements for the

degree of

MASTERS of SCIENCE in

ENERGY SYSTEMS ENGINEERING

U.S.-Pakistan Center for Advanced Studies in Energy (USPCAS-E)

National University of Sciences and Technology (NUST)

H-12, Islamabad 44000, Pakistan

February 2018

THESIS ACCEPTANCE CERTIFICATE

Certified that final copy of MS/MPhil thesis written by Mr. Haider Saif Agha, (Registration No. 00000118346), of U.S.-Pakistan Center for Advanced Studies in Energy has been vetted by undersigned, found complete in all respects as per NUST Statues/Regulations, is free of plagiarism, errors, and mistakes and is accepted as partial fulfillment for award of MS/MPhil degree. It is further certified that necessary amendments as pointed out by GEC members of the scholar have also been incorporated in the said thesis.

Signature: _____

Name of Supervisor _____

Date: _____

Signature (HoD): _____

Date: _____

Signature (Dean/Principal): _____

Date: _____

Certificate

This is to certify that work in this thesis has been carried out by **Mr. Haider Saif Agha** and completed under my supervision in, U.S.-Pakistan Center for Advanced Studies in Energy, National University of Sciences and Technology, H-12, Islamabad, Pakistan.

Supervisor: _____

Dr. Muhammad Bilal Khan
U.S.-Pakistan Centre for Advanced Studies in Energy
NUST, Islamabad

GEC member # 1: _____

Dr. Zafar ullah Koreshi
Faculty of Engineering
Air University, Islamabad

GEC member # 2: _____

Dr. Majid Khan
U.S.-Pakistan Center for Advanced Studies in Energy
NUST, Islamabad

GEC member # 3: _____

Dr. Nadia Shahzad
U.S.-Pakistan Center for Advanced Studies in Energy
NUST, Islamabad

HoD-USPCAS-E _____

Dr. Zuhair S. Khan
U.S.-Pakistan Center for Advanced Studies in Energy
NUST, Islamabad

Dean/Principal _____

Dr. Zuhair S. Khan
U.S.-Pakistan Center for Advanced Studies in Energy
NUST, Islamabad

Dedication

This work is dedicated to my Ami. May Allah bless her soul.

Acknowledgement

I would like to thank Allah Almighty without whose help I would not have been able to complete my Thesis. All the help and support from my parents and teachers were only because of Allah's will.

I would like to thank my supervisor Dr. Muhammad Bilal Khan who provided me with the necessary tools to carry out my research work.

I would like to thank my external supervisor Dr. Zafar ullah Koreshi who guided me throughout this process and gave me the freedom to explore my research interests.

I would like to especially thank Dr. Hasan Abdullah Khalid, who helped me whenever I called on him for help and guidance. He helped me on numerous occasions by taking time out of his busy routine.

I would like to thank Dr. Govindasamy Tamizhmani, Sai Ravi Tatapudi for their support throughout my stay at the Photovoltaic Reliability Lab.

I would like to thank Dr. Zuhair S Khan (HoD & Principal USPCAS-E NUST), my GEC committee, lab engineers, lab technicians, USPCAS-E and USAID for their support throughout the program.

I would especially like to thank my research fellows, Hatif bin Abdul Majeed and Farrukh ibne Mahmood who helped me in times when I had reached a dead end in my research journey.

I would also like to thank my family who supported me throughout my Master's program.

TABLE OF CONTENTS

ABSTRACT

The output of a photovoltaic (PV) solar panel under varying irradiance and temperature values, is non-linear and poses a challenge when harvesting maximum energy from the panels. The Power Voltage curves from a solar panel exhibit different behavior under changes in ambient conditions. The maximum power point is a point on this curve on which the maximum power values resides. This point changes in some cases, rapidly and in others very steadily, to make sure our system extracts the highest possible power from the panel at different conditions, we must operate/charge at this very value, for which a Maximum Power Point Tracking (MPPT) device is needed. An MPPT optimizes the power being generated from a PV panel under varying environmental conditions by virtue of algorithms controlling the duty cycle or the PWM of the DC-DC converter.

Conventionally hill-climbing and open circuit voltage methods have been deployed for this purpose which provide a cheap and easy way of tracking, however their drawbacks are low accuracy, slow operation and periodic data logging. Artificial Neural Networks (ANN), however, can quickly and accurately estimate the output based on different data sets without falling trap to local maxima.

In this thesis a Solar PV panel is modelled and later used to create data set to train a Neural Network. The trained neural network is then incorporated in an MPPT and subjected to varying environmental conditions to check for its efficiency. Lastly a comparative analysis between three MPPT techniques; Perturb and Observe (P&O), Fractional open circuit voltage (FOCV) (the models of which are also simulated) and the proposed ANN based technique is presented.

Keywords*: Maximum Power Point tracking, Artificial Neural Network, Photovoltaics, Renewable Energy.*

LIST OF FIGURES

LIST OF TABLES

LIST OF CONFERENCE PAPERS

- Haider Saif Agha, Zafar ullah Koreshi, Muhammad Bilal Khan, "**Artificial Neural Network Based Maximum Power Point Tracker for Solar Photovoltaics**" 7th International Conference on Information and Communication Technologies (IBA – ICICT Karachi, December 2017)
- Haider Saif Agha, Hatif Majeed, Farrukh Mahmood, Saddam Ali, Sai Tatapudi, Telia Curtis, Govinda Samy TamizhMani "**Temperature Coefficient of Power (Pmax) of Field Aged PV Modules: Impact on Performance Ratio and Degradation Rate Determinations**" Proceedings of SPIE Vol. No. 10370, Reliability of Photovoltaic Cells, Modules, Components, and Systems, San Diego August 2017.

LIST OF ABBREVIATIONS

PV	Photovoltaics
GHI	Global Horizontal Irradiance
AM	Air Mass
MW	Mega Watt
MPPT	Maximum Power Point Tracker
ANN	Artificial Neural Network
P&O	Perturb and Observe
FOCV	Fractional Open Circuit Voltage
IC	Incremental Conductance
FLC	Fuzzy Logic Controller
SDM	Single Diode Model
SSDM	Simplified Single Diode Model
FSDM	Further Simplified Single Diode Model
DDM	Double Diode Model
TDM	Three Diode Model
P_{MAX}	Maximum Power
V_{OC}	Open Circuit Voltage
V_{MAX}	Maximum Voltage
I_{SC}	Short Circuit Current
I_{MP}	Maximum Current
MSE	Mean Squared Error
EL	Electroluminescence
IR	Infrared
UV	Ultraviolet
IV	Current Voltage
PV	Power Voltage
FF	Fill Factor
EVA	Ethylene Vinyl Acetate
I_M	Module current

I_O	Diode leakage current
I_{SH}	Shunt current
I	Output current from panel/array
R_S	Series resistance
R_{SH}	Shunt resistance
N_p	Number of parallel connected modules
N_S	Number of series connected modules
a	Diode ideality factor
I_{PV}	Photovoltaic current
V_T	Thermal voltage
I_{SCN}	Short circuit current at nominal conditions
I_{PVN}	Photovoltaic current at nominal conditions
V_{OCN}	Open circuit voltage at nominal conditions
K_i	Temperature coefficient for current
ΔT	Difference between nominal and operating temperatures in Kelvin
G	Operating irradiance
G_N	Nominal operating irradiance
N_{CS}	Series connected cells in a panel
K	Boltzman constant
q	Charge on electron

CHAPTER 1

INTRODUCTION

This chapter gives a brief overview of the purpose of the study, its main objectives, limitations and the methodology used to carry out the research work.

1.1 Purpose of Study

With the ever increasing thirst of mankind for industrialization and development, the energy consumption globally has reached new highs as depicted by Fig.1 below. According to the International Energy Outlook [1] the world energy consumption in 2015 was estimated to be 575 quadrillion BTUs. This number is expected to rise by 28% by 2040. According to British Petroleum's Statistical review of World Energy 2017 [2], energy growth in the year 2015-2016 was the lowest over a two-year period since 1997-1998. The growth in energy production was only 1.0% which is well below the 10-year average of 1.8%. The slow growth in energy production coupled with the ever increasing demand of energy presents a very grim picture globally. In such circumstances, the world continues to gradually shift away from the conventional forms of energy. Oil continues to be world's dominant fuel, accounting for one third of world's energy consumed, however in 2016 oil gained a global market share for the second year in a row in an otherwise declining period of over sixteen years (1999-2014). Coal's market share also experienced a decline to 28.1% which is the lowest since 2004. While renewables accounted for 3.2% of global primary energy consumption [2].

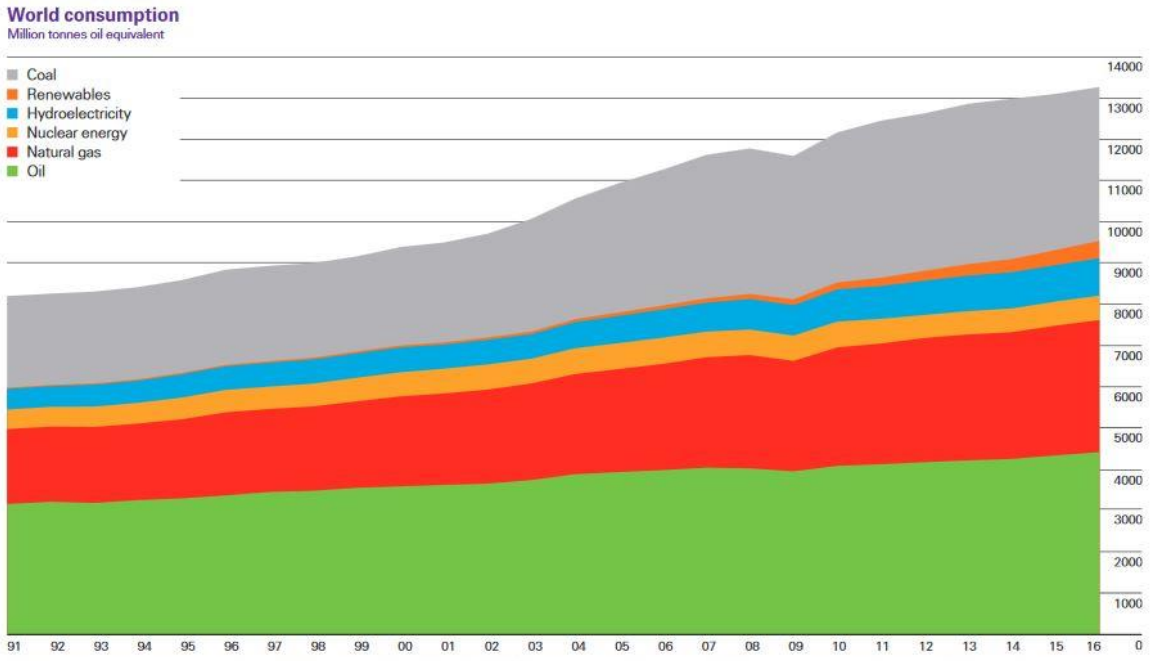

Figure 1: World energy consumption by source (MTOE)

With the global energy demand inflating and steady departure from conventional sources of energy, it is imperative to shift to renewable sources of energy. Renewables are the fastest growing energy source [3] in the world with an annual average consumption predicted to increase by 2.3% between 2015 and 2040. Renewables accounted for 24% of the electricity generation in the world [4] in 2016. Many countries in the pursuit for minimum carbon footprint have shifted towards solar and wind as their primary sources of energy such has Norway (97.9%), New Zealand (84%) and Colombia (82%).

In this long journey of shifting entirely to green energy, Pakistan is taking small measures however over the last couple of years, according to Pakistan Economic survey [5] the government added 438MW renewable energy to the grid (fiscal year 2015-16). Amongst these, Quaid e Azam Solar (Pvt) Ltd is at 100MWe capacity currently but with work in progress, the government plans to scale it upto 1000MW. This would it make it one of the biggest (capacity wise) solar parks in Asia.

Twenty seven wind power projects having a total capacity of 1347MW_e are at different stages of development and or operation whereas 308.2MW electricity is being added to the national grid. Almost all of the wind power projects being located in Thatta disctirct. Alternative Energy development board is in pursuit of 28 solar photovoltaic projects with a total capacity of 956.2MW_e while seven Independent Power Producers (IPPs) have obtained Letter of support in favor of installing 556MW_e of solar power. These numbers only tell half the story as several independent rural electrification programs, domestic usage of renewables and microhydal projects are not accounted for in these numbers.

Also, with China Pakistan Economic Corridor (CPEC) looming on the horizon, the energy sector of Pakistan will benefit greatly. A total of 10,400MW_e is expected to be added to the grid by the year 2018. It will also significantly change the energy mix, replacing expensive oil and resulting in reduction of the average cost of generation. All of these measures will help the existing commercial electricity supplies which currently stands (FY 2015-16) at 23,101MW_e (installed capacity) with generation being 73,209GW/h. While the consumption as of FY 2015-16 is at 69,545Gwh [6].

Solar photovoltaic based energy is of particular importance in not only Pakistan's renewable energy mix but also in the overall power generation. Pakistan has a total of 2.9 million megawatts solar energy potential [7] with an average of eight to nine solar hours per day.

With almost zero operational pollution, solar is the front runner in paving the pathway for Pakistan's greener future. With respect to Pakistan's energy dynamics solar is a very ideal alternative as it is dispatch-able, scalable, instantaneous, low maintenance and uncomplicated to setup. In the remote areas of Sindh, a farmer can easily reap the benefits of solar by setting up a couple of panels and harnessing the DC power without any sophistication as shown in the figure below. In such ideal conditions for solar PVs it is important to focus efforts into optimizing the PV systems for maximum profits in green energy ventures.

Figure 2: A farmer in Sindh setting up solar modules in his field [7]

1.2 Thesis Objectives

In such a case scenario where solar photovoltaics is emerging as a promising alternate energy in Pakistan, we must ensure its optimal usage and energy conversion potential. Courtesy of many advanced researches in solar cell laboratories, high efficiency solar cells have been developed capable of managing efficiencies as high as 28% (excluding multi junctional III-V solar cells which perform at an efficiency of 52% and are only used for extra-terrestrial purposes).

However the solar cells available to the Pakistani market are only as efficient as 12%-15%. This is a relatively good trade-off between a satisfactory performance and low price. For many a purposes efficiencies greater than 20% would incur a very high cost and would render the entire process of generating cheap electricity, useless.

Another way of improving the "energy rate of return" from a panel is to mount it on a tracking device. Solar trackers follow the path of the sun and ensure maximum irradiance throughout the day. Assuming a 1MW PV farm with 210W panels spread across an area of 1.282m^2 PV panels; the modules when mounted on Dual axis solar trackers (DAST) can generate an additional 1909kWhr/day as compared to Solar static solar system (SSS) [8]. Many instances where panels have to be elevated from the ground (parking lots, sheds, rooftops) can mount the entire system on a dual axis tracker and benefit from the additional units. Dual axis solar trackers cannot provide a feasible/cheap solution when the system needs to be spread out in a remote village with limited budget schemes.

Also with a country like Pakistan, experiencing eight to nine solar hours per day with a high clarity index, can perform if not better, than almost at par with DAST, systems using SSS.

One unconventional way of utilizing solar PV to its full potential is to improve the efficiency of the electronic devices which either track or convert power being generated from the panel. This technique is called Maximum power point tracking (MPPT). MPPT optimizes the power

being generated from a panel by virtue of algorithms controlling the duty cycle of the DC-DC converter.

Conventionally the hill-climbing algorithm has been used to maximize the power, in this thesis an Artificial Neural Network (ANN) based technique is developed and compared with two other conventional techniques i.e. Perturb and Observe (P&O) and Fractional Open circuit voltage method (FOCV). The system is studied for an off-grid fixed resistive load system.

The objective of the thesis is to highlight the effectiveness of using a high performance MPPT when harnessing energy from the panel. The study also sheds light on the versatility of Artificial neural networks in the field of energy.

Additionally, the effect on temperature coefficient of Power (max) is also investigated for field aged modules. The temperature coefficient of Pmax is typically assumed to not change over the lifetime of the module in the field. Therefore, this study was carried out in an attempt to investigate the validity of this assumption and current practice. Several 18-19 years old field aged modules from four different manufacturers were tested for the baseline light I-V measurements and dark I-V measurements to determine the power temperature coefficient and series resistance for each module, listed in Chapter 6.

1.3 Thesis Limitations

The study will not cover some of the aspects which otherwise can be important while dealing with a research related to MPPT. The study scope is limited to the following

1. Assumption of no shading conditions
2. Non-dynamic (fixed resistive) load
3. Module model used from one manufacturer only.

1.4 Methodology of Work

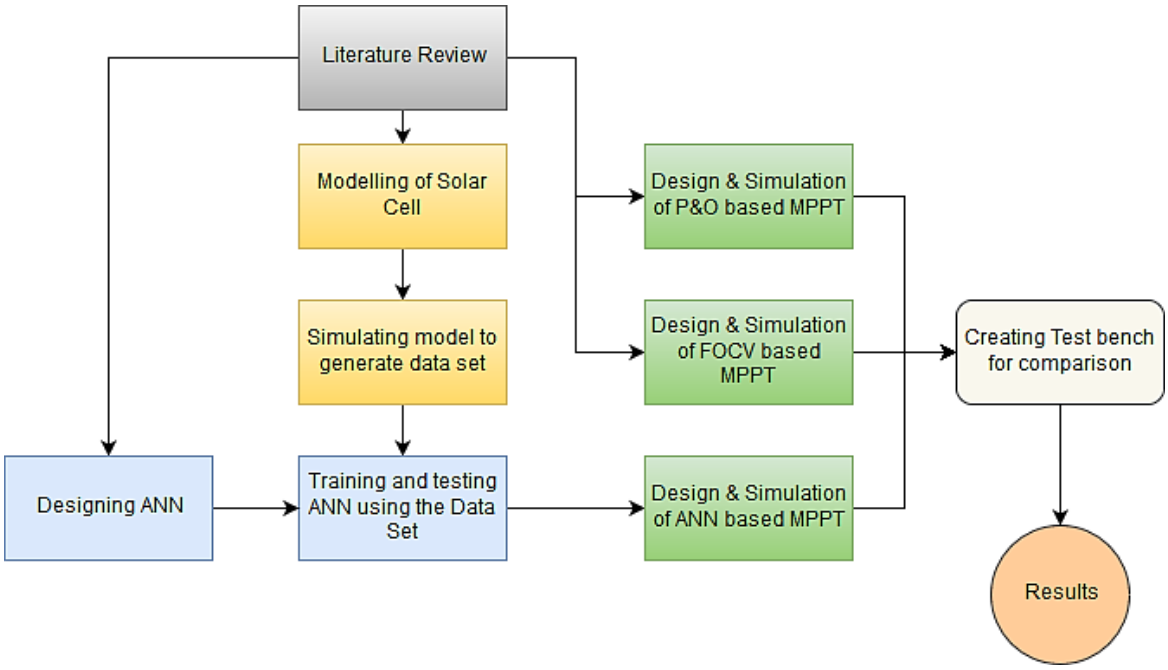

Figure 3: Methodology of Work flowchart

1.5 Thesis structure

This study is divided into six chapters based upon the work done in chronological order during the research period.

- Chapter 1: Discusses the main purpose of the study, its objectives, limitations and the methodology used for the work.
- Chapter 2: Covers the literature review regarding the problem statement; its causes, effects, current approaches being deployed for maximum power point tracking and an in-depth understanding of Artificial Neural Networks.
- Chapter 3: Presents the single diode cell model for PV along with its translational model in MATLB/Simulink. It also covers design and development of an ANN based MPPT. Two other MPPT models are also developed and simulated in this chapter
- Chapter 4: Discusses results and presents a comparative conclusion of the three techniques.
- Chapter 5: Introduces PV reliability and the study on Field aged modules.
- Chapter 6: Discussed results and analytical reason to justify the values of the found parameters.
- Chapter 7: Gives conclusion and recommendations for future work for the research studies.

Summary

This chapter gives details about the purpose and motivation of this study. The chapter also talks about the main objectives, limitations and the methodology used for carrying out the research work.

References

[1] "International Energy Outlook 2017" – U.S Energy Administration, Independent Statistic and Analysis pp 1- 5. [Online] Available https://www.eia.gov/outlooks/ieo/

[2] "BP Statistical Review of World Energy' – BP World Energy Economics Survey, June 2017. [Online] Available https://www.bp.com/content/bp-statistical-review-of-world-energy

[3] "International Energy Outlook 2017" – U.S Energy Administration, Independent Statistic and Analysis pp 18-20 [Online] Available https://www.eia.gov/outlooks/ieo/

[4] "Renewables in Energy Production" – Global Energy Statistical Yearbook 2017. [Online] Available https://yearbook.enerdata.net/renewables/renewable-in-electricity-production-share.html

[5] "Pakistan Economic Survey" – Government of Pakistan. Chapter 14. [Online] Available http://www.finance.gov.pk/survey/chapters_16/14_Energy.pdf

[6] "The Advantage of Solar Power for Pakistan" – Pakistan 360 Degrees. [Online] Available http://pakistan360degrees.com/the-advantages-of-solar-power-for-pakistan

[7] "Potential of Solar based Energy in Sindh" – Pakistan 360 Degrees. [Online]. Available http://pakistan360degrees.com/potential-of-solar-based-energy-in-sindh

[8] Lee, J. F., Rahim, N. A., & Turki, Y. A. (2013). Performance of Dual-Axis Solar Tracker versus Static Solar System by Segmented Clearness Index in Malaysia. International Journal of Photoenergy, 2013, 1-13. http://dx.doi.org/10.1155/2013/820714

CHAPTER 2

LITERATURE REVIEW

This chapter gives an insight into the Pakistan's energy mix, and covers detailed literature review on Solar cell technology, importance of MPPTs, main MPPT techniques, ANNs and their usage in MPPTs.

2.1 Pakistan's Energy Mix

Pakistan experiences an annual average Gobal Horizontal Irradiation (GHI) greater than 1600kWh/m^2. Upper Sindh and major parts of Balochistan experience an average greater than 1800kWh/m^2 as shown by the GIS data Fig. 3 [8]. The average monthly solar radiation intensity remains 136.05 to 287.36 W/m2. For a 10 hour day the average solar radiation intensity ranges from 1500W/m^2/day to 2750 W/m^2/day, especially in Southern Punjab, Sindh and Balochistan region. In an area of 100 m2, 45 MW to 83 MW power per month may be generated in the above mentioned regions [9]. Pakistan is blessed with a huge solar energy potential, stretching across the vast plains of Southern Punjab and the Upper Sindh alongwith the barren plains of Balochistan. The average annual solar radiation intensity per day (1971-2000) during the months of May, June and July in Pakistan is above 2500W/m^2 as shown in Fig. 4 below.

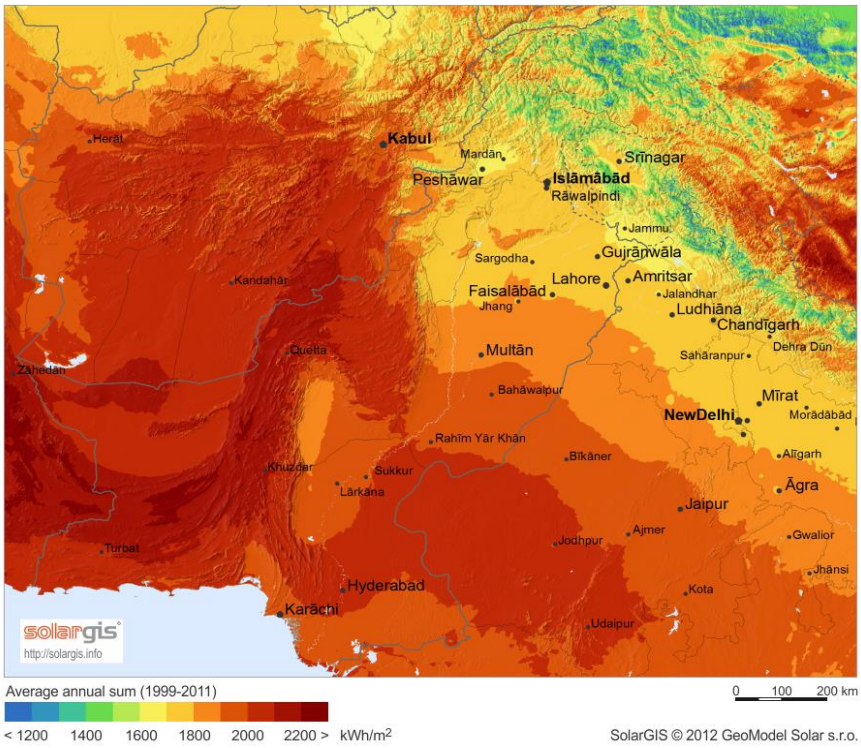

Figure 4: Average annual sum of Global Horizontal Solar irradiation in Pakistan

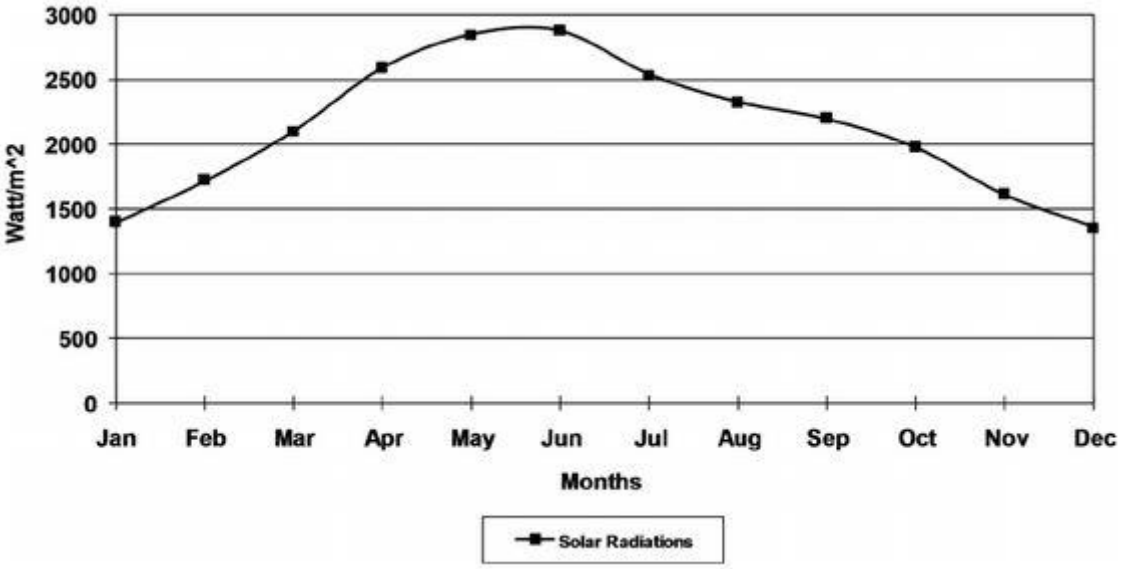

Figure 5: Average annual solar radiation intensity (W/m^2/day) in Pakistan during (1971-2000)

There is encouraging potential in many parts of the country for solar power generation. Especially in areas of Southern Punjab, Sindh and Balochistan where studies suggest that in an area of $100m^2$, 45MW to 83MW power can be generated during a month in these regions. In light of these reports, the government has initiated and completed many solar power projects. The independent private investors have also jumped on-board with the Solar power park bandwagon and are initiating many such small and large scale projects. Following is a list of Solar power projects both from public and private sectors. (Note: Projects with similar names are operating at different locations in Pakistan). Source: AEDB

.

Sr. No	Name of Project	Capacity (MWe)
1	M/s Appolo Solar Pakistan Ltd.	100
2	M/s Crest Energy Pakistan Ltd	100
3	M/s Best Green Energy Pakistan Ltd.	100
4	M/s Access Electric Pvt. Ltd	10
5	M/s Bukhsh Solar (Pvt.) Ltd	10
6	M/s Safe Solar Power Pvt. Ltd	10
7	M/s Access Solar Pvt. Ltd.	11.52
8	M/s Blue Star Hydel Pvt. Ltd.	1
9	Harappa Solar Pvt. Ltd.	18
10	AJ Power Pvt. Ltd.	12
11	M/s Integrated Power Solution	50
12	M/s Jafri & Associates	50
13	M/s Solar Blue Pvt. Ltd.	50
14	M/s R.E. Solar I Pvt. Ltd.	20
15	M/s R.E. Solar II Pvt. Ltd.	20
16	Forshine (Pakistan)	50
17	ET Solar (Pvt.) Ltd.	25

18	ACT Solar (Pvt.) Ltd	50
19	Janpur Energy Limited	12
20	Janpur Energy Limited	12
21	Blue Star Electric Pvt. Ltd.	1
22	Siddiqsons Energy Karachi	50
23	Adamjee Power Generation Pvt. Ltd.	10
24	ET Solar (Pvt.) Ltd.	50
25	Crystal Energy (Pvt.) Ltd.	2
26	Asia Petroleum Limited	30
27	First Solar (Pvt.) Ltd.	2

Table 1: Solar Projects under construction (list also includes projects which have obtained letter of support from government)

With Solar being the frontrunner in Pakistan's renewable energy initiative, it is important to make sure that solar is to be used at its maximum potential. Apart from low conversion efficiency for sub-grade quality panels, there are some intrinsic non-linear properties of a solar cell which effect its performance and limit its output. This results in power outputs which don't match with the name place rating.

2.2 Working of Solar Cell

A solar cell converts sunlight into electricity. It is essentially an electronic device which produces current and a voltage to produce power. The absorption of light forces the electron to a higher state and evidently movement of the very electron in the circuit. The mobile electron dissipates energy to the load and returns to the cell itself. Nearly all photovoltaic conversion materials are in essence a p-n junction.

The basic processes and mechanisms in the operation of a solar cell are:

- The generation of light-generated carriers;
- The collection of the light-generated carries to generate a current;
- The generation of a large voltage across the solar cell; and
- The dissipation of power in the load and in parasitic resistances.

Current from incident light is generated in two steps viz absorption of incident photons for the formation of electron hole pairs given that the energy of the incident photon is greater than the band gap. In the second step, these carriers are collected by the p-n junction. The carriers are separated by the electric field within the semiconductor. The minority carrier (generated by light) upon reaching the junction will be swept across the junction by the electric field at the junction where it will end up being a majority carrier. Connecting the base and emitter of the solar cell will lead to light generated carriers to flow through the external circuit as shown in Fig. 5.

The collection probability is the probability that a light generated carrier will be absorbed within the certain region of the junction and thus will contribute to the ligt-generated current. The probability is dependent upon distance that carrier must travel as compared to the diffusion length. The probability also depends on the surface properties. The collection probability will be low if the generated carrier is more than a diffusion length away from the junction and vice versa.

However collecting the light generated carriers in itself isn't sufficient for the generation of power. A voltage needs to be generated as well as current. Voltage is generated courtesy of "Photovoltaic effect". The movement of electrons to the n-type side and movement of holes to the p-type of the junction is caused by the collection of light generated carriers by the p-n junction. Under short circuit conditions, no charge is built up. But if the light generated carriers are not allowed to leave the cell, it would lead to a large number of electrons in the n-type side of the junction. Inevitably the number of holes at the p-type side will also increase. These polarising charges separated by the junction will lead to formation of a strong electric field. The diffusion current would increase when this electric field decreases as it acts as boundary between the two charges. An equilibrium would be formed through which a voltage would exist in the junction. The difference between the light generated current and the forward bias current is the new current generated from the solar cell. This leads to both the formation of a voltage and a current across the junction and hence power. These individual solar cells when interconnected together and encapsulated in a weather proof package is called a panel/module. Furthermore, these panels/modules when connected in series and parallel are known as an array.

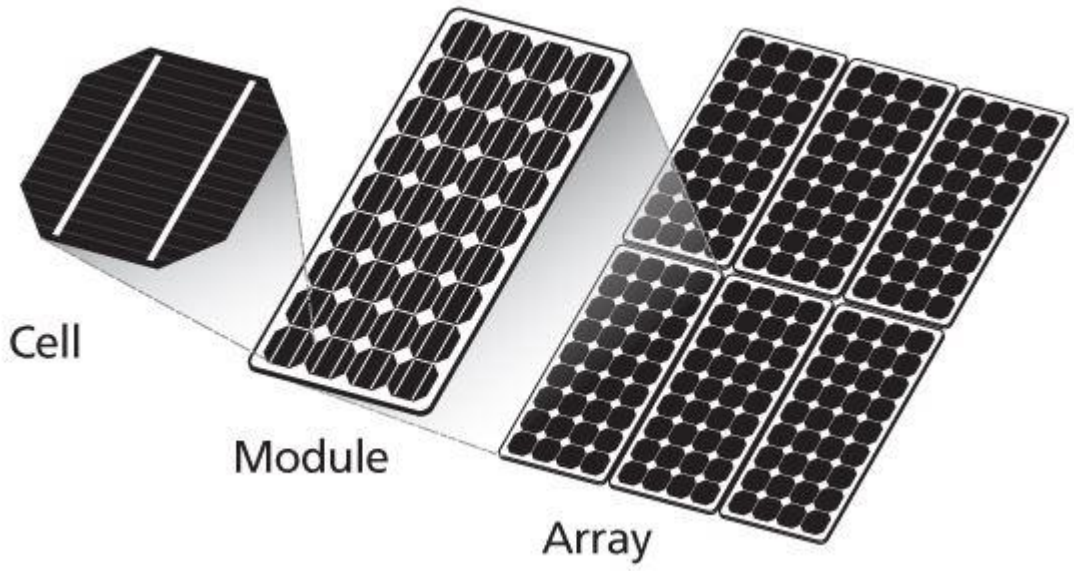

Figure 6: PV cell, module and array

The generated current voltage (IV) curve is actually a super positioned dark IV curve of a solar cell with a light generated one. For power to be extracted the IV curve must lie in the fourth quadrant. So this is the point where illumination by light comes in to help shift the curve in the fourth quadrant. Short circuit current (I_{SC}) of a solar cell is when the open circuit voltage or when the voltage across the cell is zero. This is due to the generation and collection of light generated carriers. The short circuit current depends upon the following factors.

- Area of solar cell
- Number of incident photons
- Spectrum of incident light
- Optical properties of cell

- Collection probability

Similarly, the open circuit voltage (V_{OC}) is the maximum voltage from a solar cell. The forward bias of a solar cell due to the junction characterizes this open circuit voltage. The maximum power from a solar cell is a product of I_{SC} and V_{OC}. The ratio of the maximum power from a solar cell to the product between open circuit voltage and short circuit current of a panel is known as the fill factor (FF). FF is a measure of the squareness of the IV curve (as shown in Fig 6).

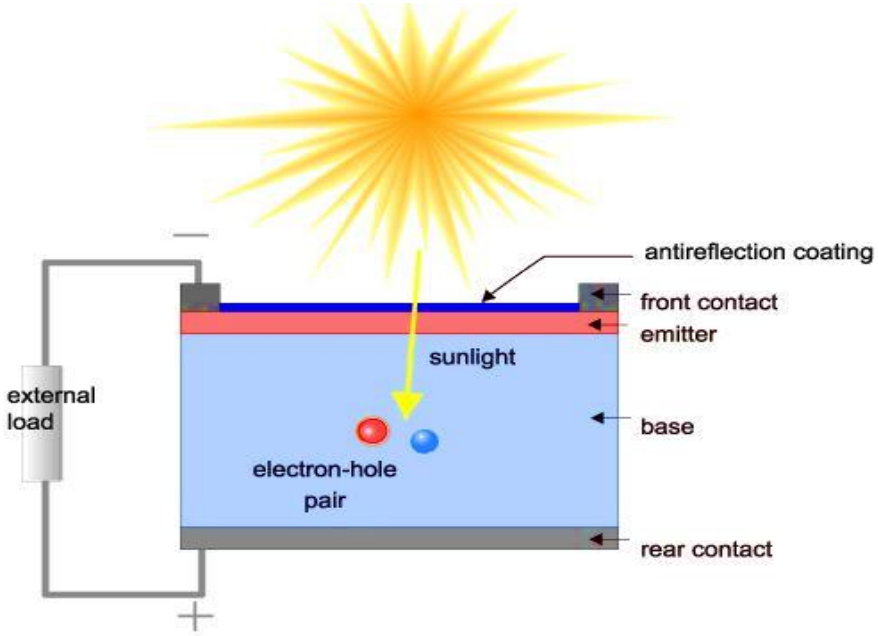

Figure 7: Solar cell structure

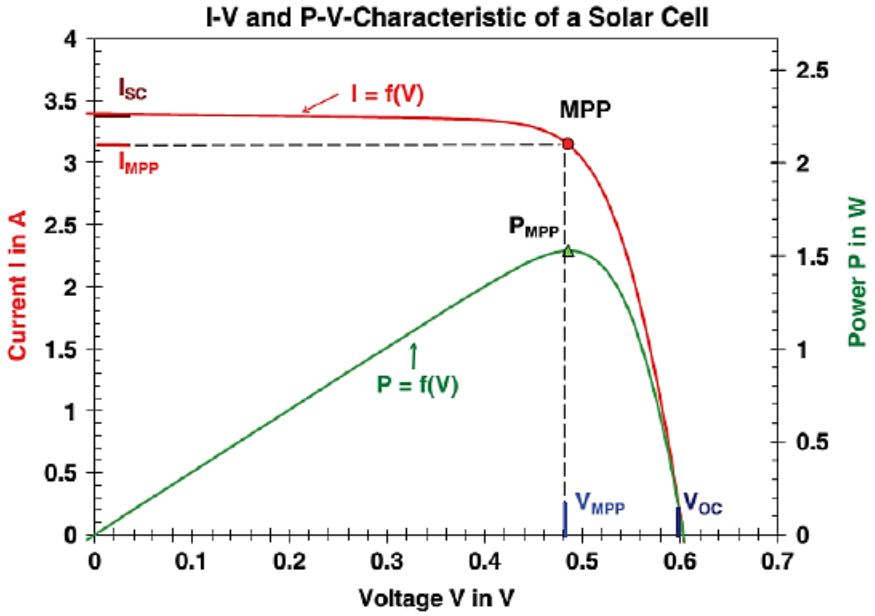

Figure 8: Characteristic IV and PV curves of Solar Cell

2.3 Non Linear Behaviour of Solar cell

The output of a solar photovoltaic cell is characterized by virtue of the current voltage (IV) and power voltage curves (PV) that it outputs. The IV curves have a non-linear behaviour with its surroundings and inevitably also with the maximum power that they generate. FF characterizes the non-linear behaviour of a solar cell. For most approximation purposes, the parameters FF,$V_{OC,}$ I_{SC} are enough to predict the electrical properties of a solar cell. For a given set of conditions, the manufacturer provides the single operating point of voltage and current at which maximum power can be harnessed from the panel.

Change in environmental conditions, such as cell temperature, solar irradiation and shading etc causes the maximum power point (MPP) to vary as the module current and the voltage are functions of thermal voltage and photovoltaic current (I_{ph}) respectively. Solar cell is a semiconductor device and thus is affected by changes in temperature. A higher temperature causes the bandgap to shrink. This causes an increase in energy of the electrons, which now require lower energy to break the bond and jump the gap. V_{OC} decreases with the increase in temperature.

A change in light intensity causes changes in all the parameters of the solar cell i.e. FF, V_{OC}, I_{SC}, efficiency and impact of series shunt resistances. The main impact of the series resistance is to reduce the fill factor. High series resistances can also reduce I_{SC}. Similarly shunt resistance severely affects the light generated current at low light conditions. (Series and shunt resistances are discussed in detail in Chapter 3).

Fig. 7 (a) and (b) represents the IV and PV curves of solar module at various operating cell temperatures and irradiances [10].

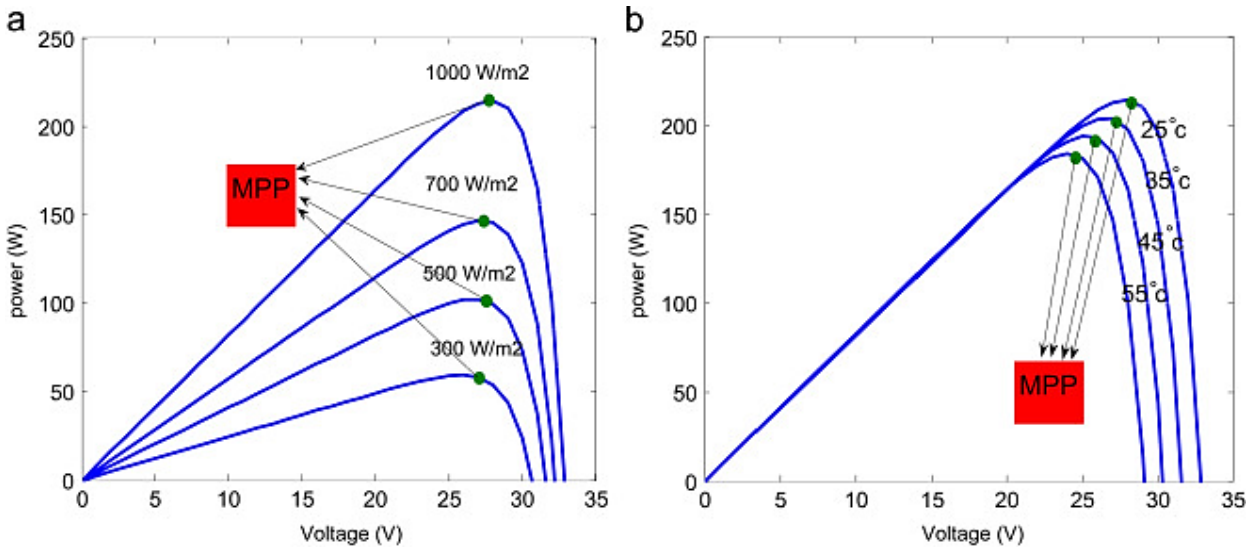

Figure 9: PV curves of Solar panel under varying irradiances (a) and varying temperatures (b)

As shown in the figure, with the varying MPP it is imperative to use an electronic device that monitors the variable voltage and current and makes sure that the system is being fed the optimum value of voltage and or current so as to make sure the panel is being used at its full potential.

2.4 Maximum Power Point Tracker

To compare the results from the three MPPT techniques and also to verify the SDM, a PV panel has to be modelled. For this purpose, the most used PV panel in literature has been modelled and simulated namely, the Kyocera KC200GT. The manufacturer claims to provide a full 130W at Standard Testing Conditions (STC). The nameplate reading suggests that the panel will output the said power at 7.39A and 17.6V. However, once this panel is installed to a 12V battery and monitored, the total output power comes to be 81.4W courtesy of 11V and 7.4A. Ultimately 48W is being lost. One of reasons for this loss of power is the fact that there is a mismatch between the battery and the panels, your battery will remain undercharge or overcharge and still not be achieving the full 130W that it is meant to. At low battery charge it'll set at 10.5V and at 13-15V with an overcharge. Let's consider the same system hooked up to a 24V battery but still not outputting a full 130W. The catch here being that the manufacturer promises 130W at STC however with changes in irradiance, temperature, wind speeds, humidity and shading etc. your output will change (as mentioned in section 2.2).

This is where Maximum power point trackers (MPPT) come into play. MPPTs are electronic devices usually embedded within an inverter or charge controller circuit. MPPT digitally track the MPP by constantly looking at the panel output and deciding which values of voltage/current are optimum to charge the system at peak power. Consider Fig. 9, the system is set to charge the battery at 24V thinking that the MPP would correspond to this value however the system can provide an additional 300W if charged at 33V. So an MPPT would alter the duty cycle to reach this output voltage.

MPPTs work by virtue of different conventional algorithms such as Perturb & observe, Fractional open circuit voltage, Incremental conductance, Current sweep etc. Unconventional methods include using Fuzzy logic controller and Artificial neural networks.

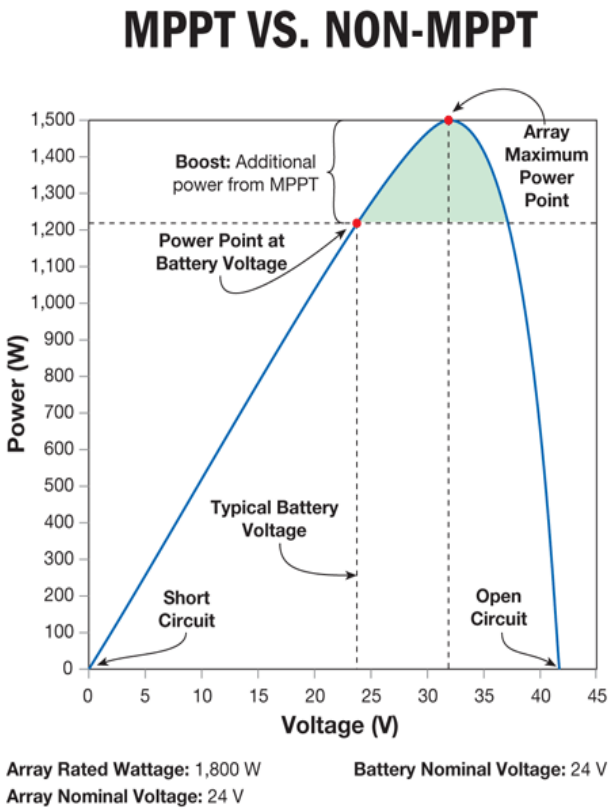

Figure 10: Using an MPPT helps extract more power from the system

A typical MPPT consists of voltage and current sensors with boost or buck boost DC-DC converters as shown in Fig. 10. Converters are classified on the basis of the magnitude they can output, a boost converter outputs voltage greater in magnitude being input to it and a buck outputs voltage less than the input voltage. While buck-boost can perform both functions. These techniques can be seen as DC transformers with stepping up or down voltage with a reference V_{IN} value. For most MPPT purposes, a boost converter is deployed (refer to Fig. 9) because mostly an MPPT is achieved by increasing the voltage value greater than the V_{IN}. However any configuration can be used to match the intrinsic impedance of the panels with the impedance of the load. MPPT is achieved by manipulating the duty ratio/cycle of the converter such that the panel operates at the MPP. The next section discusses the various conventional and unconventional methods of MPPT.

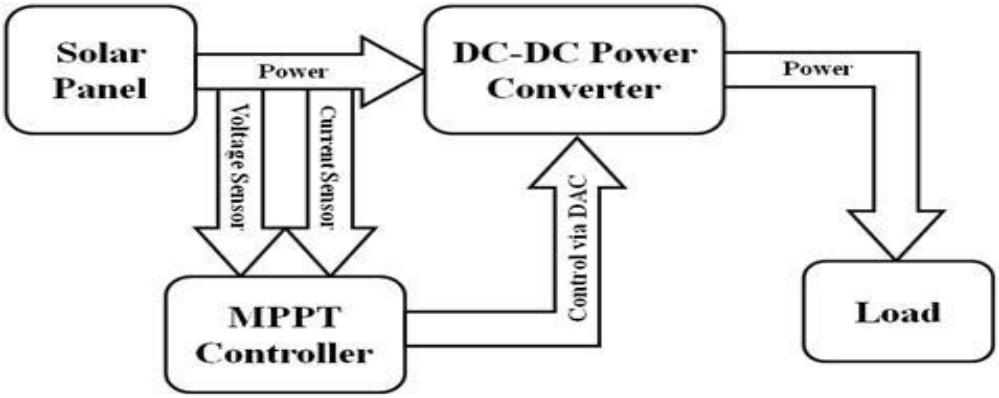

Figure 11: Generic block diagram of an MPPT

2.4.1 MPPT TECHNIQUES: PERTURB AND OBSERVE

Perturb and Observe (P&O) is a hill climbing algorithm that works by perturbing the duty cycle of the DC-DC converter and hence the operating voltage as shown in Fig.12. It then checks for the change in power output. If the power output has decreased by decreasing the voltage, it increases the voltage and checks again. If an increase in voltage results in an increase in power it keeps on increasing it until it encounters a decrease in output power; in which case, it decreases the voltage back again. This is similar to going up a hill on a car and keep throttling until a peak is reached. If you start going downhill, as a counter measure you start reversing back up. The main drawback of P&O is its inability to find a stationary point of operation. It keeps operating back and forth hence inducing oscillations. Following are some of the disadvantages of P&O

- Slow operation
- Oscillations at MPP
- Large step size can often skip the MPP
- If the MPP peak lies far from the current point of operation, P&O can take longer to track it down
- Under shading conditions, there can be multiple peaks in the PV curve and P&O can get trapped in a local maxima.

While on surface P&O might look like a very disadvantageous technique at first, it is however the most widely used technique in MPPTs. This, being the reason that

- Complexity level of algorithm is minimum
- Can be easily implemented on any microcontroller
- Medium to good tracking capability
- It can be coupled with techniques such as Fuzzy logic to make it more efficient

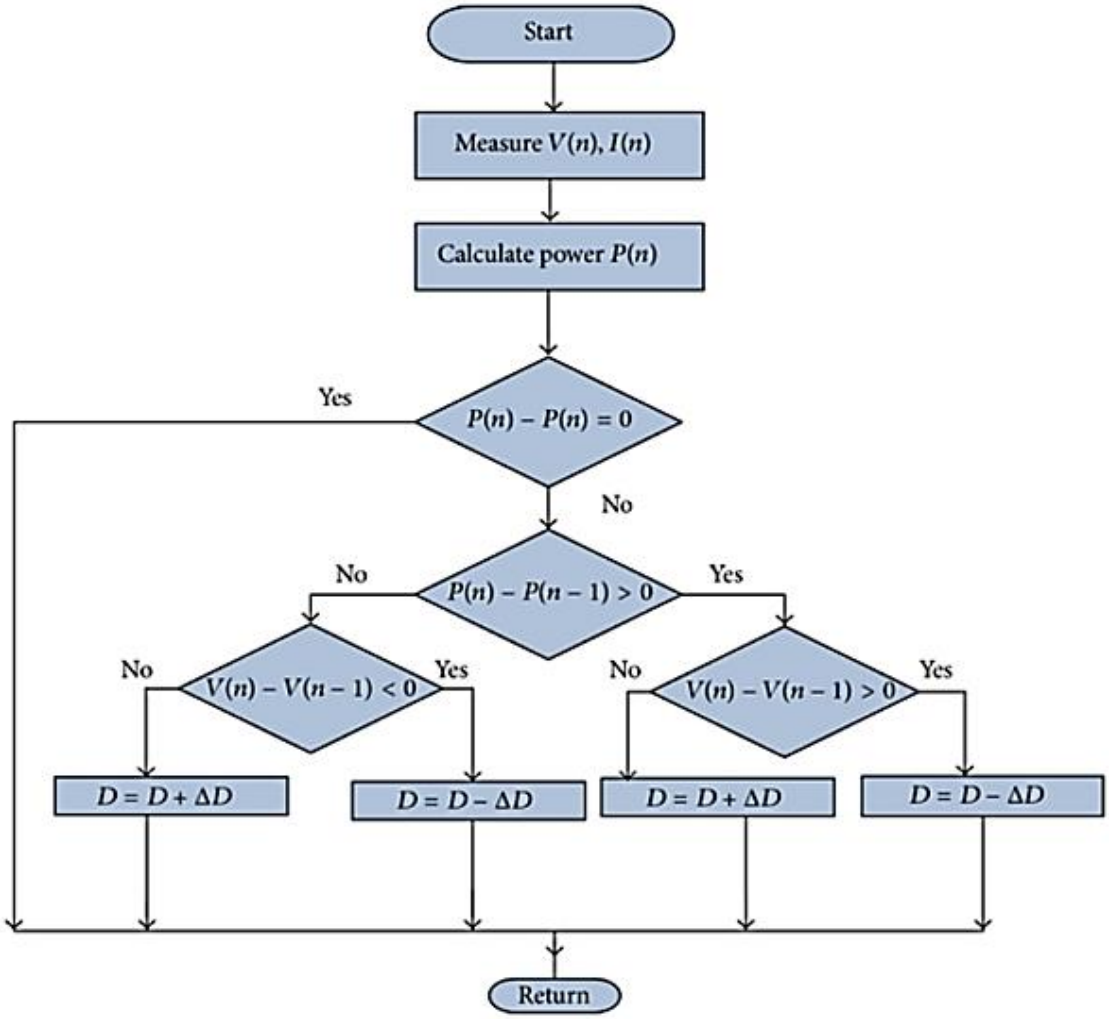

Figure 12: Working principle flowchart of P&O

2.4.2 MPPT TECHNIQUES: Fractional Open Circuit Voltage (FOCV)

FOCV works on the approximation that the V_{mpp} is linearly dependent on the open circuit voltage of the panel/array at a certain temperature and irradiance. The ratio of V_{mpp} and V_{OC} results in a linearizing coefficient. Any value being output by the panel is multiplied by this gain/coefficient to get the reference voltage. This reference voltage is then followed by the controller to ensure operation at MPP. FOCV is preferred form of MPPT algorithm for the following reasons

- Amongst all the MPPT techniques, FOCV is the simplest one
- For small scale PV projects where optimal performance isn't a requirement FOCV is a handy algorithm
- For conditions where the environmental conditions are prone to less changes or slow changes, the linearizing coefficient can predict the V_{MPP} relatively accurately.

Contrary to the simplicity and ease of usage, there are many reasons where FOCV isn't a preferred method because:

- Disconnecting the array from the load to find the open circuit voltage (Voc) at changing environmental conditions which results in operational inconvenience.
- The frequent disconnections also results in power loss. The instant at which the panel would be checked for V_{OC} it would essentially be missing out on generating power
- The linearizing coefficient is an approximation of what the value of V_{MPP} will be. It is a hit and miss method and isn't always accurate.

A hybrid P&O and FOCV method flowchart is shown below which shows the possibility of using P&O to predict the value of the linearizing coefficient without disconnecting panel from load. Fig 13 shows how the step size is determined using P&O method. This step sized is then utilized in the FOCV method to set Vpv equivalent to Vmpp.

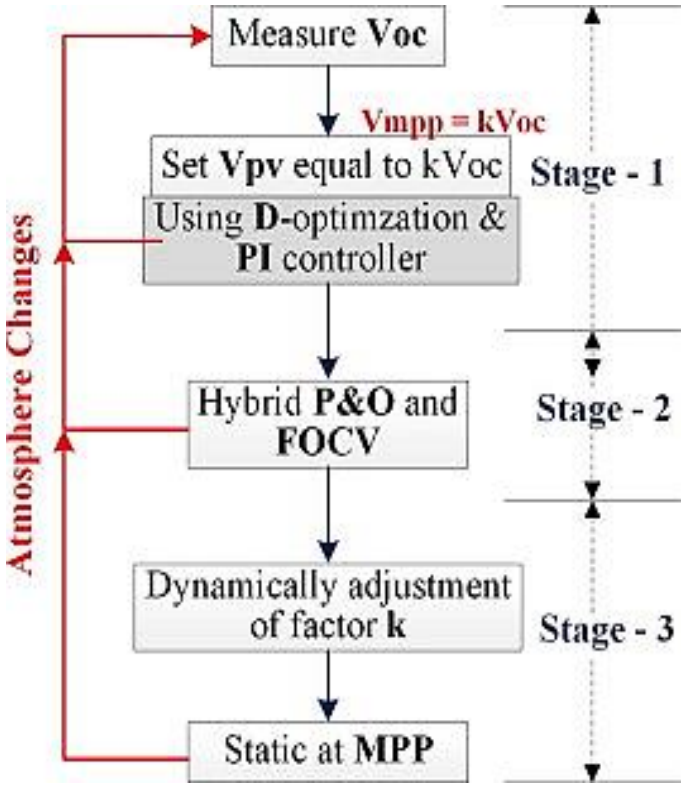

Figure 13: Working principle flowchart of Hybrid P&O and FOCV method

2.4.3 MPPT TECHNIQUES: INCREMENTAL CONDUCTANCE (IC) METHOD

Incremental conductance (IC) was developed to overcome the drawbacks of P&O method. The incremental conductance method (Fig.14) is based on the fact that the slope of the PV array power curve is zero at the MPP IC tries to reduce the tracking time and generate more power for variable conditions. It does this by using the relation between dI/dV and –I/V. Where dI is the difference between I(n) and I(n-1). Similarly dV is equivalent to difference between V(n) and V(n-1). If dP/dV is negative then MPPT lies on the right side of recent position and if the MPP is positive the MPPT is on left side. MPP is reached when dP/dV=0 [11].

$$\frac{dP}{dV} \geq 0 \; MPP \; lies \; to \; the \; left$$

$$\frac{dP}{dV} \geq 0 \; MPP \; lies \; to \; the \; right$$

$$\frac{dP}{dV} = 0 \; At \; MPP$$

Following are the advantages of IC

- Small oscillations of MPP
- Reduced tracking time as compared to P&O
- Adaptive response to dynamically environment

IC improves on the faults of P&O in a much efficient manner, with a relatively easy to understand algorithm and better tracking response. However it also suffers from some of the same drawbacks as P&O,

- Step size determination is an issue
- Complexity of programming increases
- Still cannot cater for multiple peaks or shady conditions

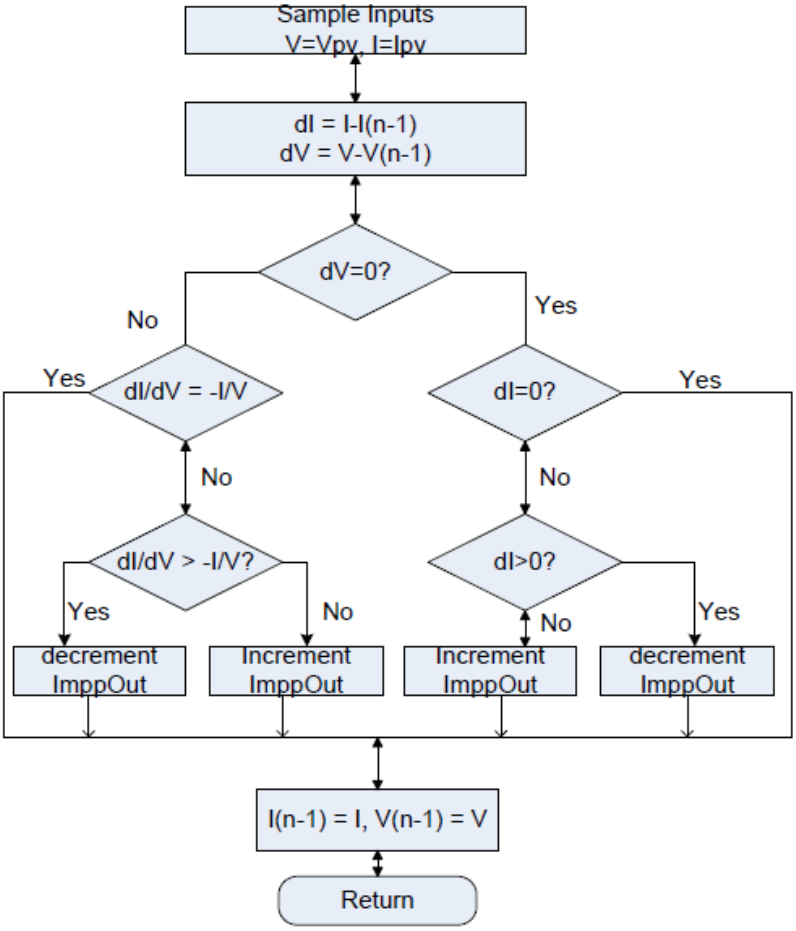

Figure 14: Working principle flowchart of current based IC method

2.4.4 MPPT TECHNIQUES: FUZZY LOGIC CONTROLLER (FLC)

Unlike conventional digital logics where a value can only exist between true (1) or false (0). Fuzzy logic control (FLC) deals with "degrees of truth". The idea was first envisioned by Dr. Zadeh at UC Berkeley in 1960s. He suggested that most of the practical decisions in life cannot simply be translated into a simple value of either 1 or 0. A lot of data and weightage needs to be fed to every aspect before making a decision. Fuzzy logic takes 1 and 0 as the extreme cases and instead answers with values in between these extremes. For e.g. a measure of hot or cold weather can be given in terms of 14° of coldness. Notice how the result is depicted with respect to an extreme case. This corresponds to in many ways how our brains work, by analysing all the aspects and forming partial truths which can be aggregated further into higher truths. Every degree of truth or aggregation is dependent upon a certain threshold.

FLC are in many ways just like artificial intelligence (AI) systems but with different working criterions. However both AI and FLC essentially take the same things into consideration while making a decision. Every input value is mapped onto a membership value (or degree) by using a curve also known as Membership function. Fuzzy logic controllers work in three basic steps

1. Fuzzification of all input values into fuzzy membership function
2. Using rule based criteria to generate fuzzy output functions
3. Getting the "crisp" output values using defuzzification

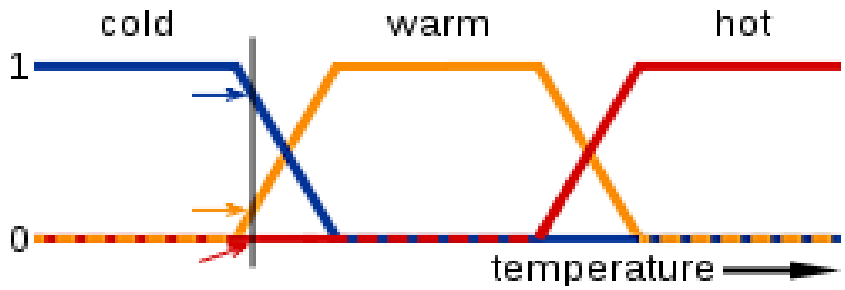

Figure 15: FLC based temperature control

Consider Fig. 15 where three truth values of cold, warm and hot are represented by functions on a temperature scale. The vertical line intersects the scale (three truth values) at various points i.e. the blue, yellow and red arrows. The red arrow can be interpreted as "not hot" because it points to zero, similarly the orange arrow pointing at 0.2 on the scale can be represented as "slightly warm" and the blue arrow as "fairly cold". This conversion of numeric values into linguistic variable is known as Fuzzification where rule based/ threshold methods have been used to classify members into functions. The above fuzzy set is a trapezoidal one. The sets can be triangular and even sigmoid functions [12].

Similar to Boolean Logic, fuzzy logic uses logic operators that mimic the AND, OR and NOT functions. MIN, MAX and 1-x replace the traditional logic operators. Once the variables have been fuzzified into linguistic variables and operators applied, the last step is to

defuzzy the data in order for the end user to understand and make sense of. This is one in four basic steps

1. Cutting the membership function at the point of truth value
2. Using the OR operator to aggregate the resulting curves
3. Finding the centre of wright under the area under of the curve of each function
4. The x position of this centre is the "crisp" output

FLCs have been used in modern day MPPTs techniques to quickly and accurately track the MPP. It works by sampling the photovoltaic current and voltage values in real time and fuzzifying them to be later used in rule based membership functions. A rule can be defined as "For an increase in V_{PV} reading greater than 10V, change the duty cycle (D) by 0.0025" etc. Such rules are then transformed into actual numeric values for the controller to understand using the defuzzifier. Fig. 16 shows a basic working methodology of FLC based MPPT [13].

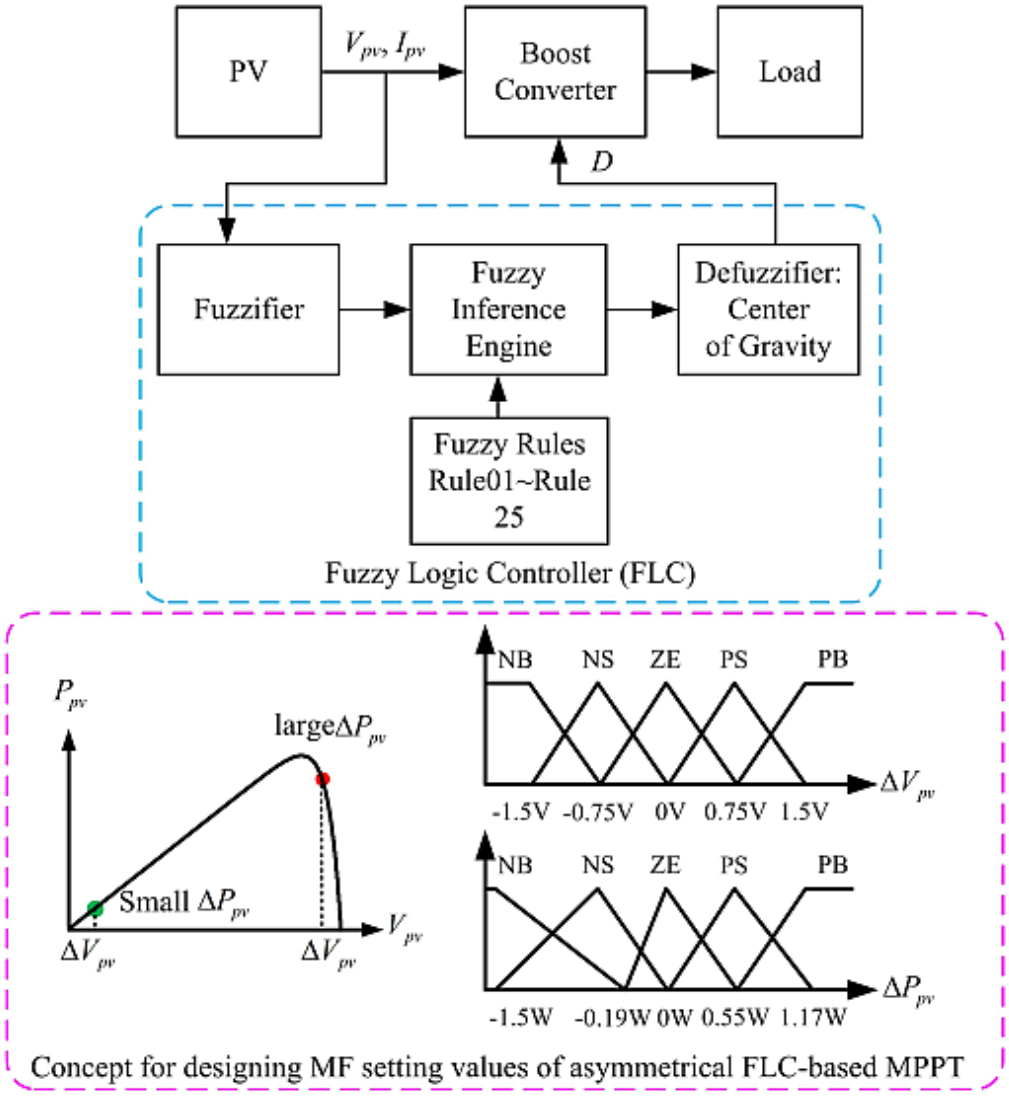

Figure 16: FLC based MPPT working principle

FLC based MPPT yields advantages which are especially useful for dealing with the pitfalls of MPPT

- FLCs are ideal for cases with non-ideal outputs such as MPPT
- FLCs are merge and operate upon uncertain information from various sources that too is similar to usage in MPPTs
- It is easy to understand with heuristic tools which incorporate "if-then" rules
- FLCs are easily customizable in natural language terms
- When used in conjunction with PI controllers, the quality of the tracking increases tremendously.

On the contrary, FLCs do have the following shortcomings aswell

- They are Complicated to design
- They Requires a detailed set of rule base
- They are Not as cheap as some of the conventionally used MPPTs
- Determination of specific step size for increase or decrease in duty cycle can be tricky to explain in rule base.

2.5 MPPT Techniques: Artificial Neural Network Based MPPT

From companies like Youtube employing Artificial Neural Networks (ANN) to teach their algorithms which videos to monetize and which to flag, to automobile newbies like Tesla Motors manufacturing self –driving cars based on Neural Nets to teach lane-keeping, obstacle avoidance and a proper driver-less mode, to Mobile manufacturer giant like Apple teaching their facial unlock technologies how to learn and adapt to an ageing facial feature and use it to unlock an iPhone, to social network powerhouse like Facebook deploying beta level chatbots based on ANNs to learn how to answer a query from a user, to search engine giant like Google funding their ANN project "Google Brain" to develop bots that can beat world's best Go player, ANN is well and truly around us and without us knowing it, we're benefitting from the rewards it brings to us in our daily lives. Our newsfeeds are catered and sorted for us to view, share and like on multiple social media platforms courtesy of ANN and Machine learning technologies which monitor our patterns or likeness and give more preference to the kind of media we consume. Our Meteorological Analysis and Predictions from all around the world is getting smarter with the day with accurate predictions having a granularity of less than five minutes within a five mile range. Our smartwatches are monitoring our heart-rates 24/7 and analysing the data to predict any abnormalities and even warn us ahead of time whether there are any chances of a heartattck. All of this has been made possible by something that tries to mimic the activity of our brain and has been in the works for over half a century now. ANN has matured leaps and bounds from the time since 1958 when the first perceptron was developed by Frank Rosenblatt to explain how the human brain works, to a point where it is now applicable for all our practical purposes. In such a case scenario it is the

right time to move ahead with the changing society and adapt and move along with the tide of time.

2.5.1 What is an ANN?

The basic functional unit in our brain is known as "Neuron" as shown in Fig 17. The term "neural networks" has been derived from the very same word. This gives as an idea how ANNs are analogous to our brains. ANNs by definition are computational models based on biological neural networks (Fig 18). It has a set of inputs that enter the network and goes through the architecture of the network, modifying it, inheriting knowledge or inferring information to it, thereby learning and adjusting according to the desired outputs. A complicated non-linear relation between an input and output are modelled and patterns are found [14].

Both the human brain and the neural network acquire knowledge through learning procedures, scenarios, events or identification of patterns from data sets. Similarly the knowledge is stored within inter-neuron (synapses) spaces known as synaptic weights. To further illustrate the analogy, consider the biological neuron shown below. The dendrites are the entry points for the signals into the network, while the cell body sums up all the information which is being collected by the dendrites to form an input. The axon is merely a mode of transfer. It transfers the input when the sum crosses a certain threshold, at which point it fires it to the next neuron. The space between one neuron to the next is known as a synapse. How much signal will be transferred to the next neuron is determined by the weights in the synapses. Biologically, the synapse is a void with salts, the more material (weight) there is in the synapse, better the data transmission on the next neuron and so forth. The connections can either inhibit flow of signals or boost them depending on the weights assigned. Interconnections of billions of such neurons results in the organ that is our brain.

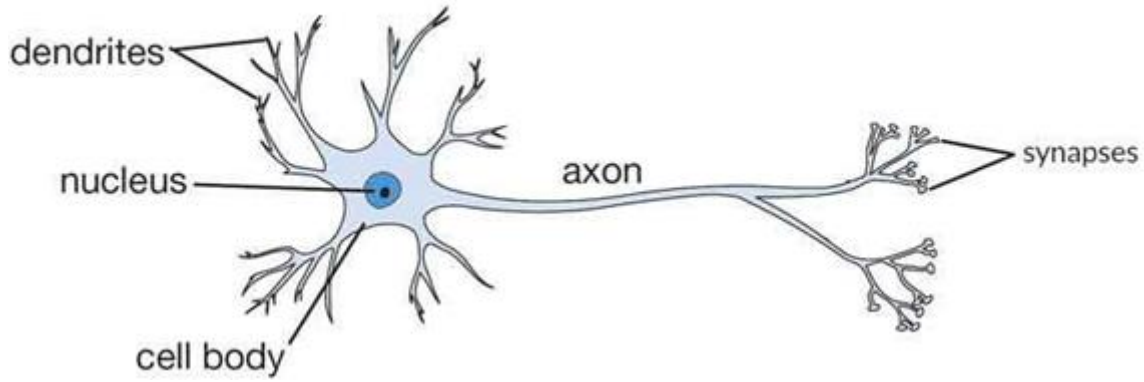

Figure 17: Structure of biological neuron [15]

The above biological structure of a neuron can be modelled and developed to work in a similar manner. The equivalent model of the biological structure is shown below.

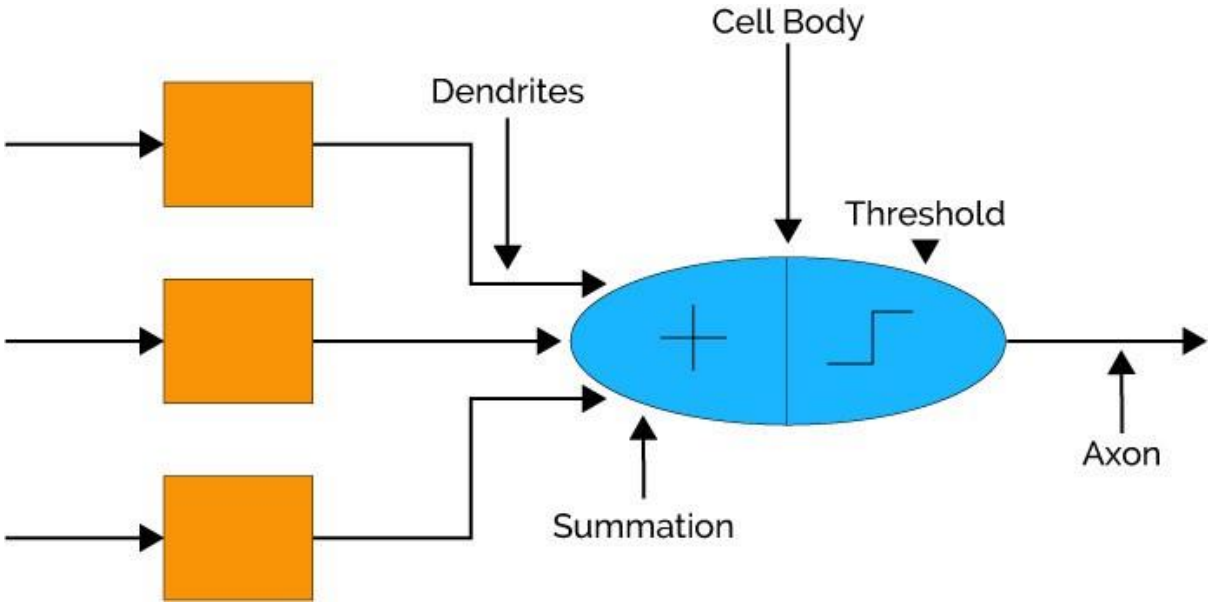

Figure 18: Equivalent mode of a biological neuron

The input blocks act as the dendrites collecting signals and parsing them through to summation block. The summation block keeps summing up the signals to generate an input until a set threshold is crossed. Upon crossing the threshold, the signal is fired through via the axon while being assigned a weight to it. This is completely analogous to how a biological neuron works.

2.5.2 Working of ANN

In a Neuron model (Fig 19), the weight (w), refers to the strength of the synapse, while the signal from the axon is represented by a. The bias, b, is more of a constant input of 1 which can also be omitted in many cases. Continuing the discussion from the previous section, let's consider a scalar input p incoming to a "dendrite". This input is multiplied with the scalar weight w. This becomes one of the terms that are sent to the accumulator (summer). While the other input 1, is multiplied by a bias b and then forwarded to the summer. The summer outputs, n, into the activation function.

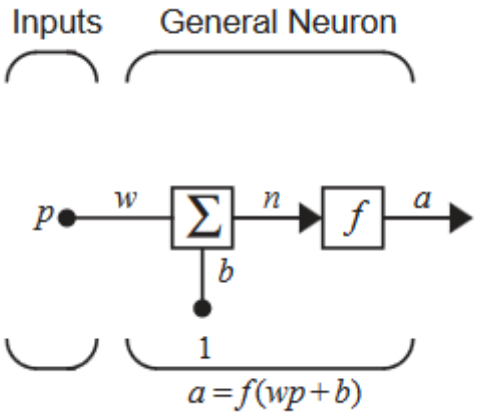

Figure 19: Single Input Neuron

So the output of the Neuron can be simply written as

$$a = f(wp + b) \tag{1}$$

For w = 3, p = 2 and b = -1.5, then the function becomes

$$a = f(3(2) - 1.5) = f(4.5) \tag{2}$$

The weight and bias are two arbitrary value which will solely depend upon the learning rule that the ANN employs [16]. The output of the neuron depends upon the transfer function and is chosen by the designer according to the requirement.

A transfer function is selected to satisfy a specific problem that the neuron is aimed at solving. It can either be linear or non-linear. There are several transfer functions to choose from. Some of the basic transfer functions are as follows

- Hard limit transfer function
  This transfer function distinguishes outputs into two categories; input function argument being less than 0 – in which case the output will be 0 and the input function argument being greater than or equal to 0 – in which case the output will be 1.

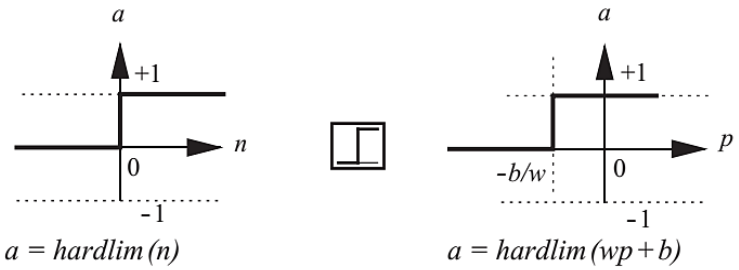

Figure 20: Hard Limit transfer function

- Linear Transfer Function
  The output of a linear transfer function is equivalent to its input. Notice how the bias and weight affects the output of the function

$$a = n$$

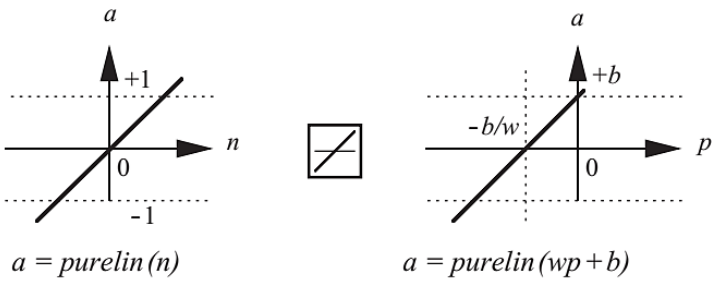

Figure 21: Linear Transfer Function

- Log Sigmoid Transfer Function
  Unlike the above two functions whose outputs are either binary or linear, the output of Log Sigmoid transfer function ranges between 0-1. The input output relationship is mapped using the following equation

$$a = \frac{1}{1 + e^{-n}} \tag{3}$$

This transfer function is more popular with multi-layered back propagation networks.

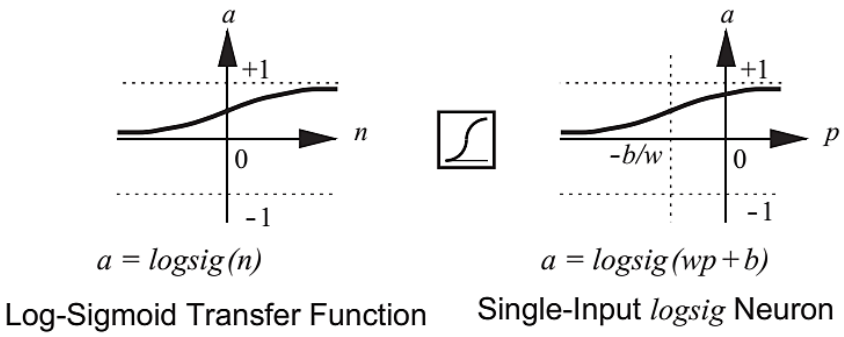

Figure 22: Log Sigmoid Transfer Function

ANNs are considered to be Universal Functional Approximations which roughly means they can predict and learn anything be it detecting a song to developing and mastering a game. Literally, any function can be mapped onto a neural network for it to learn from. In such a case scenario, there can be many types of problem statements/equations i.e. Linear, non-linear etc. So there must be an equal number of transfer function which can make it easy for us to map such non-linearities. For e.g the most common transfer functions include, the sigmoid and ReLu functions. Sigmoid functions were very popular particularly due to their ease of use however they suffered from vanishing slope (which is necessary for back propogation) so ReLu became a very good alternative. However sigmoid still remains a good tradeoff between performance and ease of use. It depends upon the designer of the network to decide which network best suits his/her or their problem. Following is a list of transfer functions with their equivalent MATLAB commands and input/output relation.

Name	Input/Output Relation	Icon	MATLAB Function
Hard Limit	$a = 0 \quad n < 0$ $a = 1 \quad n \geq 0$		hardlim
Symmetrical Hard Limit	$a = -1 \quad n < 0$ $a = +1 \quad n \geq 0$		hardlims
Linear	$a = n$		purelin
Saturating Linear	$a = 0 \quad n < 0$ $a = n \quad 0 \leq n \leq 1$ $a = 1 \quad n > 1$		satlin
Symmetric Saturating Linear	$a = -1 \quad n < -1$ $a = n \quad -1 \leq n \leq 1$ $a = 1 \quad n > 1$		satlins
Log-Sigmoid	$a = \frac{1}{1+e^{-n}}$		logsig
Hyperbolic Tangent Sigmoid	$a = \frac{e^{n}-e^{-n}}{e^{n}+e^{-n}}$		tansig
Positive Linear	$a = 0 \quad n < 0$ $a = n \quad 0 \leq n$		poslin
Competitive	$a = 1$ neuron with max n $a = 0$ all other neurons		compet

Table 2: Transfer functions

So far, a single input feed-forward ANN has been seen with a simple transfer function. However there can be multiple inputs to a neuron. All the inputs are just like the above mentioned cases, multiplied with the weights and added to the corresponding bias in a summing block. The output of multiple weight and input products can be rewritten in a matrix form as W.

$$n = w_{1,1}p_1 + w_{1,2}p_2 + w_{1,3}p_3 \ldots\ldots w_{1,R}p_R$$

The above expression can be written in matrix form as,

$$n = W_p + b$$

The neuron output becomes

$$a = f(W_p + b)$$

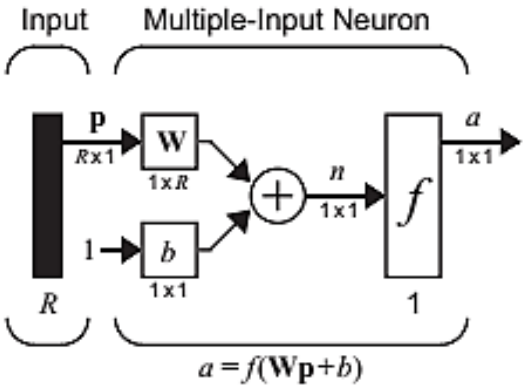

Figure 23: Neuron with R inputs

The number of inputs which are to be fed to the network depend upon, again, the problem. For instance a car that needs just needs to keep in a lane (within a controlled lab environment) must look at inputs from line marking sensors on both sides and front and back. So the total number of inputs to a network become four. Similarly for our case an MPPT that needs to track the MPP should get inputs about the surroundings i.e. irradiance and the temperature sensors. A simple neuron with multiple R inputs is shown in Fig. 22.

ANN architecture is classified on the basis of different layers. A single neuron receiving inputs may be insufficient to properly train or quickly train so there are five to ten neurons operating in parallel; this parallel operation of neurons is called a layer. Mostly, the input layer is also referred to as a layer in itself as it contains a matrix information about the inputs. While the second layer also known as the hidden layer contains the weights, bias, summers etc. The output layer contains the output of the transfer function. It is not necessary for all the neurons to have the same transfer functions, they all can have a different function associated to them. The weight matrix, W (SxR), indicates the target neuron, the weight corresponding to it and the source of input for the weight. All of this can be combined and rewritten in the S by R form as shown in Fig. 23. Notice how the weight matrix which was previous a 1xR matrix has now turned into an SxR matrix signifying multiple inputs.

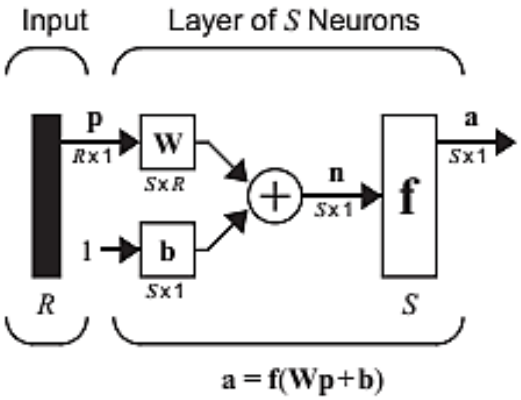

Figure 24: Layer of S neurons

The network output of a neuron that is also the network output is called the output layer (similar for the input layer) and the layers other than these two are known as hidden layers as shown in Fig. 24.

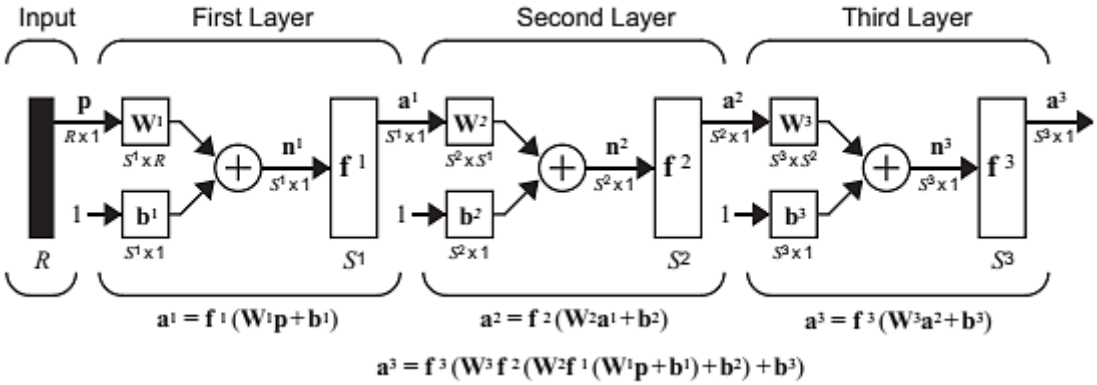

Figure 25: Three layer network

A single layer network is very inefficient as compared to a multiple layer network. Assigning two different transfer functions to a couple of layers in a three layered network can be trained to approximate most functions. So we can now develop an understanding of the parameters we need to change to develop our very own network. Suppose we have a system with two inputs, so we'll use two inputs to the first layer. Similarly we'll use the respective neurons in the output layer to map the output. Determination of transfer function mostly depends upon the requirement at the output layer. Whether an output ranging between -1 to +1 is required or a simple 0 or 1, this all goes into thinking while choosing the transfer function. Most practical neural nets have two to three layers. Networks having more than four layers are rarely used.

Now that a complete multi layered architecture of an ANN has been presented, we begin to see the procedure or "learning rule" through which the network modified the weight and biases or readjusts them to make sure the input is being mapped to the desired output. This is known as the Learning Rule/ Training algorithm. In general all the learning rules are classified into three categories

- Supervised Learning
  As evident from the name, the learning rules in this type of learning is provided with a set of examples in the training set. Target values (**t)** is the desired value while (**p)** is the input value. With each iteration, the inputs are compared with the target values and the subsequent error is calculated and the weights and the biases are adjusted based on the learning rule.

- Unsupervised Learning
  This type of learning is particularly interesting because there isn't a specific target value or set grade of performance that needs to be met. In unsupervised learning, the rule base is applied to the inputs only; the inputs are clustered together and patterns amongst them are found.

- Reinforced learning
  Reinforced learning is very similar to supervised learning except that in supervised each input is checked by mapping onto the target values however in reinforced learning a particular threshold or grade is set for performance. This grade is a measure of the network performance over a subsequent set of output values. Reinforced learning is not really commonly used.

Learning rules and techniques is an area of particular interest for researchers. There are different algorithms that fall into the above mentioned categories. But for the sake of simplicity and understanding of this thesis, we discuss the basic Perceptron learning rule or the Perceptron algorithm.

In simple terms, a Perceptron is a single layered neural network and the Perceptron learning algorithm is considered as the simplest and basic level of ANN.

Consider a two input perceptron with one neuron. The transfer function used is *hardlim.* Typically weight matrix, W is written as such

$$\mathbf{W} = \begin{bmatrix} w_{1,1} & w_{1,2} & \cdots & w_{1,R} \\ w_{2,1} & w_{2,2} & \cdots & w_{2,R} \\ \vdots & \vdots & & \vdots \\ w_{S,1} & w_{S,2} & \cdots & w_{S,R} \end{bmatrix}.$$

Re-writing W in terms of a vector composed of the elements in the *ith* row

$${}_i\mathbf{w} = \begin{bmatrix} w_{i,1} \\ w_{i,2} \\ \vdots \\ w_{i,R} \end{bmatrix}.$$

The partitioned W can be written as

$$\mathbf{W} = \begin{bmatrix} {}_1\mathbf{w}^T \\ {}_2\mathbf{w}^T \\ \vdots \\ {}_S\mathbf{w}^T \end{bmatrix}.$$

The output of the network can then be easily written using the *hardlim* function in the following manger

$$a_i = hardlim(n_i) = hardlim({}_i\mathbf{w}^T\mathbf{p} + b_i).$$

We know the *hardlim* function has the following output type

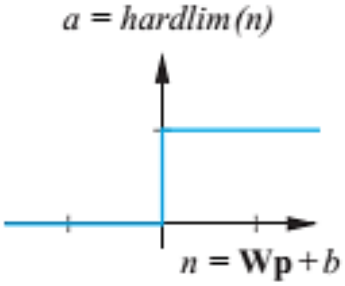

Figure 26: Hardlim function output

By manipulating the weight matrix, it becomes clear that if the product of the *ith* row of the weight matrix and the input vector is greater than or equal to $-b_i$ the output will be 1 and 0 vice versa. From the above figure it is visible that the each neuron divides region into two separate spaces. The entire objective in a learning rule is to determine the bias and weights that would cause these neurons to shift to a different region. The decision boundary is the region for which the input is 0.

$$n = {}_1\mathbf{w}^T\mathbf{p} + b = w_{1,1}p_1 + w_{1,2}p_2 + b = 0.$$

By choosing initial values for w and b, we can derive an equation in terms of p_1 and p_2. Similarly to find the point of intercepts of the decision boundary on the graph, we can place p_1 and p_2 zero in turns and find the intercepts. Supposing the method yields p = [1 1]. The graph of the decision boundary is shown as below. To check as to which region of the boundary would result in an output of 1 or 0 a simple check with test points can be made.

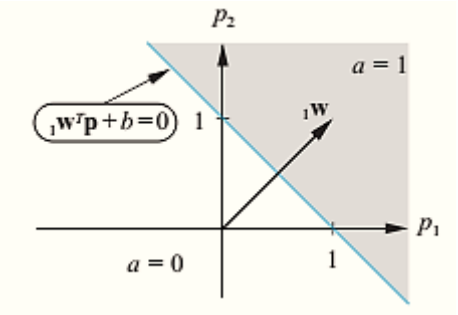

Figure 27: Decision boundary of a two input perceptron

Now that there exists a decision boundary, we need to determine the weight and bias. In case of weight, there is a simple rule which governs the relation between the boundary and weight itself. The boundary is always orthogonal to the weight. So we can choose a point such as [2 2] which would still be orthogonal to be the boundary. While the bias is found by the following equation

$${}_1\mathbf{w}^T\mathbf{p} + b = 0.$$

The boundaries and the weight functions adjust how far and how steep the line should be to classify two sets of different points. The perceptron learning rule is the most basic ANN.

Other algorithms stem from the entire concept of adjusting the weight and bias of the neurons to reach desired values.

2.5.3 Previously Deployed ANN Based MPPT Techniques

With a clearer understanding of how some of the most basic ANNs work, it is easier to understand the implementation of ANN for MPPT purposes. ANN based MPPT is an active area of research not because higher levels of tracking have not been achieved with other methods but because of the versatility of using Neural networks. Following are some of the prominent techniques

1. ANN based MPPT method in conjunction with Incremental conductance [17].
2. 2 sensor based (PV voltage and current) ANN for MPPT [18].
3. Fixed voltage grid connected ANN based MPPT technique [19].
4. Array voltage trained Neural network for MPPT design [20]
5. dP, dV, Irradiance, Temperature (inputs) for Smart MPPT (ANN) method [21].

All these techniques differentiate from each other on the basis of number of inputs, training schemes, grid connected systems or stand-alone systems. The fundamental target value however remains the same for all, to track the maximum value of power at various instances. Following figure gives a list of almost all the MPPT techniques and a modest overview [22].

MPPT technique	PV array dependent?	True MPPT?	Analog or digital?	Periodic tuning?	Convergence speed	Implementation complexity	Sensed parameters
Hill climbing/P&O	No	Yes	Both	No	Varies	Low	Voltage, current
Incremental conductance	No	Yes	Digital	No	Varies	Medium	Voltage, current
Fractional V_{OC}	Yes	No	Both	Yes	Medium	Low	Voltage
Fractional I_{SC}	Yes	No	Both	Yes	Medium	Medium	Current
Fuzzy logic control	Yes	Yes	Digital	Yes	Fast	High	Varies
Neural network	Yes	Yes	Digital	Yes	Fast	High	Varies
RCC	No	Yes	Analog	No	Fast	Low	Voltage, current
Current sweep	Yes	Yes	Digital	Yes	Slow	High	Voltage, current
dc Link capacitor droop control	No	No	Both	No	Medium	Low	Voltage
Load I or V maximization	No	No	Analog	No	Fast	Low	Voltage, current
dP/dV or dP/dI feedback control	No	Yes	Digital	No	Fast	Medium	Voltage, current
Array reconfiguration	Yes	No	Digital	Yes	Slow	High	Voltage, current
Linear current control	Yes	No	Digital	Yes	Fast	Medium	Irradiance
I_{MPP} and V_{MPP} computation	Yes	Yes	Digital	Yes	N/A	Medium	Irradiance, temperature
State based MPPT	Yes	Yes	Both	Yes	Fast	High	Voltage, current
OCC MPPT	Yes	No	Both	Yes	Fast	Medium	Current
BFV	Yes	No	Both	Yes	N/A	Low	None
LRCM	Yes	No	Digital	No	N/A	High	Voltage, current
Slide control	No	Yes	Digital	No	Fast	Medium	Voltage, current
β Method	No	Yes	Digital	No	Fast	High	Voltage, current
System oscillation method	No	Yes	Analog	No	N/A	Low	Voltage
Constant voltage tracker	Yes	No	Digital	Yes	Medium	Low	Voltage
Lookup table method	Yes	Yes	Digital	Yes	Fast	Medium	Voltage, current, Irradiance, temperature
Online MPP search algorithm	No	Yes	Digital	No	Fast	High	Voltage, current
Temperature method	No	Yes	Digital	Yes	Medium	High	Voltage, irradiance, Temperature
Three point weight comparison	No	Yes	Digital	No	Varies	Low	Voltage, current
POS control	No	Yes	Digital	No	N/A	Low	Current
Biological swarm chasing MPPT	No	Yes	Digital	No	Varies	High	Voltage, current, Irradiance, temperature
Variable inductor MPPT	No	Yes	Digital	No	Varies	Medium	Voltage, current
INR method	No	Yes	Digital	No	High	Medium	Voltage, current

Figure 28: Review of MPPT techniques

Summary

The chapter discusses Pakistan's energy trends and discusses why it is imperative to take small steps towards a green renewable future with a steady departure from conventional sources of energy i.e. fossil fuels. The chapter goes into details about solar cell technology, importance of MPPTs, its types and the proposed ANN based method.

References

[9] Solar energy potential in Pakistan. (2013). *Journal of Renewable and Sustainable Energy, 4*(032), 71st ser., 5-30. doi:ne: http://dx.doi.org/10.1063/1.4712051

[10] Hou, Y., & Li, E. (n.d.). *Research on Testing Methods of I-V Characteristics of Solar Photovoltaic Cell Array* (1st ed., Vol. 1, Ser. 1). 2007

[11] Soon, T. K., & Mekhilef, S. (2013). Maximum Power Point Tracking With Improved Incremental Conductance Method for Fast Changing Solar Irradiation Level. *IOP Conference Series: Earth and Environmental Science, 16*, 012017. doi:10.1088/1755-1315/16/1/012017

[12] Logic and Fuzzy Systems. (2010). *Fuzzy Logic with Engineering Applications*, 117-173. doi:10.1002/9781119994374. Chapter 5. Chu Li.

[13] Sujith, S., & Kathiravan, N. (2016). Comparison of fuzzy logic based MPPT with P&O for solar PV pumping system. *2016 International Conference on Emerging Technological Trends (ICETT)*. doi:10.1109/icett.2016.7873755

[14] What is an Artificial Neural Network (ANN)? - Definition from Techopedia. (n.d.). Retrieved December 16, 2017, from https://www.techopedia.com/definition/5967/artificial-neural-network-ann

[15] X. (2017, July 17). Overview of Artificial Neural Networks and its Applications. Retrieved December 16, 2017, from https://medium.com/@xenonstack

[16] Hagan, M. T., Demuth, H. B., Beale, M. H., & Jesús, O. D. (2016). *Neural network design*. S. l.: S. n. MATHWORKS

[17] Vinay, P., & Mathews, M. A. (2014). Modelling and analysis of artificial intelligence based MPPT techniques for PV applications. *2014 International Conference on Advances in Green Energy (ICAGE)*. doi:10.1109/icage.2014.7050144

[18] Rizzo, S. A., & Scelba, G. (2015). ANN based MPPT method for rapidly variable shading conditions. *Applied Energy, 145*, 124-132. doi:10.1016/j.apenergy.2015.01.077

[19] Diab, H., El-Helw, H., & Talaat, H. (2012). Intelligent maximum power tracking and inverter hysteresis current control of grid-connected PV systems. *2012 International Conference on Advances in Power Conversion and Energy Technologies (APCET)*. doi:10.1109/apcet.2012.6302065

[20] Dzung, P. Q., Khoa, L. D., Lee, H. H., Phuong, L. M., & Vu, N. T. (2010). The new MPPT algorithm using ANN-based PV. *International Forum on Strategic Technology 2010*. doi:10.1109/ifost.2010.5668004

[21] Messalti, S., Harrag, A. G., & Loukriz, A. E. (2015). A new neural networks MPPT controller for PV systems. *IREC2015 The Sixth International Renewable Energy Congress*. doi:10.1109/irec.2015.7110907

[22] Gupta, A. K., & Saxena, R. (2016). Review on widely-used MPPT techniques for PV applications. *2016 International Conference on Innovation and Challenges in Cyber Security (ICICCS-INBUSH)*. doi:10.1109/iciccs.2016.7542321

CHAPTER 3
SYSTEM MODELLING

The chapter presents the single diode cell model and its Simulink implementation and verification. Two conventional MPPT techniques are also modelled and implemented in Simulink. Lastly the ANN based MPPT implementation is shown.

3.1 Single Diode Cell Model

The working principle of the solar cell is known as the "photovoltaic effect". PV effect refers to the generation of potential difference at the P-N junction of the diode when exposed to visible or other radiation (as elaborated in Chapter 1). In essence, if PV effect is eliminated, the solar cell is nothing but a conventional diode in which the carriers are separated by the junction. This generates an electric field and thus an electric current, I_{PV}. Therefore the PV cell is modelled as a diode. There are various mathematical models of the PV cell;

- The double diode model (DDM)
- Three diode model (TDM)
- Simplified single diode model (SSDM)
- Further simplified single diode model (FSDM)

In literature the most commonly used model is the Single diode model (SDM). It consists of a series resistance (R_S) and shunt resistance (R_{SH}) – these resistances mimic the parasitic resistances caused by various defects. For e.g. R_{SH} occurs mainly due to manufacturing defects. Lower the shunt resistance, greater the alternate path for the light generated current to travel [23]. This causes less current to flow from the junction and a subsequent drop in voltage. R_{SH} has greater impacts at low light levels. Series resistance is caused to the current movement from emitter to base of the cell, the contact resistance between the metal contact and silicon cell and also due to the top and bottom metal resistive contacts. Just like R_{SH} , R_S also affects the impact factor greatly. The SDM also consists of a current source along with a diode in parallel. The SDM model is shown in Fig. 28 below:

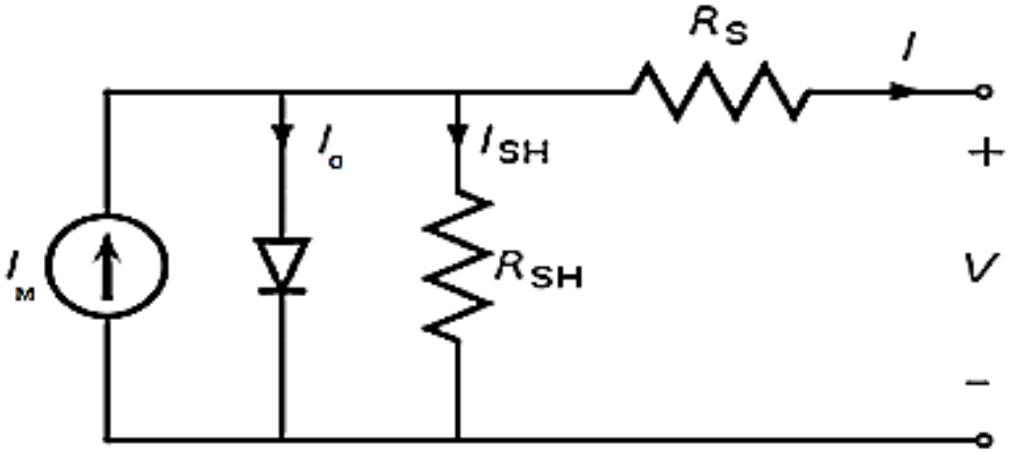

Figure 29: Single diode model of PV cell

According to Kirchoff's law

$$I = I_M - I_O - I_{SH} \tag{4}$$

I_M is given by

$$I_M = I_{PV} - I_O N_P \left[exp\left(\frac{V + R_S \left(\frac{N_S}{N_P}\right) I}{V_T a N_S} \right) \right] - 1 \tag{5}$$

The diode leakage current can be found from.

$$I_O = \frac{(I_{SCN} + K_i \Delta T) G}{\exp\left(\frac{V_{OCN} + K_i \Delta T}{a V_T}\right) - 1} \tag{6}$$

The photovoltaic current is given by,

$$I_{PV} = \frac{(I_{PVN} + K_i \Delta T) G}{G_N} \tag{7}$$

The thermal voltage (V_T) can be calculated using the following equation;

$$V_T = \frac{N_{CS} k T}{q} \tag{8}$$

N_{CS}: Series connected cells in a panel

K: Boltzman constant ($1.38064852 \times 10^{-23}$)

q: Charge on electron ($1.60217662 \times 10^{-19}$C)

Once we have all the governing equations for the currents across the Single Diode model. We can replace them in Kirchoff's current law to find out the module or array current. The PV

panel model parameters of Kyocera KC200GT were used to simulate the SDM. The manufacturer's parameters were obtained using the KC200GT data sheet (appended in A1). The parameters used are shown in the table below.

Quantity	Value
I max power	7.61A
V max power	26.3V
P max	200.143 W
I short circuit	8.21A
V open circuit	32.9V
I leakage	9.825×10^{-8} A
I photovoltaic	8.211A
Diode ideality constant (a)	1.3
Parallel resistance	415.406Ω
Series resistance	0.221Ω

Table 3: KC200GT module parameters used in simulating SDM

3.2 SIMULINK Model of SDM

Equations 4-8 were modelled and simulated in MALTAB/Simulink (Fig 30-33) to generate the SDM. The SDM was simulated to generate the training points for the ANN.

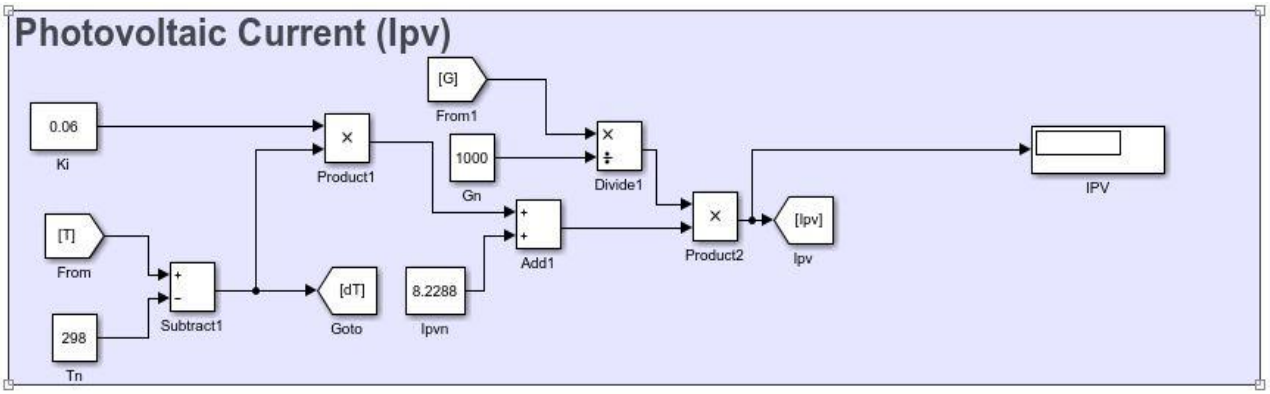

Figure 30: Simulink Model - Photovoltaic current

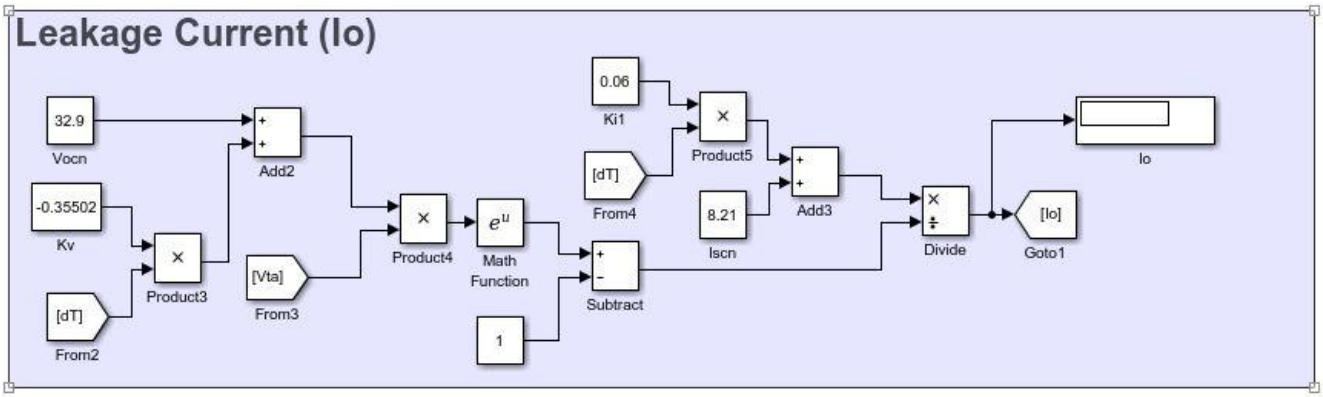

Figure 31: Simulink model - Leakage Current

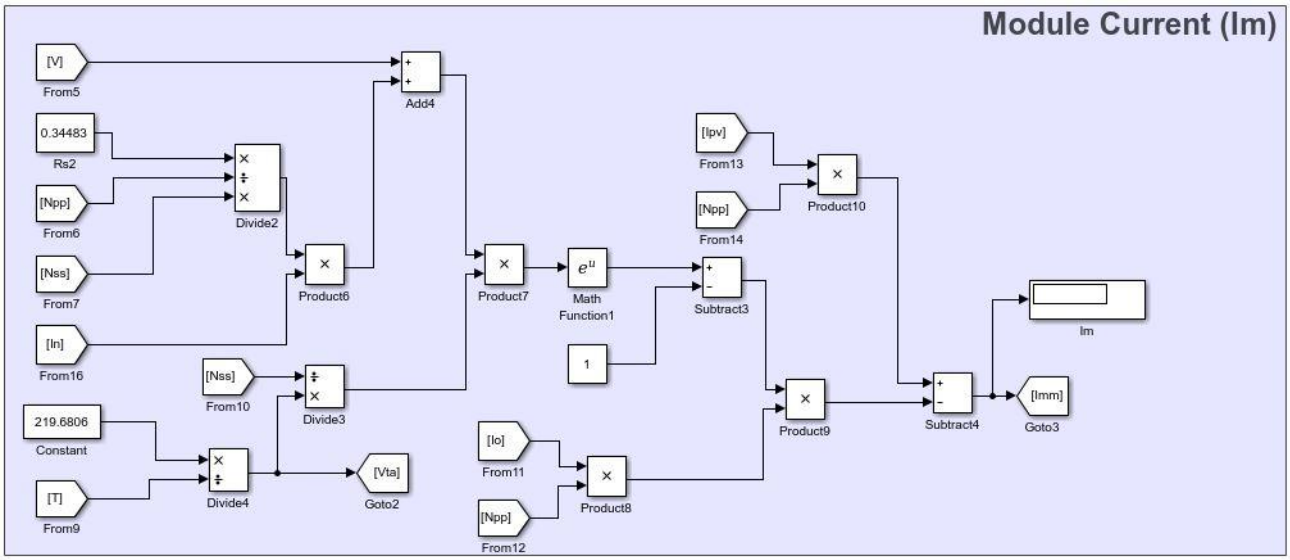

Figure 32: Simulink Model - Module Current

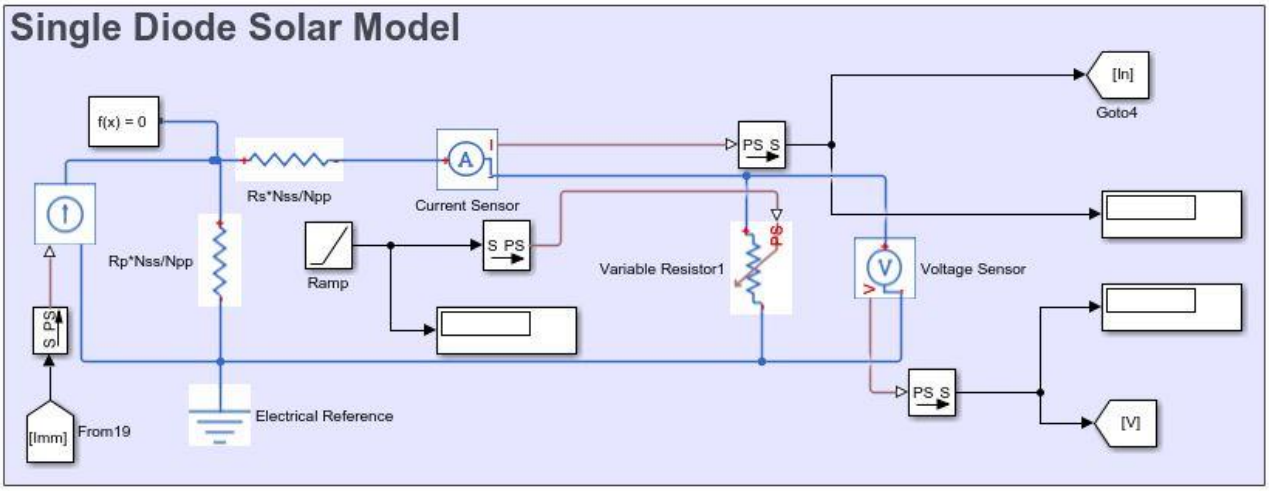

Figure 33: Simulink Model – SDM

3.3 Model Verification

The Simulink model Fig 30-33 were simulated with the parameters given in Table 3. The model was simulated under different conditions. The verification of the model accuracy is confirmed by the output values under Standard testing conditions i.e 25C and 1kW/m^2. According the manufacturer's data sheet (A.1), the output Maximum Power (P_{MAX}) at STC should be 200W at V_{Max} 26.1V and I_{MAX} equivalent to 7.61A which is in agreement with the results shown in the graphs below. The figures below show the operation of the SDM at fixed irradiance and varying temperatures (Fig. 33) and variable irradiance with fixed temperature (Fig. 34).

Once the panel output has been obtained and verified using SDM, now an array is designed by simply connecting the panels in 15 by 2 series configuration. The total output power for the array at STC should be 6.0kW. This array is also subjected to different conditions of temperature and irradiance, the result of which are shown in Fig. 35. The output powers of the array at these conditions will become our test bench for gauging the ANN based MPPT.

The same SDM based array model is now simulated over a range of 109 different values of temperature and irradiance to obtain test data for the ANN. The test set will be explained in detail in Chapter 4.

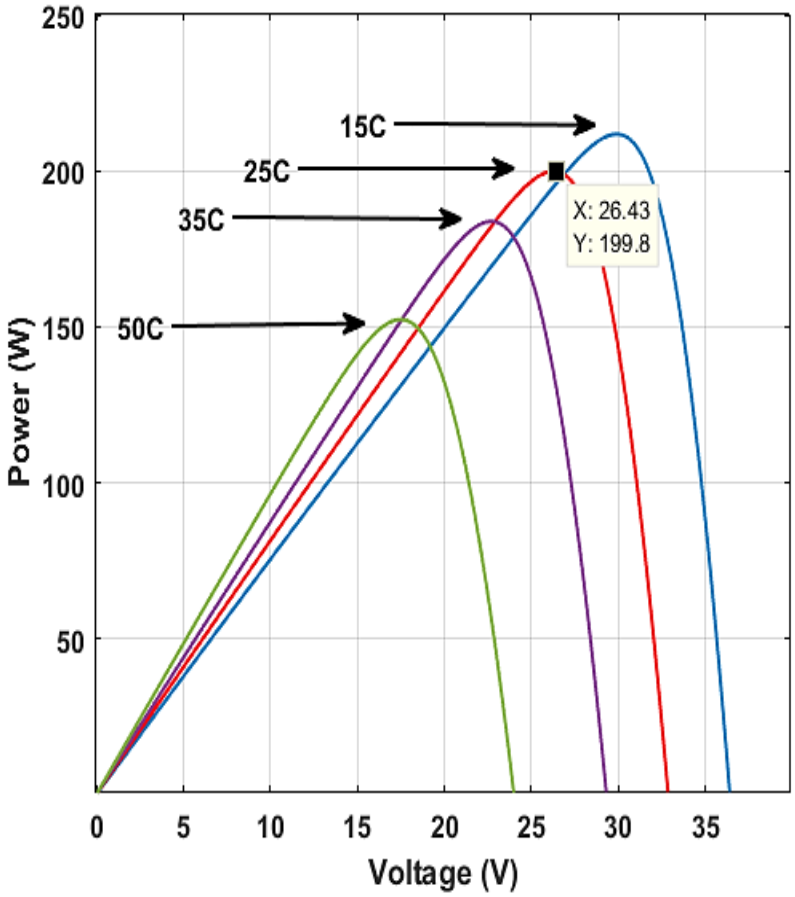

Figure 34: KC200GT module PV curves @1kW/m2 & Variable Temperatures

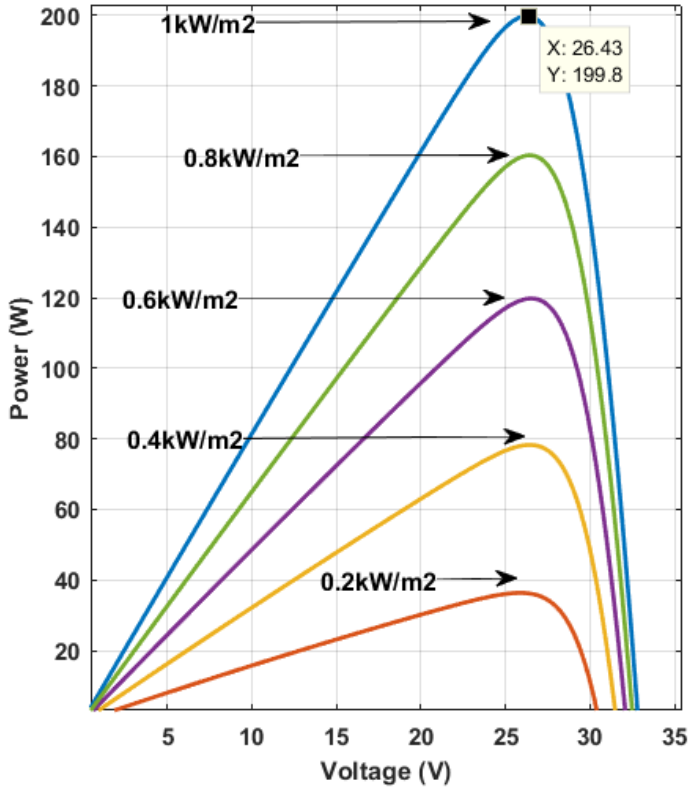

Figure 35: KC200GT module PV curves @25C & Variable Irradiances

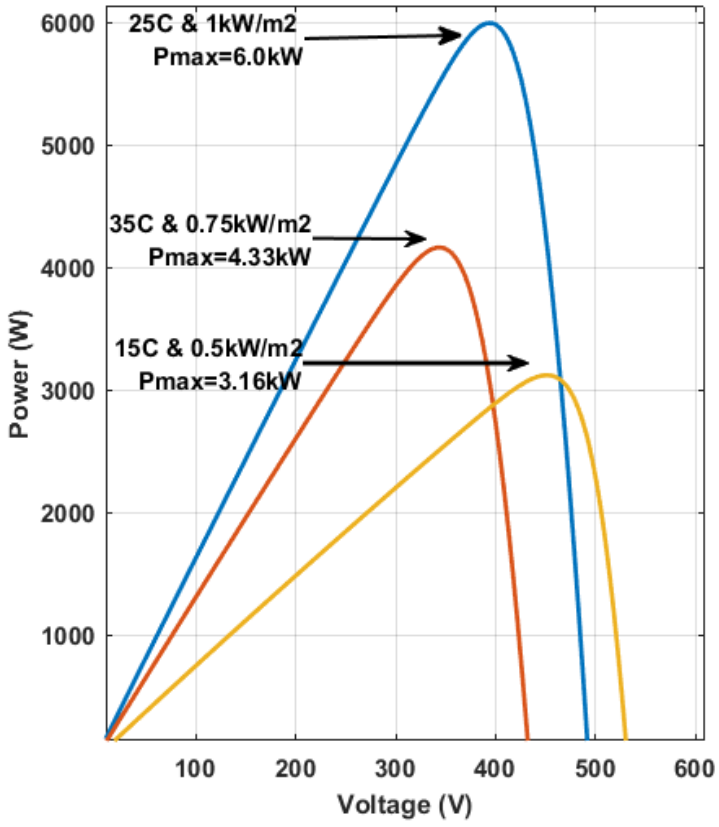

Figure 36: KC200GT Array PV curves at Variable Irradiances & Temperatures

3.4 Design & Development of ANN

This research work proposes developing a two-input and one-output artificial neural network. The idea behind doing so is to train the ANN on a set of input data consisting of different combinations of temperature and irradiances. The network learns for the set of environmental condition inputs what the target output operating voltage should be for which the maximum power point would be reached.

The ANN consists of three layers the input layer, hidden layer and the output layer. The input layer comprises of two neurons (temperature and irradiance) while the hidden layer has ten neurons and the output has one neuron (Vmpp).

Activation function for the hidden layer and the output layers are tansig and purelin respectively.

The input layer is given a total of 105 training point combinations of temperatures (varying between 15-40C) and irradiances (200-1200W/m^2). These set of points mimic the harsh and normal operating environmental conditions which the panel might be exposed to.

The output layer also corresponds to 105 different target values of V_{MPP} corresponding to different maximum power points obtained using single diode model. The ANN predicts the reference voltage ($V_{MPP)}$ at which the system should operate using the boost converter to achieve maximum power point.

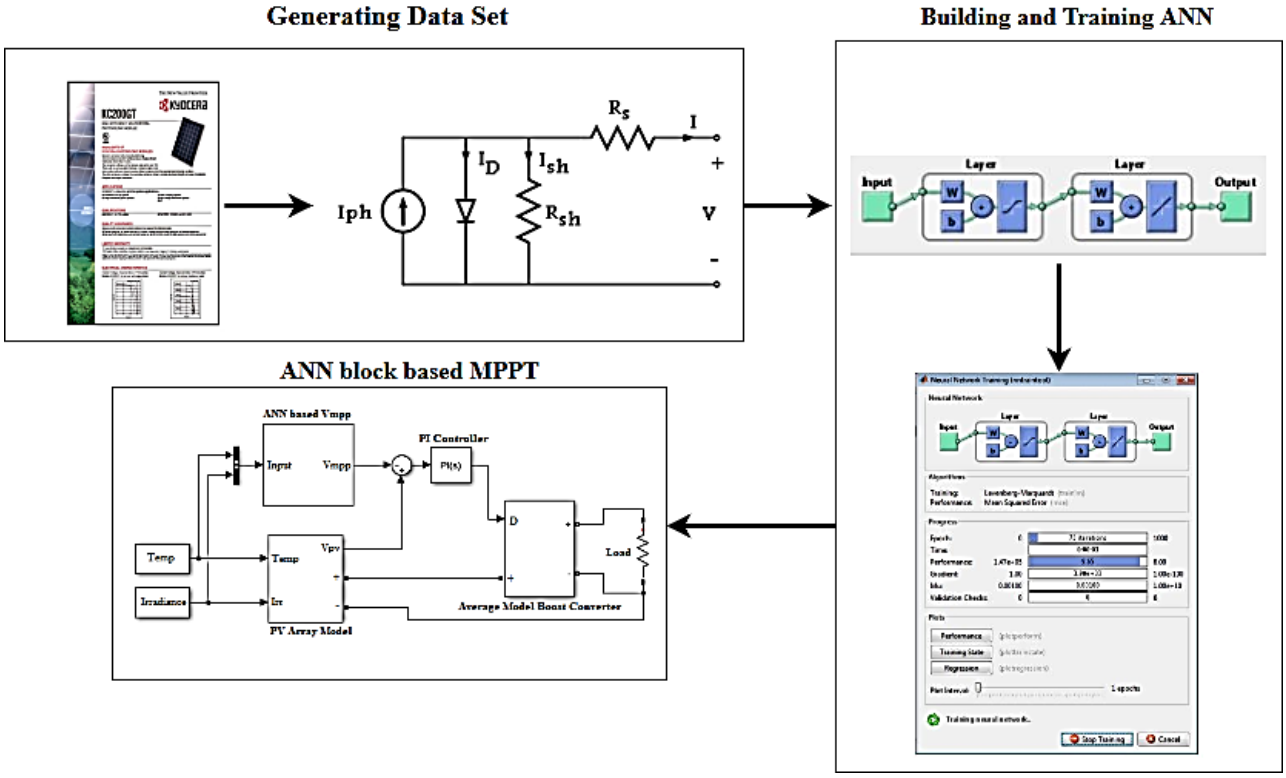

Figure 37: Methodology of work

3.5 Selecting Activation/Transfer Function

As mentioned in Chapter 2 a transfer function is selected to satisfy a specific problem that the neuron is aimed at solving. It can either be linear or non-linear. The activation function can be considered as the ON-OFF switch. The activation function generates an output when a certain threshold is reached or crossed. Some of the activation functions have been discussed in detail in Chapter 2, however the choosing a transfer function depends entirely upon the requirement of the problem. In this case a "*tangsigmoid"* (hidden layer) and "*purlin"* transfer functions (Output layer) have been used. The reason for selecting the two is discussed below.

3.5.1 Tan Sigmoid Transfer Function

Sigmoid functions are more commonly used with ANNs because of their ability to output a cluster of values between -1 and 1 unlike other functions whose outputs are just binary. The simplest of sigmoid function maps outputs based on the following relation

$$a = \frac{1}{1 + e^{-n}} \tag{9}$$

A sigmoid function produces an "S" shaped curve. In general, a sigmoid function is real-valued and differentiable, having a non-negative or non-positive first derivative, one local minimum, and one local maximum. Sigmoid function caters for the non-linearity in the system (in our case the non-linearity exists between the input set of values and the target values due to the single diode model). The tan sigmoid function satisfies the property between the derivative and itself such that it is computationally easy to perform [24]. Derivatives of the sigmoid function are easy to employ in our case of learning. Another reason for using tan sigmoid is because it provides a good trade-off between speed and exact shape of the curve [25].

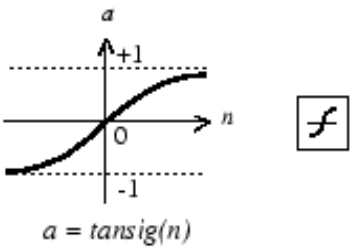

Figure 38: Tan Sigmoid transfer function and MATLAB symbol

Tan Sigmoid Syntax is given below

$$A = \text{tansig}(N,FP) \tag{10}$$

A = tansig(N,FP) takes N and optional function parameters

N: S-by-Q matrix of net input (column) vectors

FP: Structure of function parameters (ignored)

Which returns A, the S-by-Q matrix of N's elements squashed into [-1 1].

3.5.2 Pure Linear Transfer Function

Linear transfer functions work as linear relation between input and output. Linear transfer functions are used almost exclusively on the output layer where the output values are required continuously if a certain threshold is being crossed. It makes sense to use *purelin* transfer function on the output and not the hidden layers. It would render the purpose of training the network useless, if the hidden layers are activated by a linear relationship while we have non-linearities to deal with. *Purelin* is used in function approximations and regression tasks.

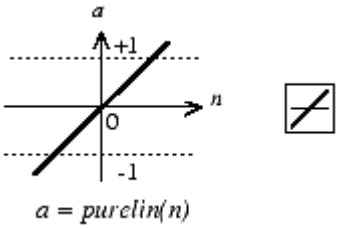

Figure 39: Purelin transfer function and MATLAB symbol

Pure Linear Syntax is shown below

A = purelin(N,FP)
info = purelin('*code*')

A: purelin(N,FP) takes N and optional function parameters

N: S-by-Q matrix of net input (column) vectors

FP: Structure of function parameters (ignored)

3.6 Selecting Network Architecture

The network input and output architecture is straightforward and simple. The number of neurons in the input layer is entirely dependent on the training features in the data. In this case, there are two input features i.e. Irradiance and Temperature; hence the input layer contains three neurons. Similarly the output layer neurons depend upon the number of output features. Again, in this case, V_{MPP} is the only output so there will be one neuron in the output layer.

Selecting the number of hidden layers and the neurons in them is not as simple as the above two layers. However it has become common to use a single hidden layer and judge the performance, if the said performance is not desirable, amongst all the steps that can be taken to enhance performance, one of the measures could be to increase the number of hidden layers. But for majority of the problems a single hidden layer suffices. Selecting the number of neurons in the hidden layer is a topic of active research and discussion. The following formula was used to find out the number of neurons in the hidden layer [26].

$$N_h = \frac{N_S}{\alpha(N_I + N_O)} \tag{11}$$

N_h: Neurons in the hidden layer
N_S: Number of sampling points in the data set
N_I: Number of input neurons
N_O: Number of output neurons
α: Scaling factor between 2-10

$$N_h = \frac{109}{3.5(2+1)} \tag{12}$$

$$N_h \approx 10$$

The network architecture becomes

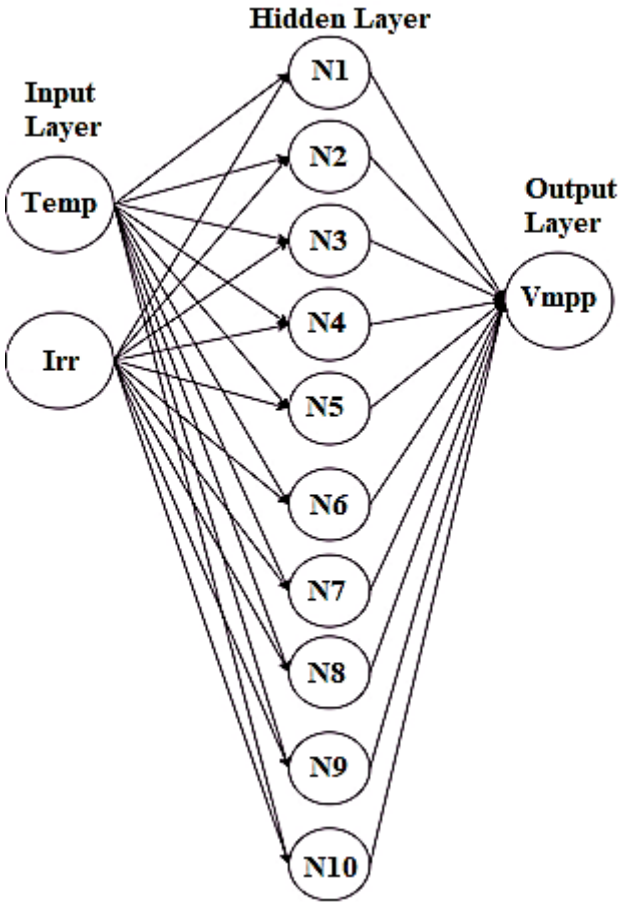

Figure 40: Network Architecture

3.7 Training the Network

MATLAB Neural Network toolbox (*nntool)* is used to create and train the network on the coded set of input points. The *trainlm* command uses the Levenberg Marquardt [27] algorithm as a learning rule (discussed in detail in Chapter 2). While the performance is checked using the Mean Squared error (mse). The total training time for the simulation is under 5 seconds, which is a good tradeoff between performance and convenience. The performance check results in 9.65. The performance in scaled between $1.5e^{05}$ to 0. In such a scenario, the resulting performance is acceptable. Once the network has been trained, it is tested with multiple values of irradiance and temperatures (some of which are present in the training points and some aren't) and the results are compared to simulations from the SDM. The ANN gives accurate and consistent results which suggests that it can be used in an MPPT model.

3.8 ANN Based MPPT System Model

The ANN model is converted into a Simulink block using *genism* command. This ANN block is incorporated in the MPPT model which consists of a Kyocera KC200GT PV array, signal builder blocks to generate variable patterns of irradiance and temperature, duty cycle controlled average model boost converter, a fixed resistive load and a Proportional Integral (PI) controller in conjunction with a summing (+-) junction. The system block diagram is shown below

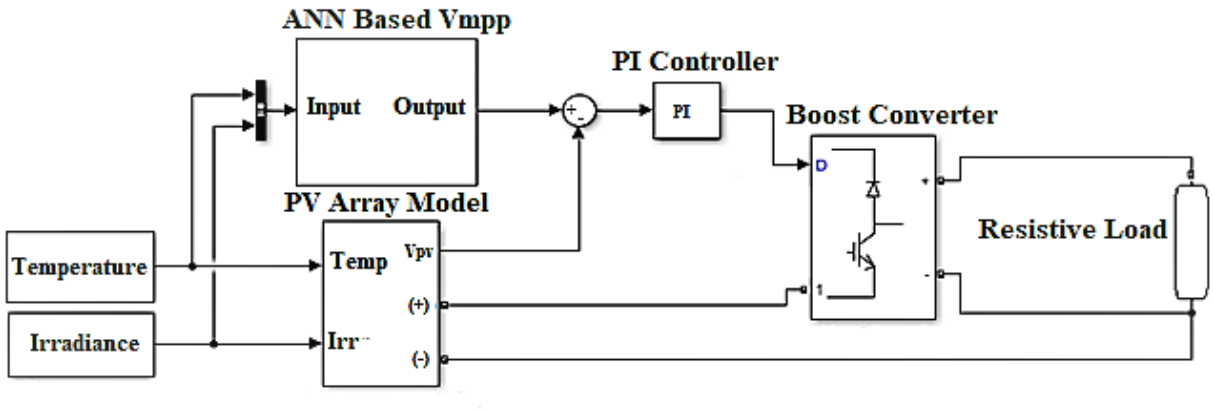

Figure 41: ANN based MPPT system block diagram

The ANN block generates a reference voltage at which the system should be operating (V_{MPP}). The same inputs for irradiance and temperature results in the panel operating at $V_{PV.}$ The properly tuned PI controller forces V_{PV} to be equivalent to V_{MPP} by manipulating the boost converter's duty cycle (discussed in Chapter 2). The Simulink model for the MPPT is shown below

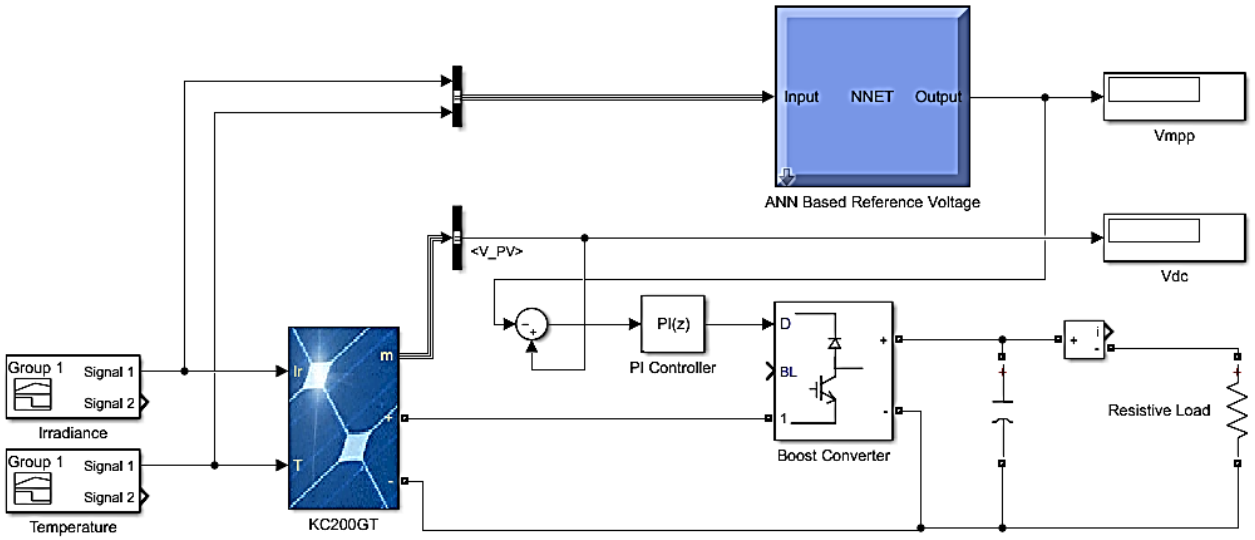

Figure 42: Simulink Model of ANN based MPPT

3.9 P&O Based MPPT

The P&O algorithm is coded in MATLAB/Simulink function file. The function file block is added to the same MPPT model as the one shown above. The P&O algorithm takes the runtime inputs of current and voltage from the PV panel and uses it to calculate power and compare it with the previous value of power, it correspondingly checks for voltage as well and updates the duty cycle [28]. This cycle continues until the new power is equal to the old power. The flowchart for the method is shown in Chapter 2 Fig. 11. Following table shows some of the parameters used in the P&O method.

Parameters	Values
Initial Duty cycle	0.7
Maximum Duty cycle	1
Minimum Duty cycle	0
Delta (step size) Duty cycle	0.001

Table 4: Parameters for P&O method

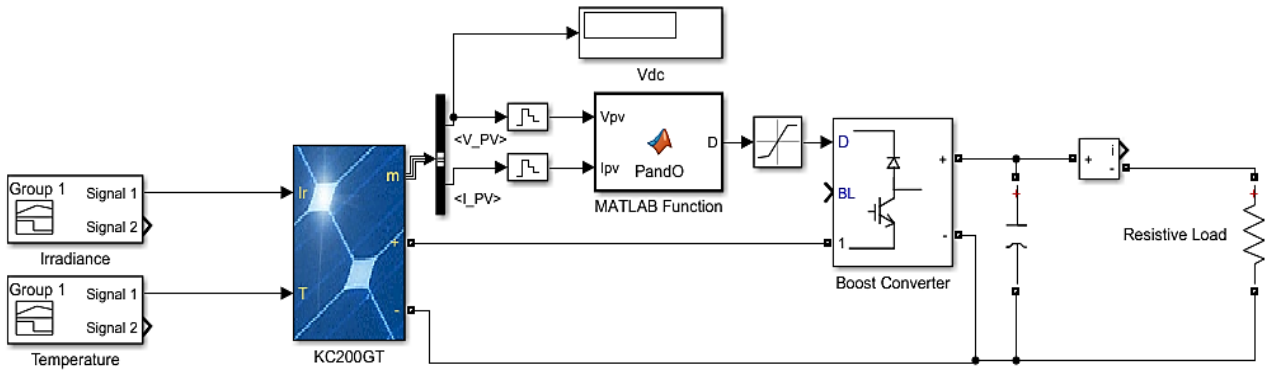

Figure 43: Simulink Model of P&O based MPPT

3.10 FOCV Based MPPT

As discussed earlier in Chapter 2, FOCV method assumes that the maximum power point voltage will always be a fraction of the open circuit voltage at any given condition. The ratio of V_{mpp} and V_{OC} results in a linearizing coefficient. Any value being output by the panel is multiplied by this gain/coefficient to get the reference voltage. This reference voltage is then followed by the controller to ensure operation at MPP [29]. To simulate the FOCV method, the open circuit voltages at the three testing conditions were already noted down and fed to the controller at the specific instances using a signal builder block. Parameters used for this method are summarized in Table 5. While the system Simulink diagram is shown in Fig. 43.

Parameter	Values
Linearizing coefficient	0.79939
Series connected cells in array	810
$V_{OC\text{-}Ref}$ (25C, 1kW/m^2)	493.48V
$V_{OC\text{-}Ref}$ (35C, 0.75kW/m^2)	469.9V
$V_{OC\text{-}Ref}$ (15C, 0.5kW/m^2)	497.33V

Table 5: Parameters for FOCV method

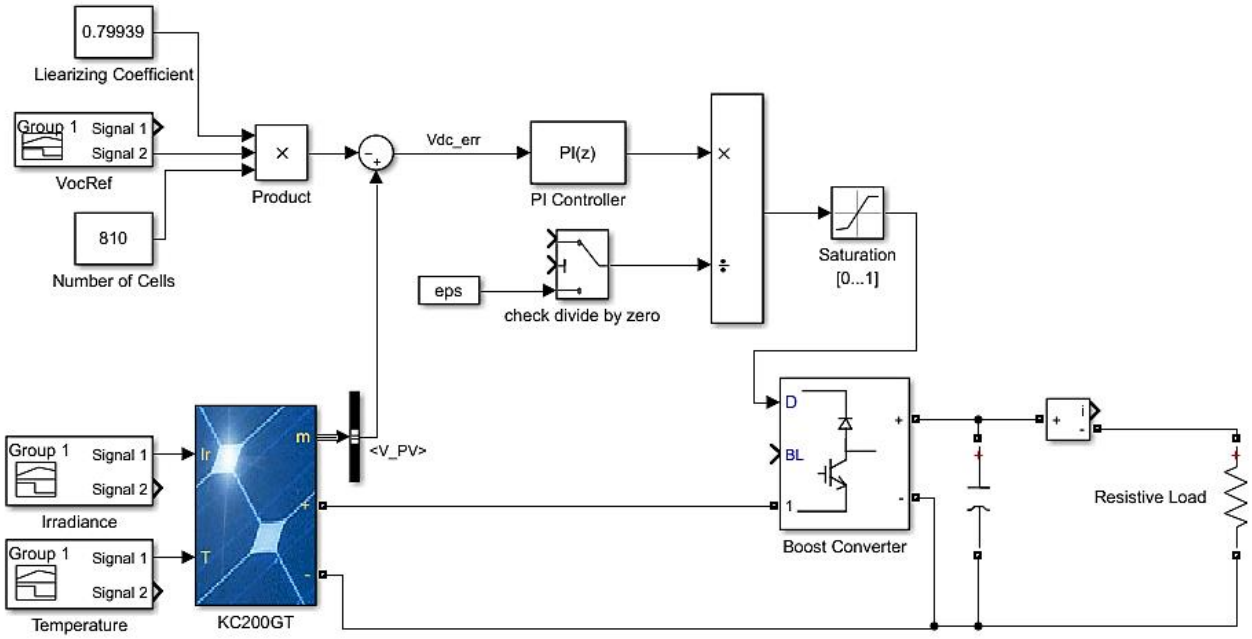

Figure 44: Simulink Model of FOCV based MPPT

Summary

The chapter discusses the modelling and implementation of the SDM in Simulink. Working principal of ANNs is also discussed with step by step guide on what parameters to choose for the proposed task. The ANN model is also implemented in Simulink alongwith P&O and FOCV models.

References

[23] Shunt Resistance. (n.d.). Retrieved December 16, 2017, from http://www.pveducation.org/pvcdrom/shunt-resistance

[24] Namin, A. H., Leboeuf, K., Muscedere, R., Wu, H., & Ahmadi, M. (2009). Efficient hardware implementation of the hyperbolic tangent sigmoid function. *2009 IEEE International Symposium on Circuits and Systems*. doi:10.1109/iscas.2009.5118213

[25] Logsig. (n.d.). Retrieved December 16, 2017, from https://www.mathworks.com/help/nnet/ref/tansig.html

[26] Thomas, L., V, M. K., & B, A. (2016). Discovery of optimal neurons and hidden layers in feed-forward Neural Network. *2016 IEEE International Conference on Emerging Technologies and Innovative Business Practices for the Transformation of Societies (EmergiTech)*. doi:10.1109/emergitech.2016.7737353

[27] Hagan, M., & Menhaj, M. (1994). Training feedforward networks with the Marquardt algorithm. *IEEE Transactions on Neural Networks, 5*(6), 989-993. doi:10.1109/72.329697

[28] Niasar, A. H., Zare, Z., & Far, F. R. (2015). A low-cost P&O based maximum power point tracking, combined with two-degree sun tracker. *The 6th Power Electronics, Drive Systems & Technologies Conference (PEDSTC2015)*. doi:10.1109/pedstc.2015.7093260

[29] Penella, M. T., & Gasulla, M. (2014). A Simple and Efficient MPPT Method for Low-Power PV Cells. *International Journal of Photoenergy, 2014*, 1-7. doi:10.1155/2014/153428

CHAPTER 4
RESULTS & DISCUSSIONS

The chapter discusses the environmental conditions used as a test bench to run the simulations on the three models. Voltage and power curves for all three methods are also presented.

4.1 Test Bench

The system is subjected to three different environmental conditions. 25C and 1kW/m^2, 35C and 0.75kW/m^2, and lastly 15C and 0.5kW/m^2

For the first four simulation seconds, the system operates at Standard operating conditions. At the fourth second mark, the temperature is increased by 10C and the irradiance is decreased to 0.75kW/m^2. After three seconds, the system is subjected to the greatest change by decreasing the temperature down to 15C and the irradiance to 0.5kW/m^2. It is understandable that such abrupt changes cannot take place in reality. But the purpose of these abrupt changes is to showcase the ability of the proposed MPPT system under the worst case scenario. It is also noteworthy that apart from the first operating condition, the second and third conditions were not used as an input data point to train the ANN based MPPT system. The system trained itself and using its learning rules, figured out the operating voltage for which the power would be optimized. All three systems are running the same; KC200GT array of 15 by 2 (series by parallel panels in an array), average model boost converter, fixed resistive load of 100Ω and the same capacitor for reducing the oscillations. The figures below show the testing conditions being provided, individual plots of the voltage versus time series and power versus time series. For comparison purposes, the power versus times curves of all three methods are taken together in one plot.

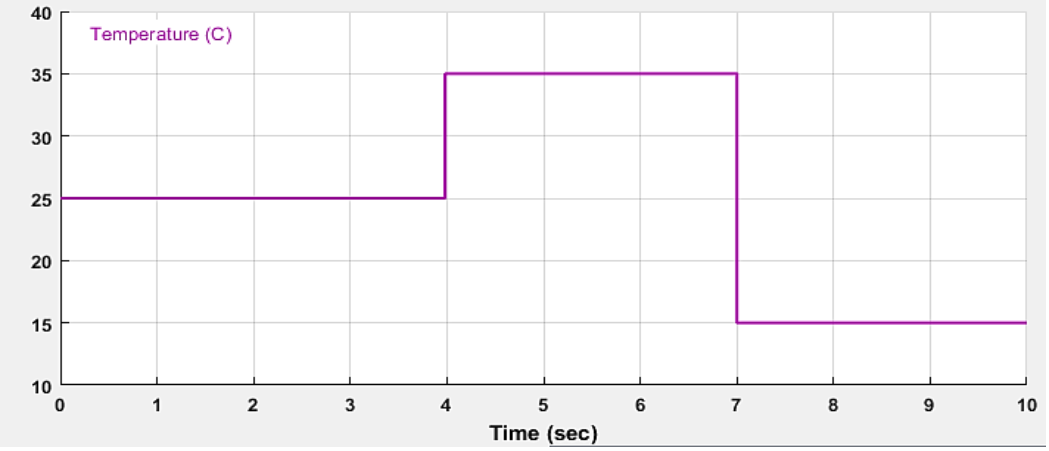

Figure 45: Temperature Input Conditions

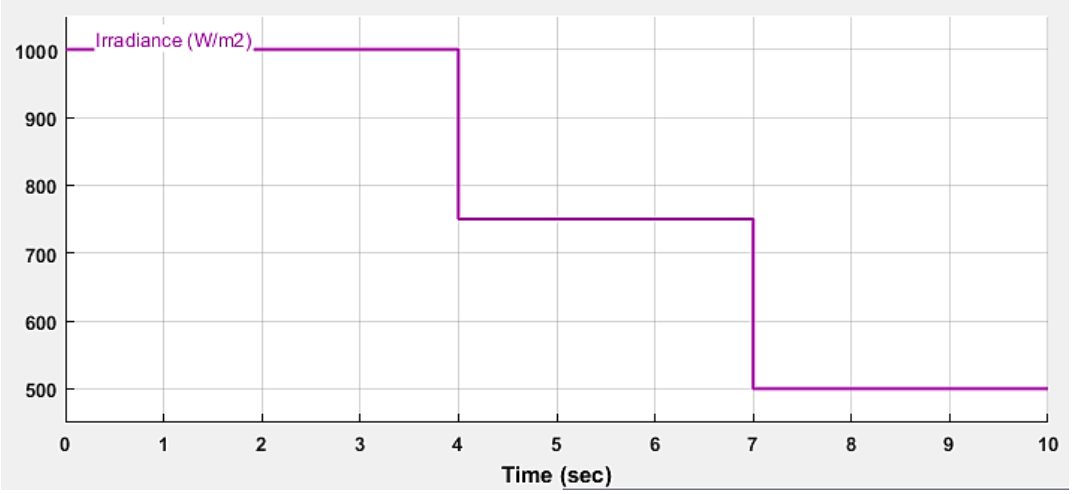

Figure 46: Irradiance Input Conditions

4.2 P&O Results

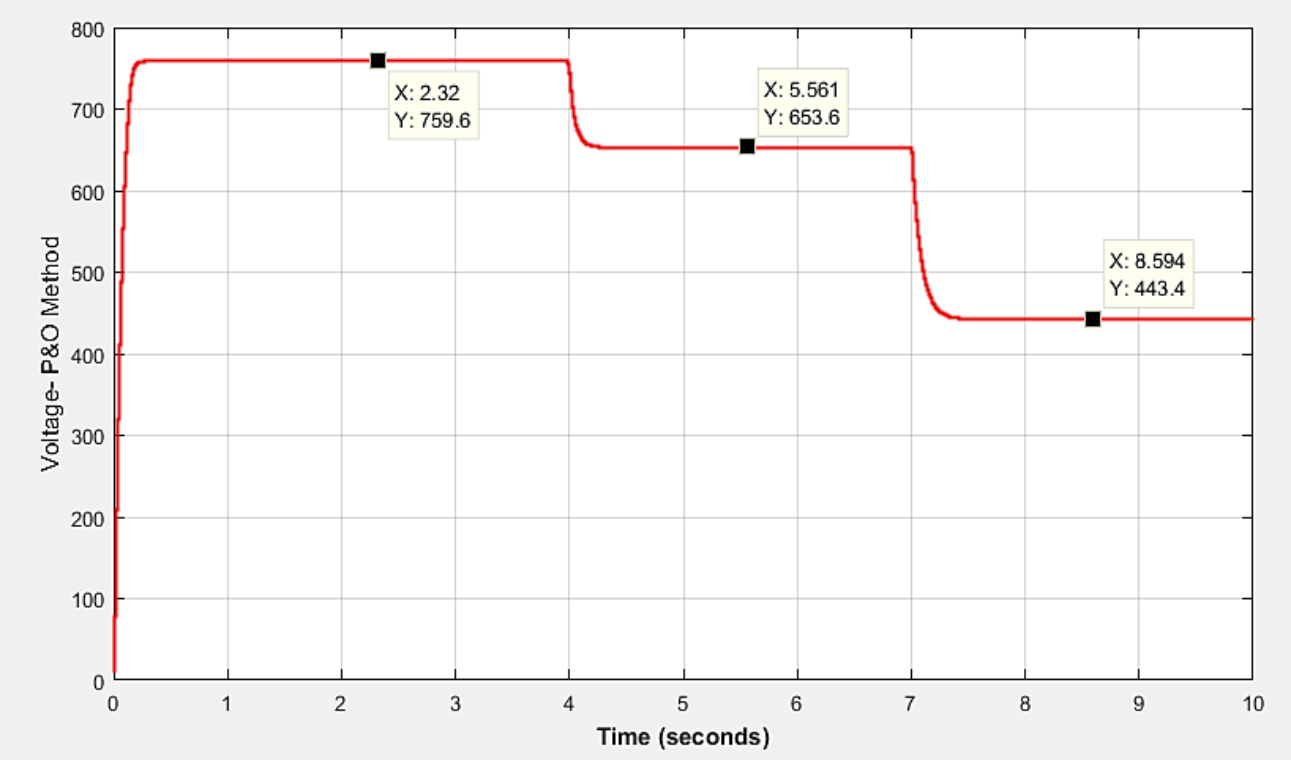

Figure 47: P&O Method - Voltage output

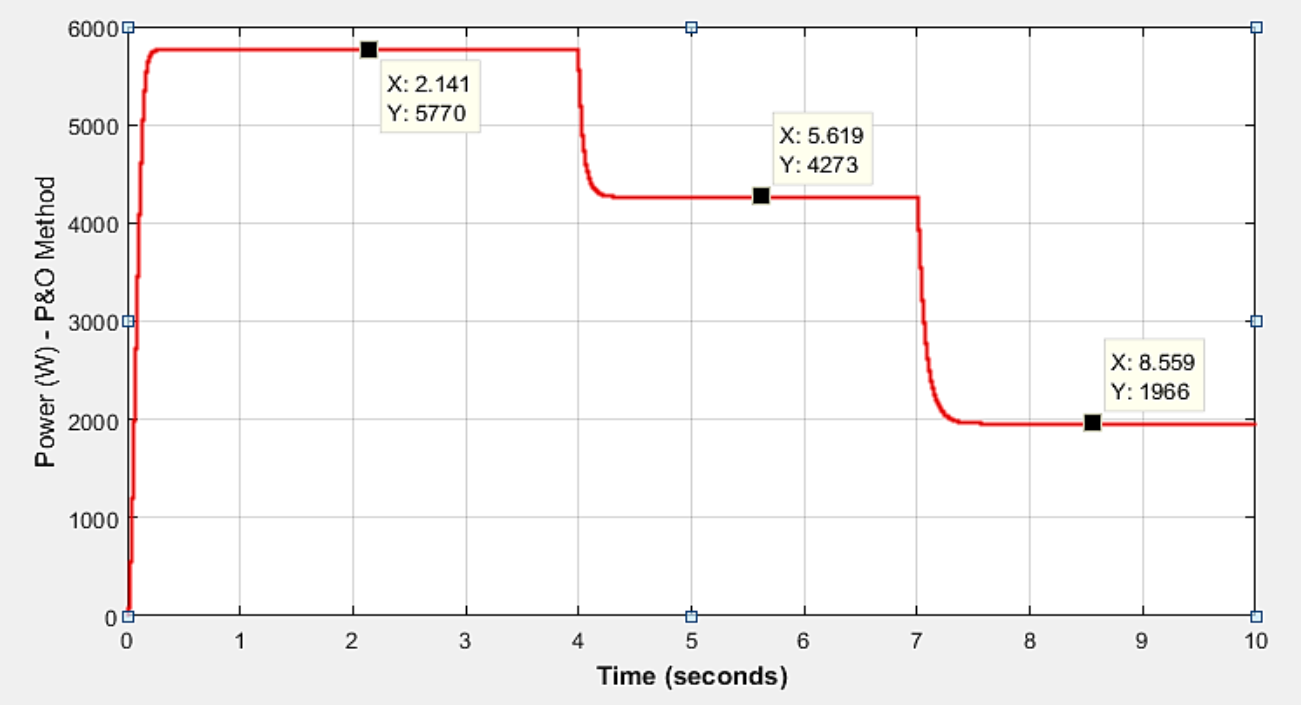

Figure 48: P&O Method - Power output

4.3 FOCV Results

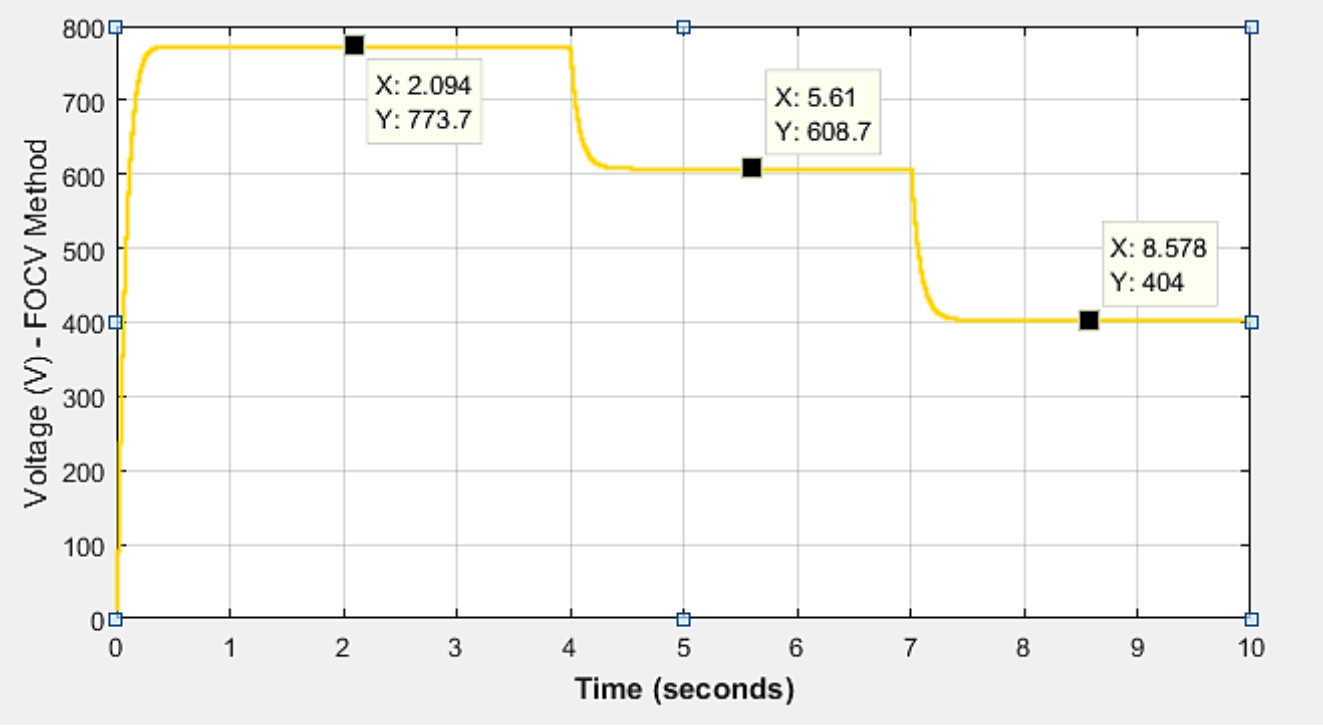

Figure 49: FOCV Method - Voltage output

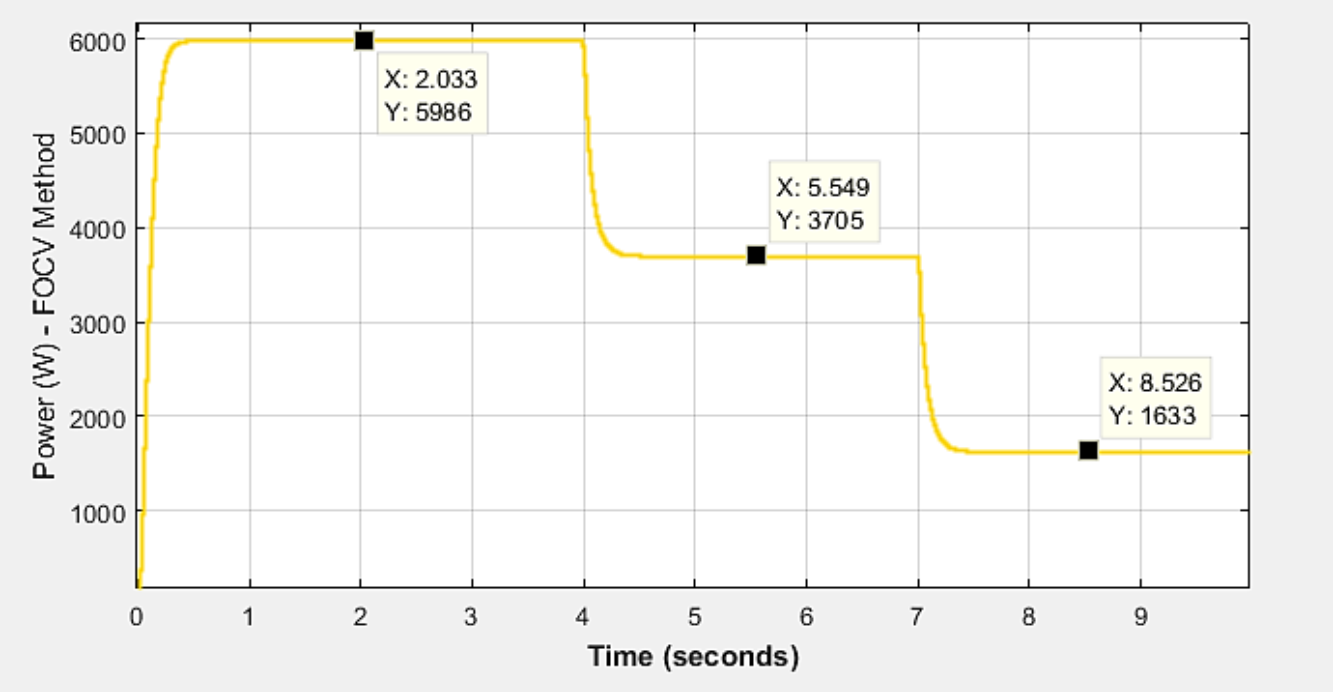

Figure 50: FOCV Method - Power output

4.4 ANN Method Results

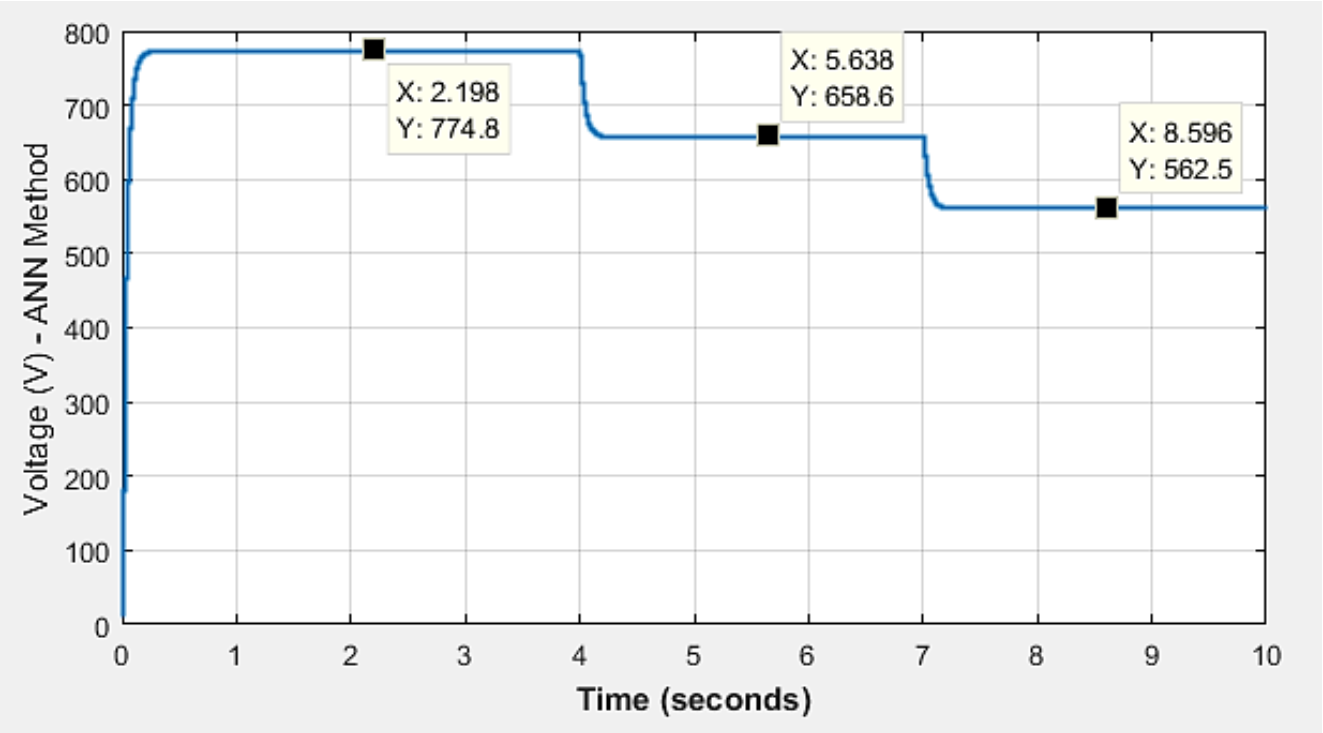

Figure 51: ANN method - Output Voltage

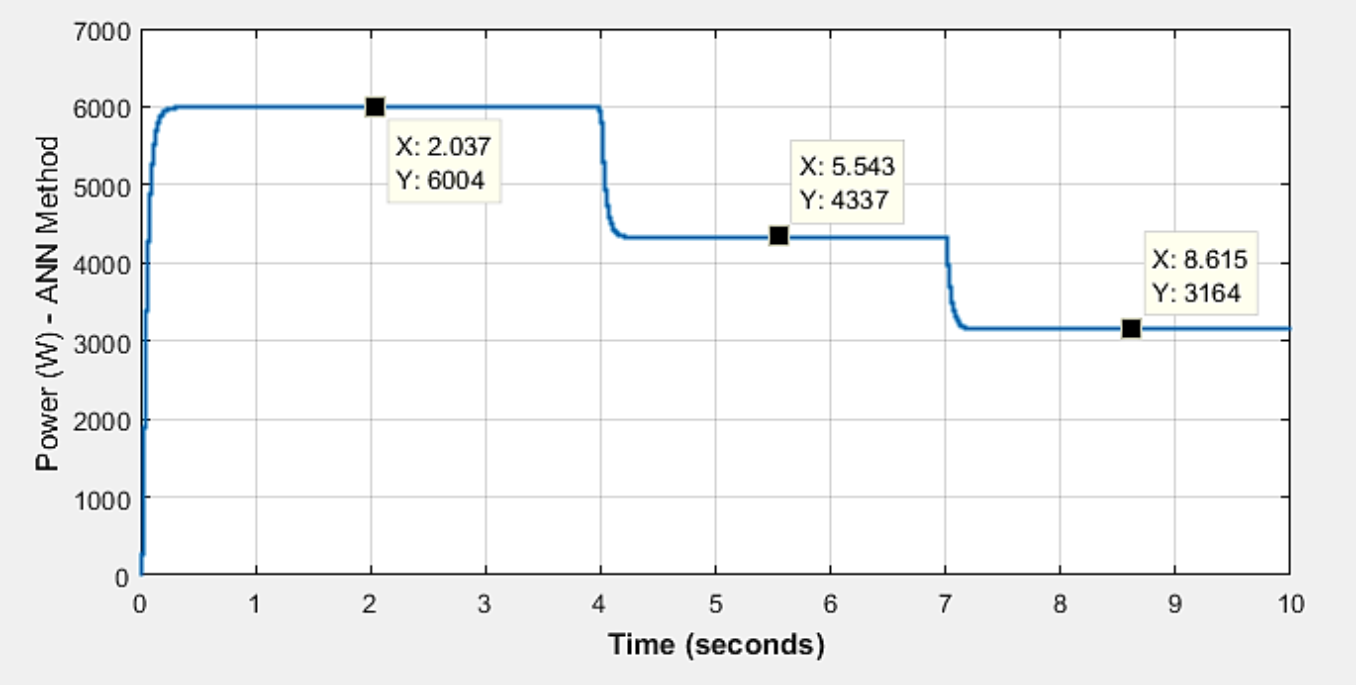

Figure 52: ANN method – Output Power

4.5 Output Comparisons of three methods

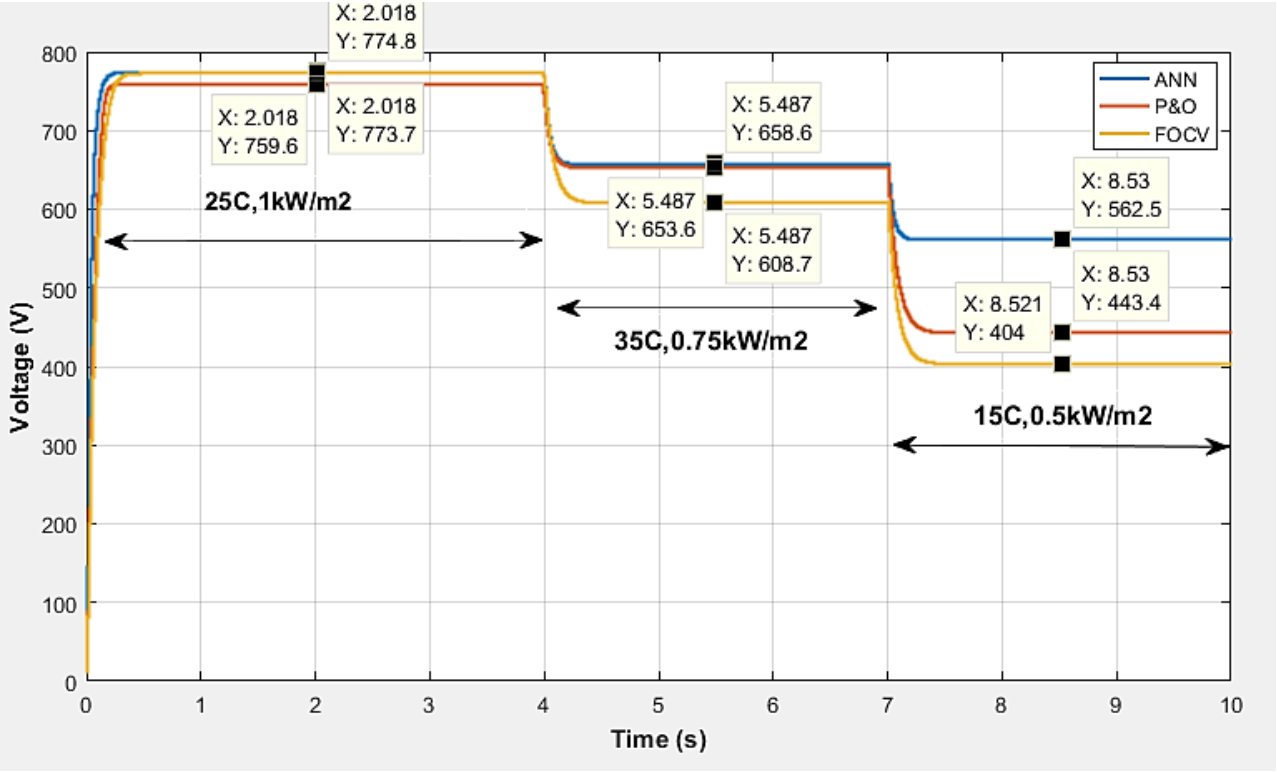

Figure 53: Voltage Comparisons of Three Methods

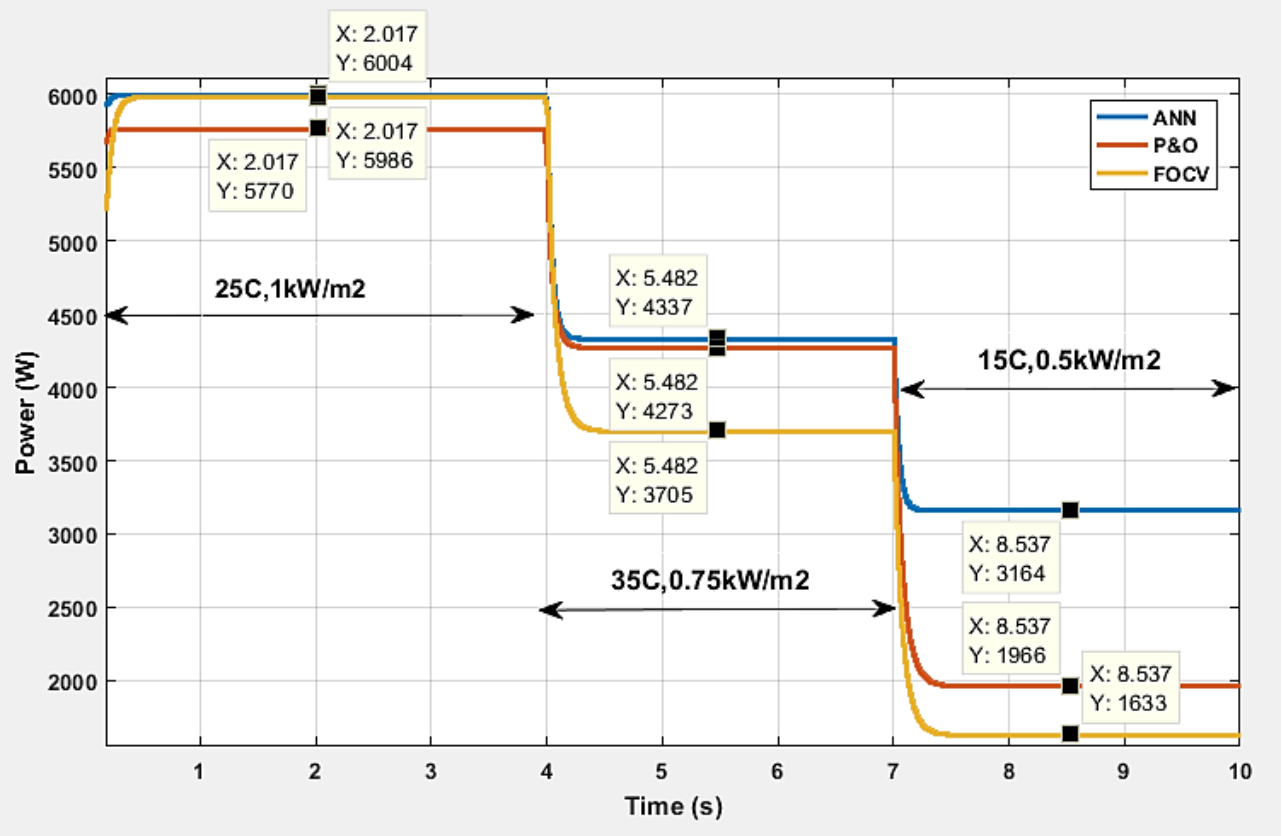

Figure 54: Power Comparisons of Three Methods

4.6 Discussions

For the first operating condition i.e. Standard operating conditions, the three methods track the MPP relatively accurately, however P&O does suffer from local maxima trap. Most of the times, for the FOCV method, the V_{MPP} at STC is actually an accurate linear approximation of V_{OC} therefore at STC FOCV method generally manages to track the MPP accurately. The ANN based method is extremely accurate not only because of the advantages that Neural networks exhibit but also because the STC points were provided at data inputs while training the network.

Operating Conditions	Maximum Power (W)	ANN Power (W)	P&O Power (W)	FOCV Power (W)
Condition 1	6004	6004	5986	5770
Condition 2	4339	4337	4273	3705
Condition 3	3169	3164	1966	1633

Table 6: Comparison of Output Powers

For the second condition, contrary to the previous ability, P&O manages to track the MPP relatively accurately as compared to FOCV method. However in totality it is still lagging behind the MPP by 100W. This is due to the fact that P&O method samples points in intervals and during the transition between conditions, the sampling point did not keep up with the computations and hence it led to inaccurate tracking. The linear approximation based V_{MPP} in this case fails and inevitably so does the FOCV tracking. FOCV method underestimates the linear approximation coefficient. The proposed ANN method however, tracks the MPP accurately with only an error of 0.04%.

For the third and last condition, both the conventional methods fail to keep up with the abrupt change and fail with a difference greater than 1kW whereas ANN based method tracks the MPP quickly and accurately with an error of only 0.15%.

All of these differences in operating points owe to the fact that the conventional methods fail to reach V_{MPP}. The voltage difference becomes greater than 150V for the last condition. This means, that the conventional systems are way off target in their quest to reach the maximum power point voltage. These huge differences in voltage operating points in evidently impacts the output power.

The results clearly suggest that the proposed ANN based method is superior to the conventionally applied techniques. The benefits of the proposed method are of major importance when it comes to large systems such as the one simulated where conventional methods incur losses greater than 1kW.

Summary

The chapter presents the results of the three proposed methods. The MPPTs were subjected to three different conditions while holding all the other variables such as load, PV array model and boost converter constant. The results clearly show the ANN based technique to be superior over the two conventional ones.

CHAPTER 5
PERFORMANCE OF FIELD AGED MODULES

This chapter introduces the work carried out at Photovoltaic Reliability Lab (Arizona State University). Important terms in photovoltaic reliability and testing are introduced along with objectives, methodology and limitations.

5.1 Introduction

The general perception around the world related to solar photovoltaics field age is not accurate. Most of the times, a shift towards Solar PV is made to ensure a sustainable long lasting alternative. However, in many cases the life of modules may vary from the presumed constant of 25 years [1]. This is due to the fact that in the field, the modules are subjected to all kinds of intrinsic and extrinsic wear and tear. Therefore it is imperative to ensure the reliability of PV to certify their performance. PV reliability also cross checks whether a certain module is living up to the claims of its manufacturer's datasheet. Photovoltaic reliability lab at Arizona State University works on reliability issues of PV modules. Their work involves predicting the lifetime of solar PV modules using statistical analysis obtained using tests such as accelerated stress testing, outdoor testing, module characterization and material characterization. Testing is divided into two main categories, non-destructive testing and performance testing. Visual inspection, EL imaging, IR imaging and UV imaging, diode circuit failure and electrical insulation testing constitute non-destructive testing. Baseline light IV, dark IV, cell IV, quantum efficiency measurements and reflectance tests come under performance testing [2].

One of the important parameters while determining the performance of a module is known as the "Temperature coefficient" - A temperature coefficient describes the relative change of a physical property that is associated with a given change in temperature. There are numerous properties of a module that can be affected over time such as maximum power, short circuit current, open circuit voltage, maximum power point voltage, FF and overall efficiency. In the industry it is a common norm to assume the maximum power (P_{MAX}) temperature coefficient constant throughout the age of the module [3]. While calculating the performance ratio of a field aged module, the same value of P_{MAX} temperature coefficient is used which was associated with it before deploying it in the field. This could result in incorrect results for performance ratio.

This study focuses on testing the industrial assumption about temperature coefficient of P_{MAX} being constant. For this purpose a total of 24 field aged modules from four manufacturers were used. These modules were subjected to various performance tests such as light IV, dark IV, EL imaging, IR imaging and UV imaging. Light and dark IV results help in finding out the P_{MAX} temperature coefficient, FF, series and shunt resistance.

According to the findings of this study, the temperature coefficient of P_{MAX} varies over time which is contrary to the industrial assumption. The implications of the research can have a valuable impact on the PV reliability industry.

5.2 Objectives

- Finding field aged modules with from four different manufacturers
- Performing performance tests such as Light and dark IV
- Calculating temperature coefficients
- Calculating series and shunt resistance
- Performing imaging tests such as EL, IR and UV

5.3 Limitations

- Usage of standard thermocouples [4]
- All the modules were not precisely cooled to the same temperature before taking the IV. The environmental chamber temperature may not necessarily correspond to the module temperature
- Readings taken between 9AM to 3PM. All efforts were made to test panels in same conditions however some readings may differ due to a partial cloud cover. This measure was due to time constraints.
- During IR imaging the module can heat up

5.4 Methodology

- Shortlisting the 24 panels from different manufacturers
- Fullfilling the criteria on the visual inspection checklist
- Performing IV tests
- Calculating temperature coefficient for the six main performance indicators [4]
- Calculating series and shunt resistance using IV tests
- Performing imaging tests such as EL to find cracks in modules
- Performing IR to look for hotspots on the modules
- Performing UV fluorescence to determine browning or delamination defects [5]

Summary

The chapter discuss the importance of PV reliability, its indicators and the industrial assumption which serves as the basis for the research objective. Limitations and methodology of the study are also mentioned.

References

[1] Misbrener, K. (2017, October 10). What is the life expectancy of a solar array? Retrieved December 16, 2017, from https://www.solarpowerworldonline.com/2017/01/life-expectancy-solar-array/

[2] Huang, B., Lin, T., Hung, W., & Sun, F. (2001). Performance evaluation of solar photovoltaic/thermal systems. *Solar Energy*, *70*(5), 443-448. doi:10.1016/s0038-092x(00)00153-5

[3] Measuring the temperature coefficient of a PV module. (2016, February 12). Retrieved December 16, 2017, from http://sinovoltaics.com/solar-basics/measuring-the-temperature-coefficients-of-a-pv-module/

[4] Shaukatullah, H., & Claassen, A. (n.d.). Effect of thermocouple wire size and attachment method on measurement of thermal characteristics of electronic packages. *Ninteenth Annual IEEE Semiconductor Thermal Measurement and Management Symposium, 2003.* doi:10.1109/stherm.2003.1194345

[5] Park, N., Han, C., Hong, W., & Kim, D. (2011). The effect of encapsulant delamination on electrical performance of PV module. *2011 37th IEEE Photovoltaic Specialists Conference*. doi:10.1109/pvsc.2011.6186147

CHAPTER 6

EXPERIMENTATION AND RESULTS

Methodology, results and conclusion of the research carried out at PV reliability lab (Arizona State University) is discussed in this chapter.

6.1 Methodology

6.1.1 Module Selection

Following table lists the modules selected for carrying out the performance tests

Table 7: Modules used for study

Manufacturer	Module Type	Number of Modules	Time in the field (years)	Rated Power (Watts)
A	Monocrystalline Silicon	7	18	120
B	Monocrystalline Silicon	8	18	175
C	Monocrystalline Silicon	6	18	120
D	Monocrystalline Silicon	3	19	75

Nameplate data of the four manufacturer's modules are shown below:

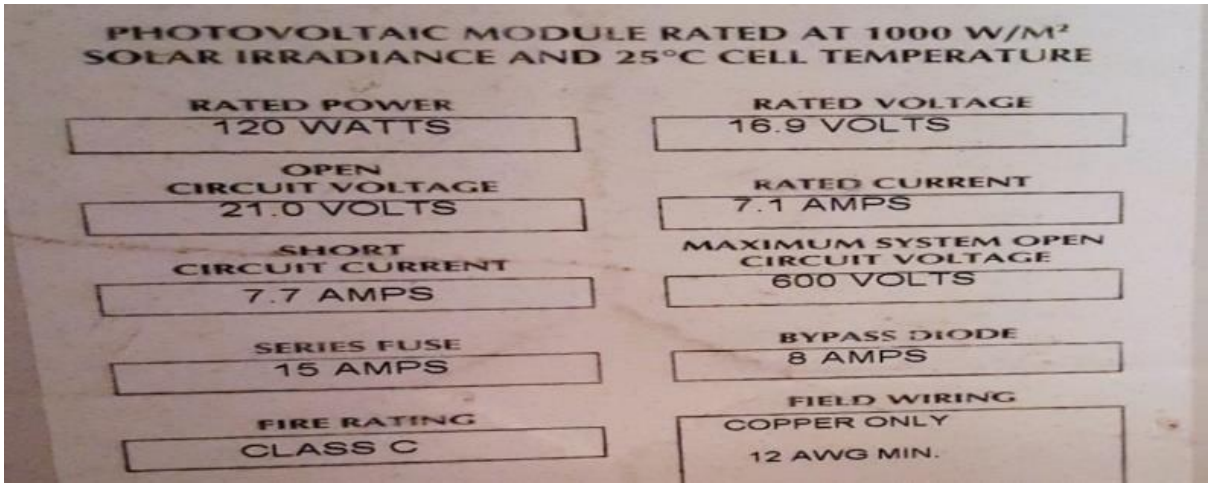

Figure 55: Nameplate - Manufacturer A

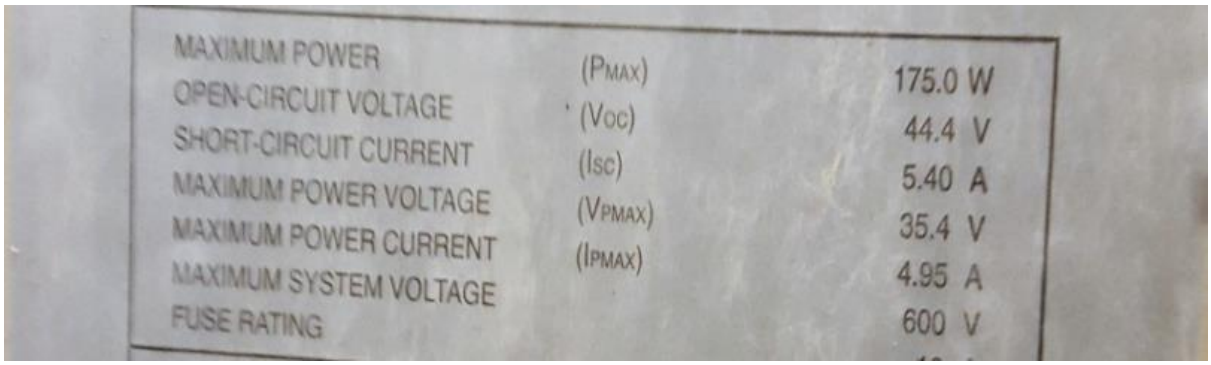

Figure 56: Nameplate - Manufacturer B

Figure 57: Nameplate - Manufacturer C

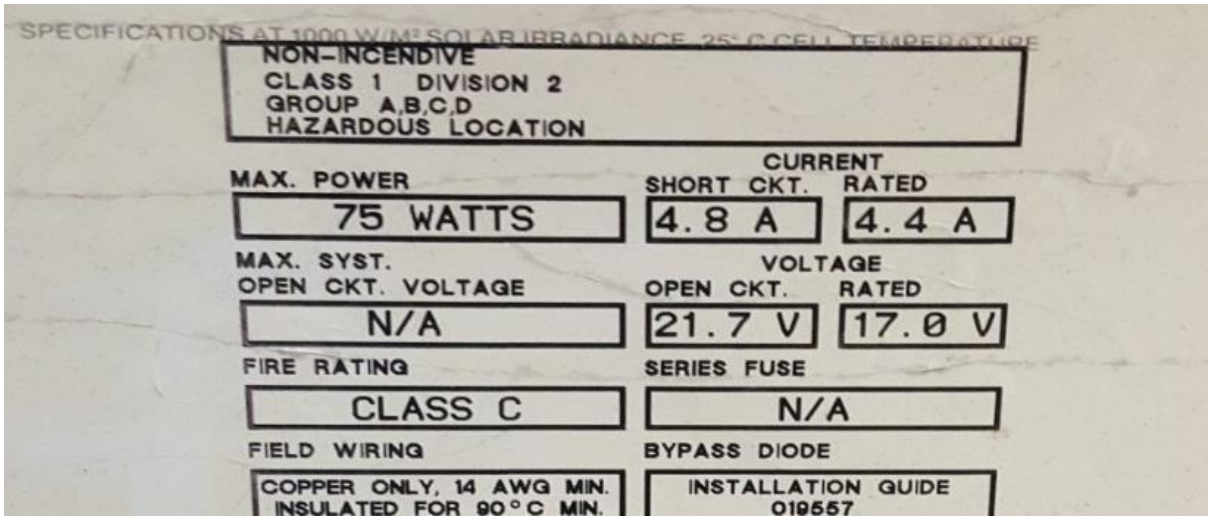

Figure 58: Nameplate - Manufacturer D

6.1.2 Performing Baseline Light IV

Baseline Light IV is performed by first cooling the module down to a certain temperature by placing it in the environmental chamber. The temperature is brought down to 15C. Once the temperature is achieved the module is removed from the chamber while covering it with a Styrofoam sheet. The module is mounted on a three axis rack facing the sun so as to replicate AM1.5 conditions and 1000W/m^2 irradiance level [1]. Once the panel is in position and the rack tilted, the thermocouples are attached. Once at the centre and one at the edge of the panel to double check the values of temperatures. The panel is also meanwhile connected to the IV tracer. Once the entire setup is ready, the Styrofoam is removed and IV curves are taken courtesy of the IV tracer. The readings should be taken for a module temperature increase of 25C to 40C if achievable. There should be no cloud cover and the temperatures for taking the IV curves should be between 9AM to 3PM. The process is repeated for all modules. The results are used to calculate short circuit current, open circuit voltage, maximum power point current, maximum power point voltage, maximum power, FF and efficiency.

6.1.3 EL Imaging

Electroluminescence is the opposite of the photoelectric effect. In the photoelectric effect, the panel gives out current in response to irradiance however in Dark IV the panel is fed current via a DC supply source equivalent to its short circuit current. The panel in turns gives out IR irradiance in the near IR region. The entire process takes place in a dark room and the IR images are captured using a near IR camera [2]. All this while, the panel is set on a rack. The EL image shows defects or cracks in the module cells. The process is repeated for all panels

6.1.4 DARK IV

Dark IV is carried out in a chamber where again it is fed with DC power. The chamber is a dark place where, when, DC power is fed, the panel acts like a diode. The dark IV carriers give results are further calculated to find series and shunt resistances [3]. The series and shunt resistances are cross checked with those found by the baseline light IV. The process is repeated for all panels

6.1.5 IR IMAGING

Infra-red imaging used a simple IR camera which captures an IR image of a panel that it mounted on to a rack. IR images give information about 'hotspots'. Hotspots are regions of elevated temperatures on the panel surface [4]. IR imaging gives information about faulty cells. As the cells are connected in series, one faulty cell could lead to non-faulty cells discharging their power into the faulty one. IR imaging tells about solder bond degradation and or cracks. The process is repeated for all the panels.

6.1.6 UV IMAGING

Ultraviolet imaging utilizes UV lamp lights to find faults in a module. The module is again set on a rack in a dark room. The UV lights are shone at an angle of 45 degrees onto the panel surface to avoid glare while taking pictures. A camera takes the photo of the panel being illuminated by the UV light [5]. UV imaging gives information about browning. Browning occurs when the encapsulatant layer which is composed of EVA breaks down UV illumination.

6.2 Result and Discussion

6.2.1 Temperature Coefficient

Two temperature coefficients are calculated for P_{MAX} and open circuit voltages. The temperature coefficient for open circuit voltage remains the same as expected because it depends on the band gap of the material. Because the band gap doesn't change over time in the field, hence the temperature coefficient for the open circuit voltage also doesn't change.

However the temperature coefficient for P_{MAX} is found to be 0.5%/C to 0.6%/C. These values are different as compared to temperature coefficient of P_{MAX} for new modules – 0.4%/C to 0.5%/C [6]. The FF shows a decrease due to increase in series resistance therefore causing the coefficient of P_{MAX} to increase. The results clearly show that the normal assumption of using temperature coefficient of fresh module for calculating performance ratio is not the right method. Temperature coefficient for P_{MAX} and V_{OC} are shown below

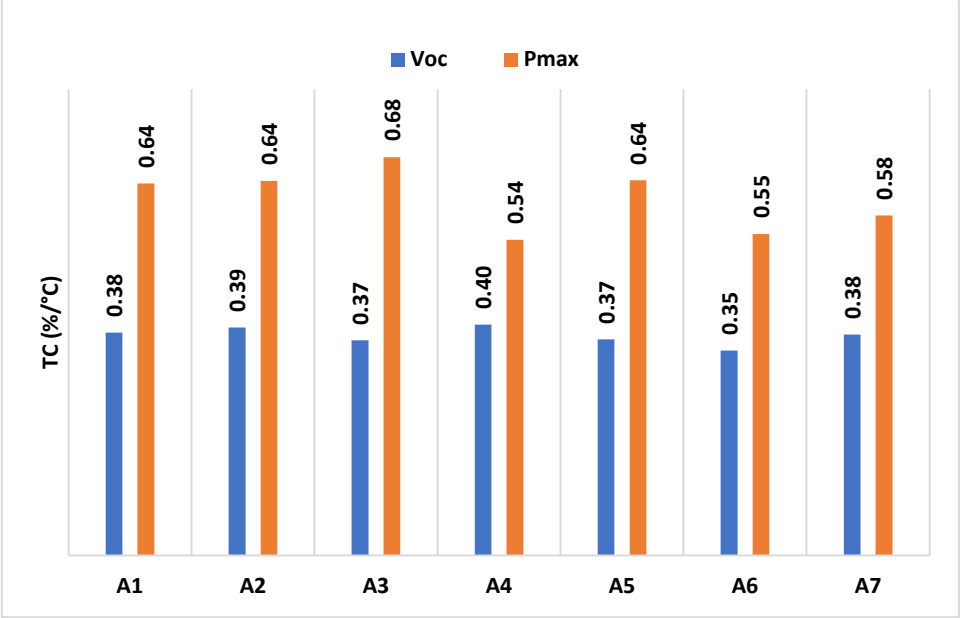

Figure 59: Temperature coefficient for Pmax and open circuit voltage for modules from manufacturer A

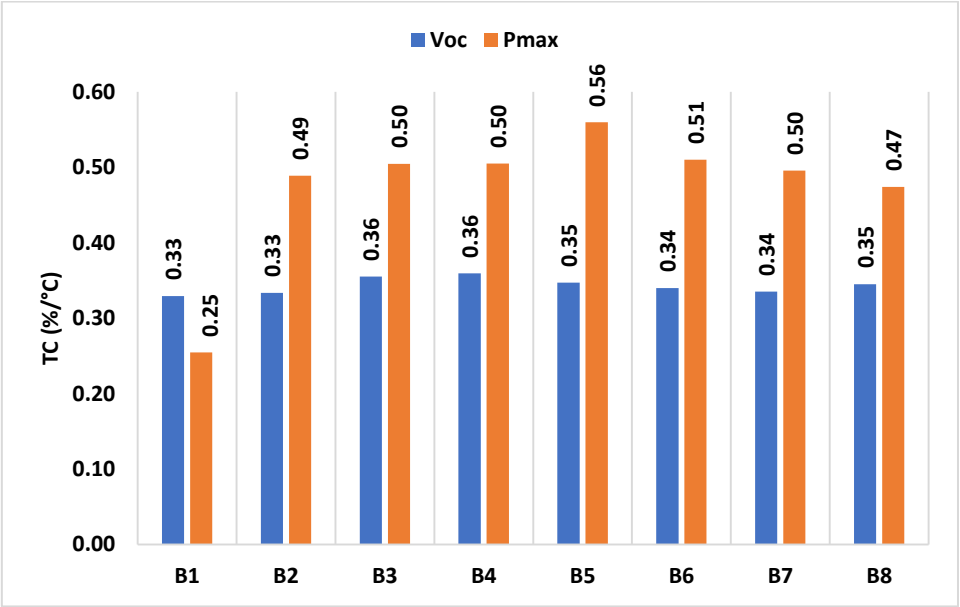

Figure 60: Temperature coefficient for Pmax and open circuit voltage for modules from manufacturer B

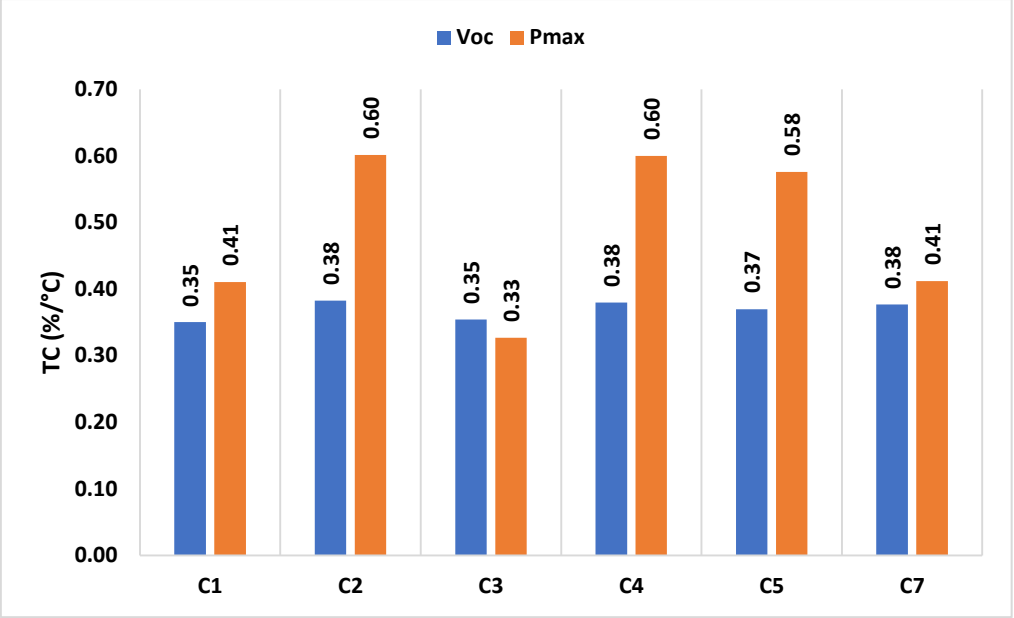

Figure 61: Temperature coefficient for Pmax and open circuit voltage for modules from manufacturer C

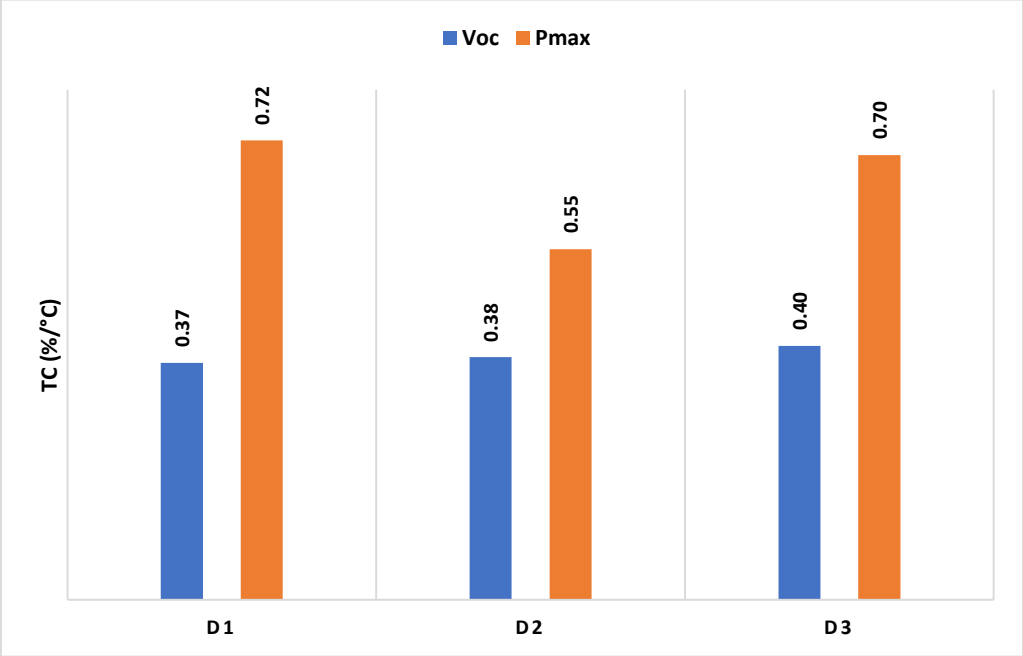

Figure 62: Temperature coefficient for Pmax and open circuit voltage for modules from manufacturer D

The following figures show the temperature coefficient of short circuit current. The temperature coefficient of short circuit for new modules are in the range from 0.2%/°C to 0.3%/°C. The results are also in this range apart from some outliers which could be due to experimental errors such as thermocouple placement. Thus, the temperature coefficient for

short circuit does not change as expected because it is dependent on the bandgap of the material which does not change due to the aging of the module.

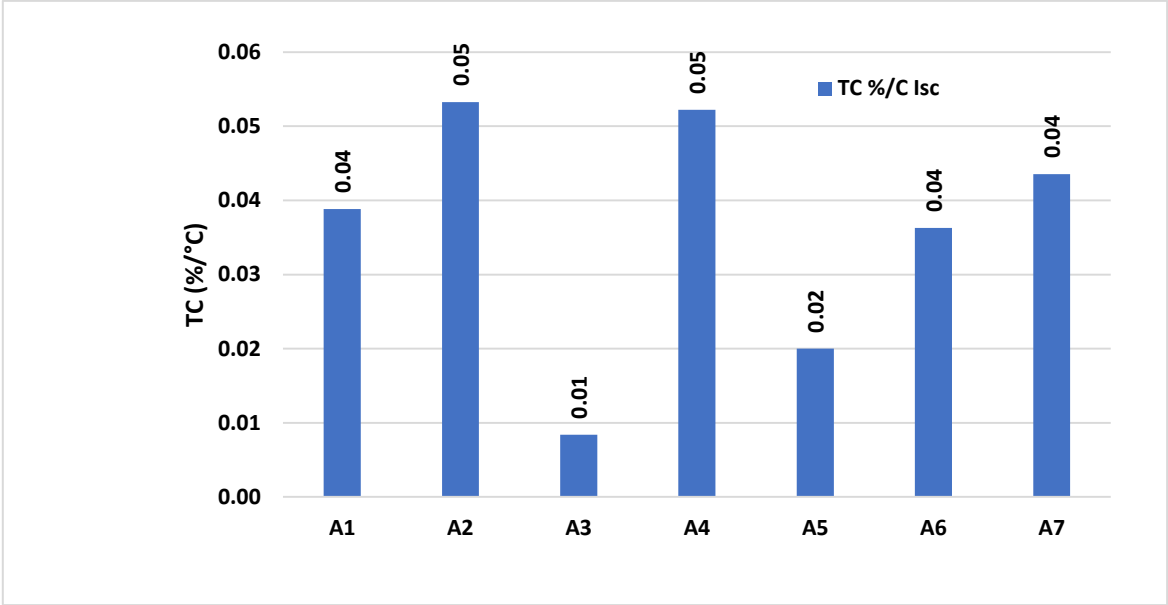

Figure 63: Temperature coefficient for short circuit current for modules from manufacturer A

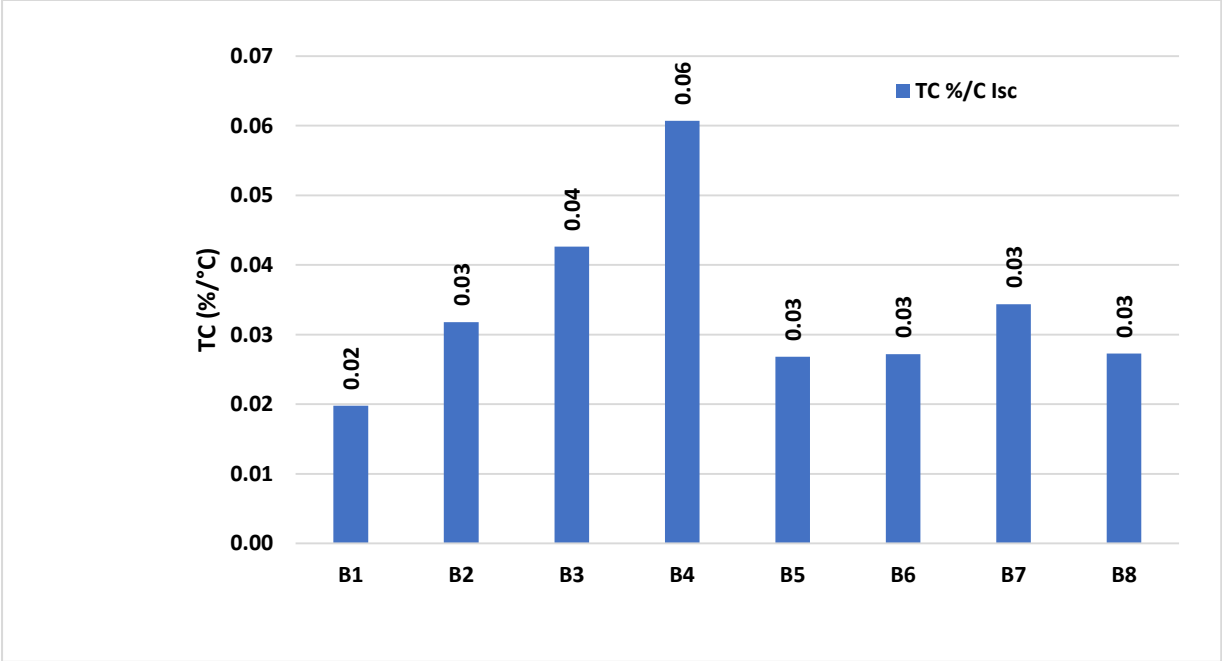

Figure 64: Temperature coefficient for short circuit current for modules from manufacturer B

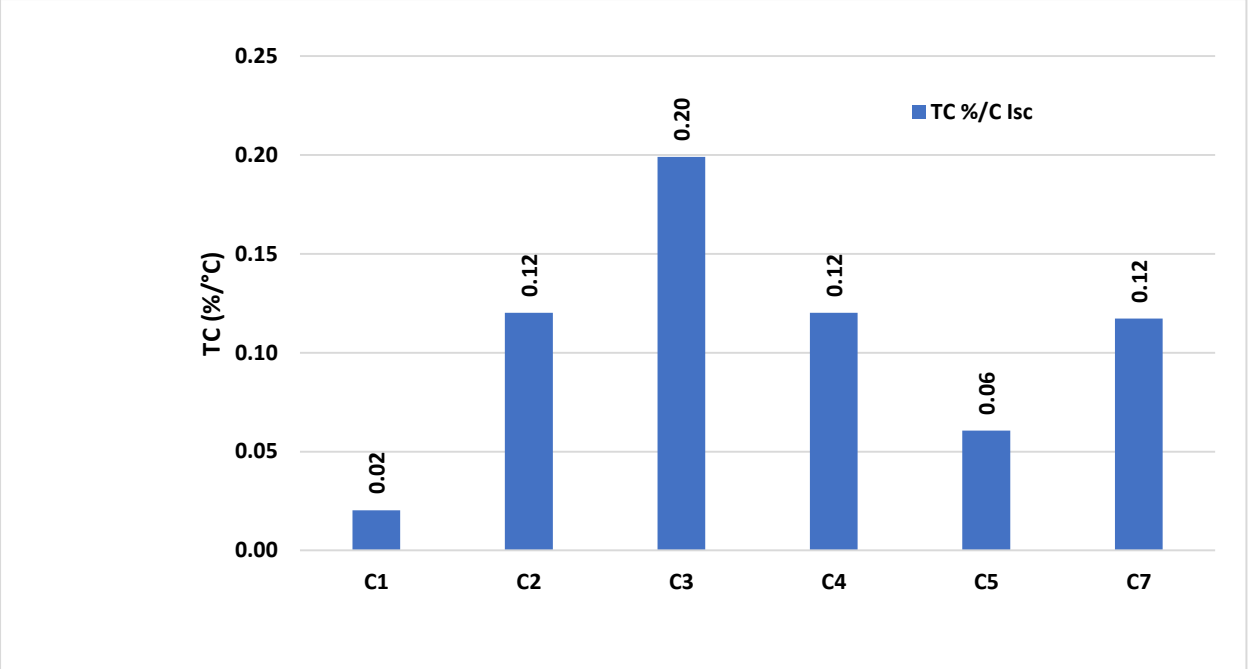

Figure 65: Temperature coefficient for short circuit current for modules from manufacturer C

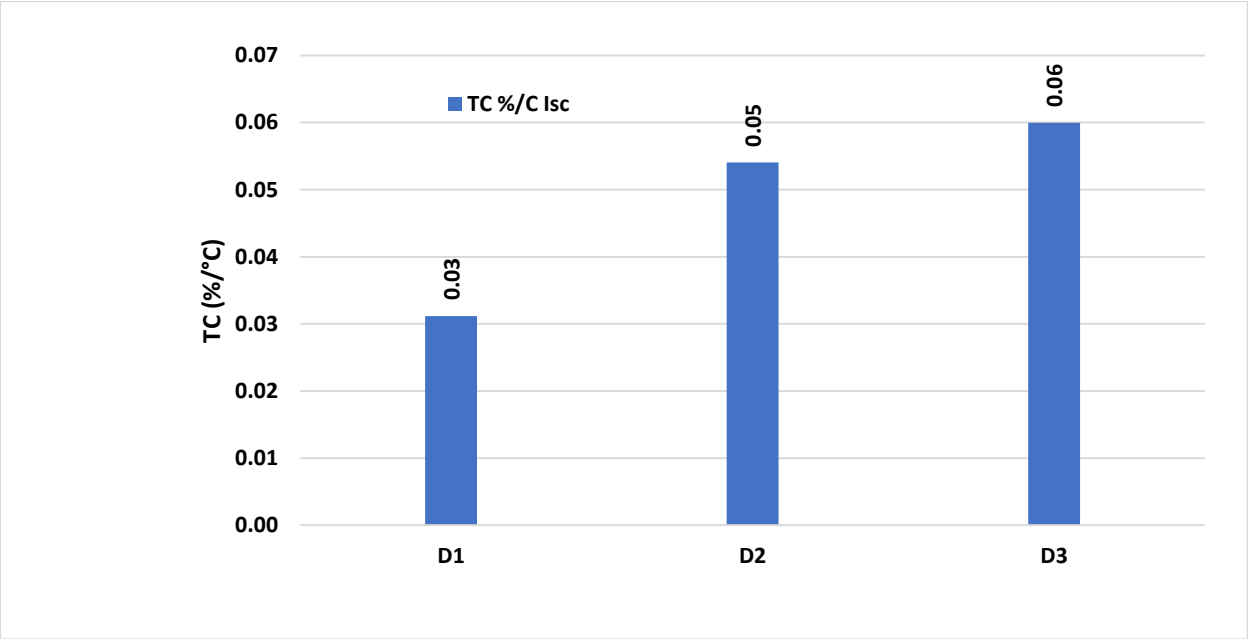

Figure 66: Temperature coefficient for short circuit current for modules from manufacturer D

6.2.2 Resistances

The figures below show the series and shunt resistance calculated from baseline light and dark IV. Dark IV exhibits series resistance values which are less compared to those calculated by dark IV. While shunt resistances calculated from baseline IV method are lower as compared to those calculated by dark IV. The study shows that dark IV is a superior method for calculating the resistances. Due to the decrease in FF and increase in temperature

coefficient for P_{MAX} the series resistance show in increase. This is caused by solder bong degradation.

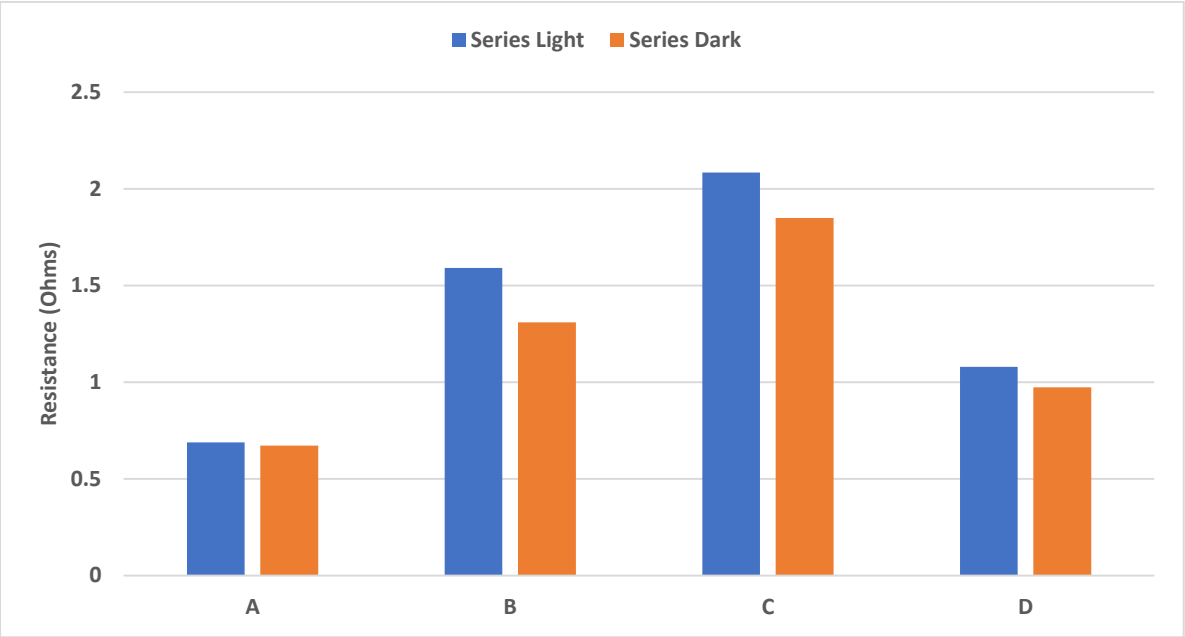

Figure 67: Series resistance from baseline light and dark IV for all modules

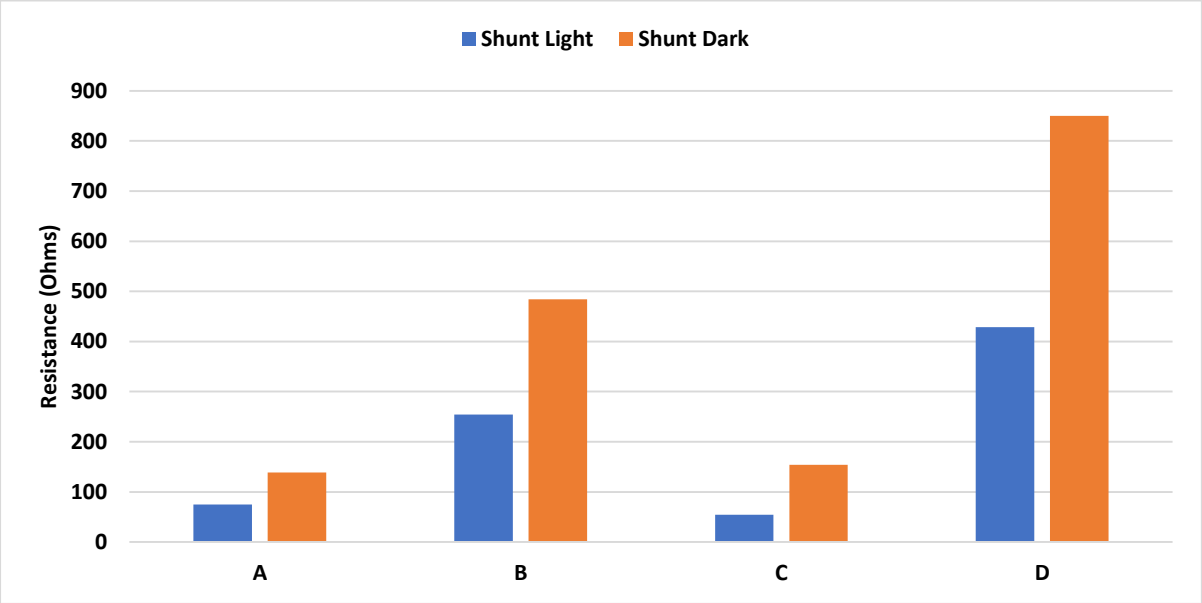

Figure 68: Shunt resistance from baseline light and dark IV for all modules

6.2.3 EL IMAGING

Not all the EL images have been shown in the results. Mostly the images which correspond to cracks or faults have been shown. The cracks and defects could hinder the performance of the panel considerably. Panels from manufacturer D were faulty and no current could be fed to them for EL purposes.

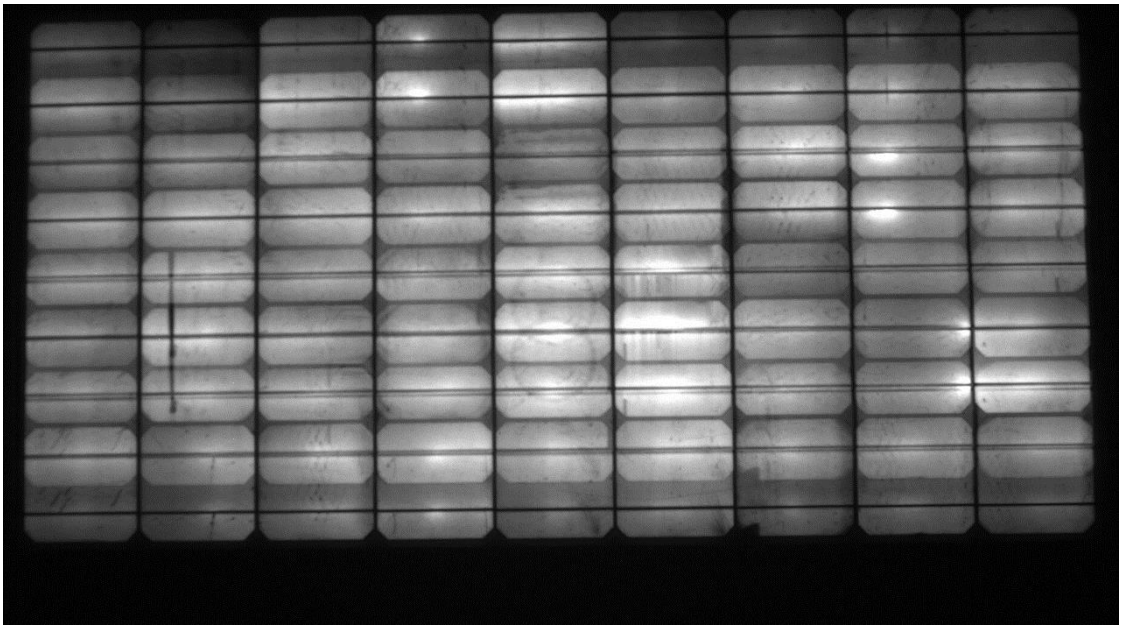

Figure 69: Module from Manufacturer A

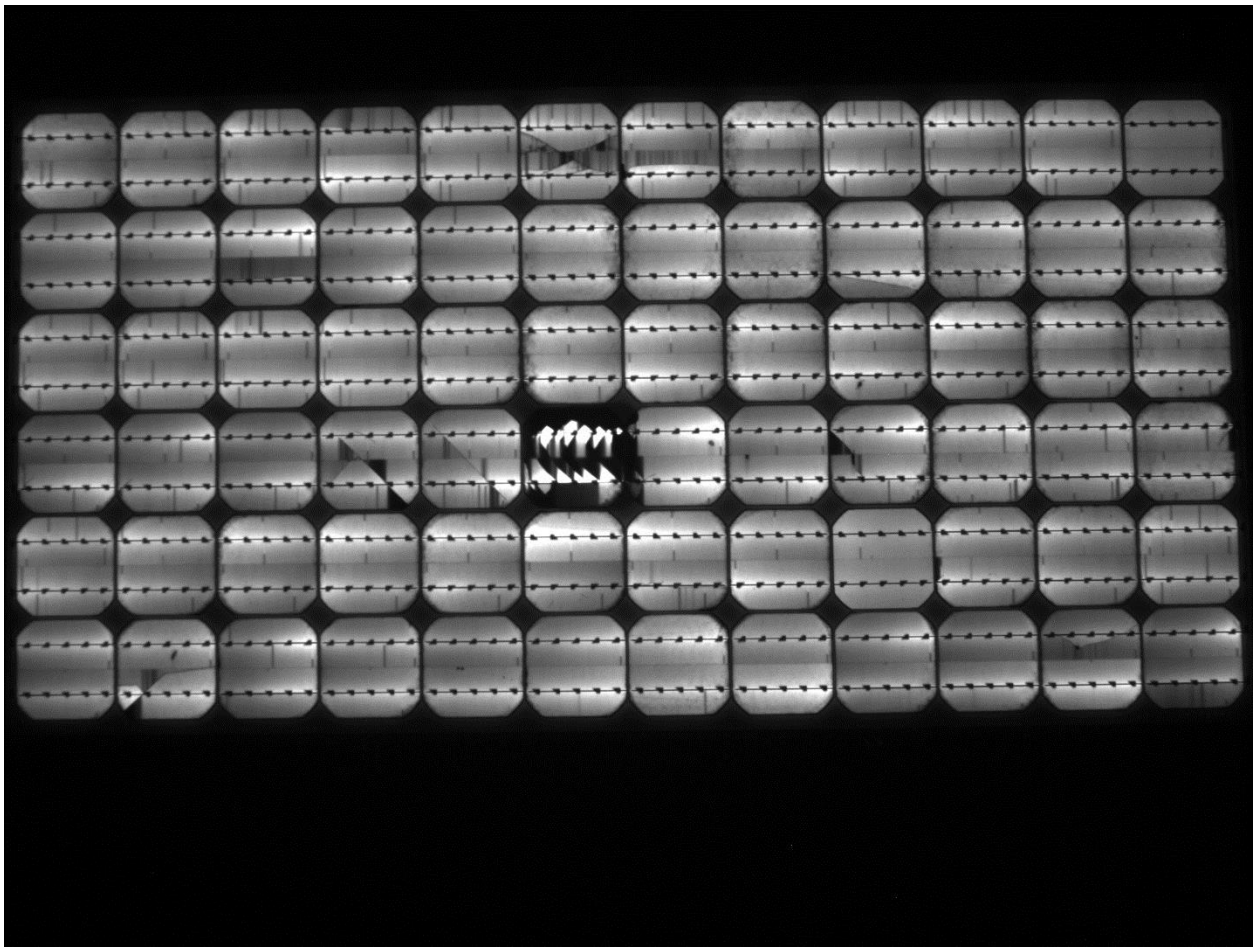

Figure 70: Module from Manufacturer B

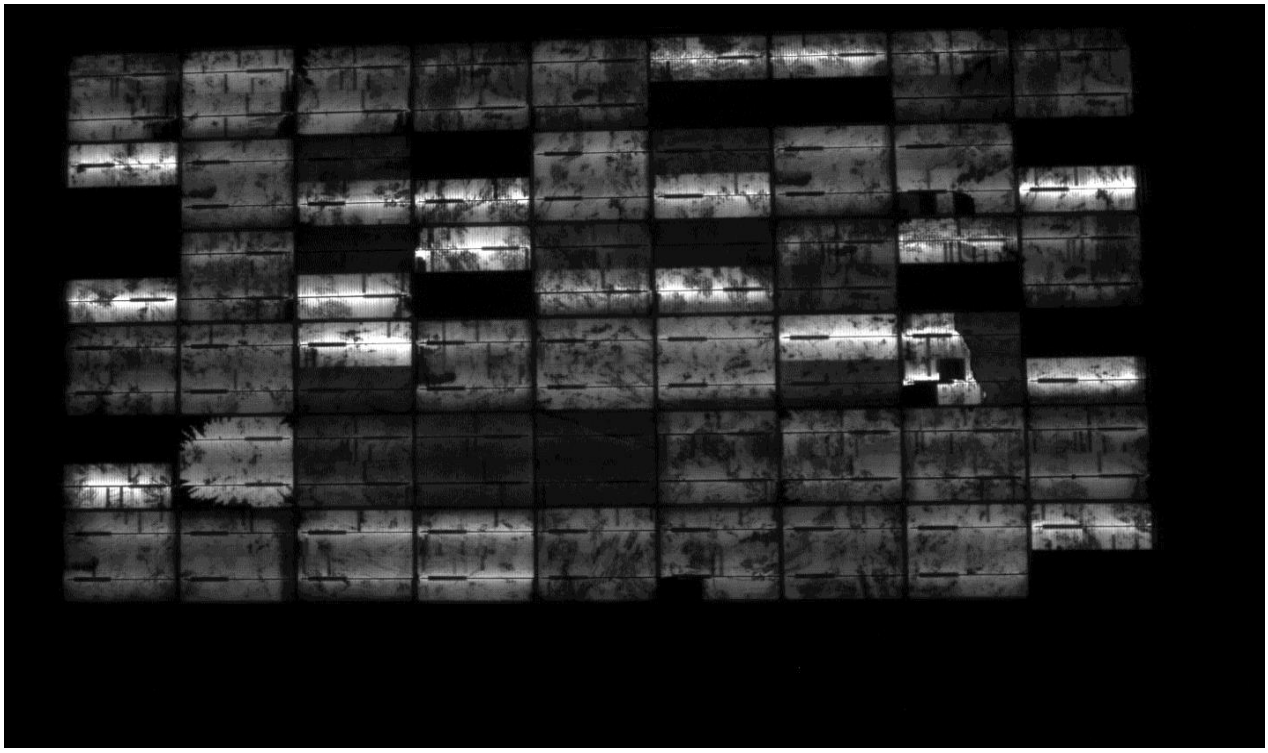

Figure 71: Module from Manufacturer C

6.2.4 IR Imaging

Similarly for IR images, not all the results have been shown. Following figures shows some of the main IR images where the hotspots were visible. As mentioned above the hotspots are caused by faulty cells which limit the output performance of the neighbouring cells.

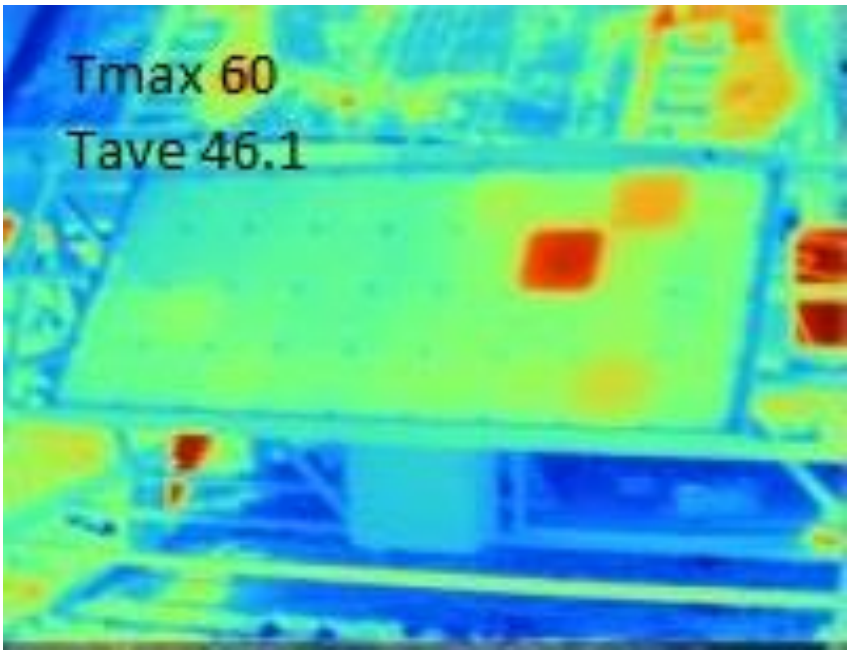

Figure 72: Module from manufacturer A

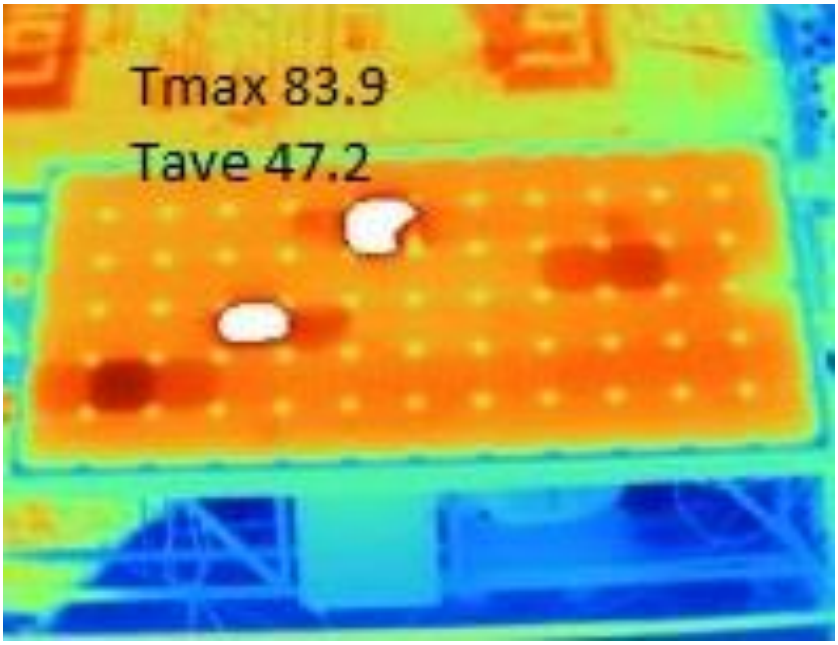

Figure 73: Module from manufacturer B

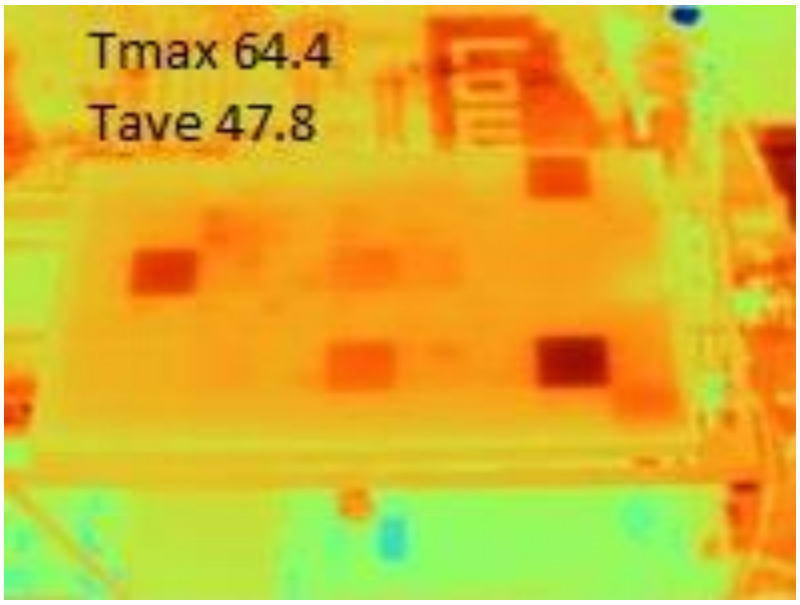

Figure 74: Module from manufacturer C

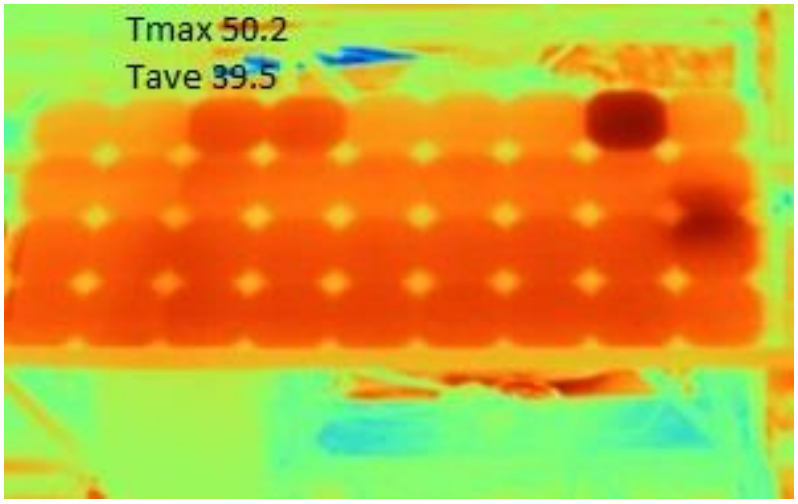

Figure 75: Module from manufacturer D

6.2.5 UV Imaging

UV images show browning which can be related to EVA breakdown. Browning reduces the light available to the cells and hence decrease in maximum power. Following figures show the UV images of different panels.

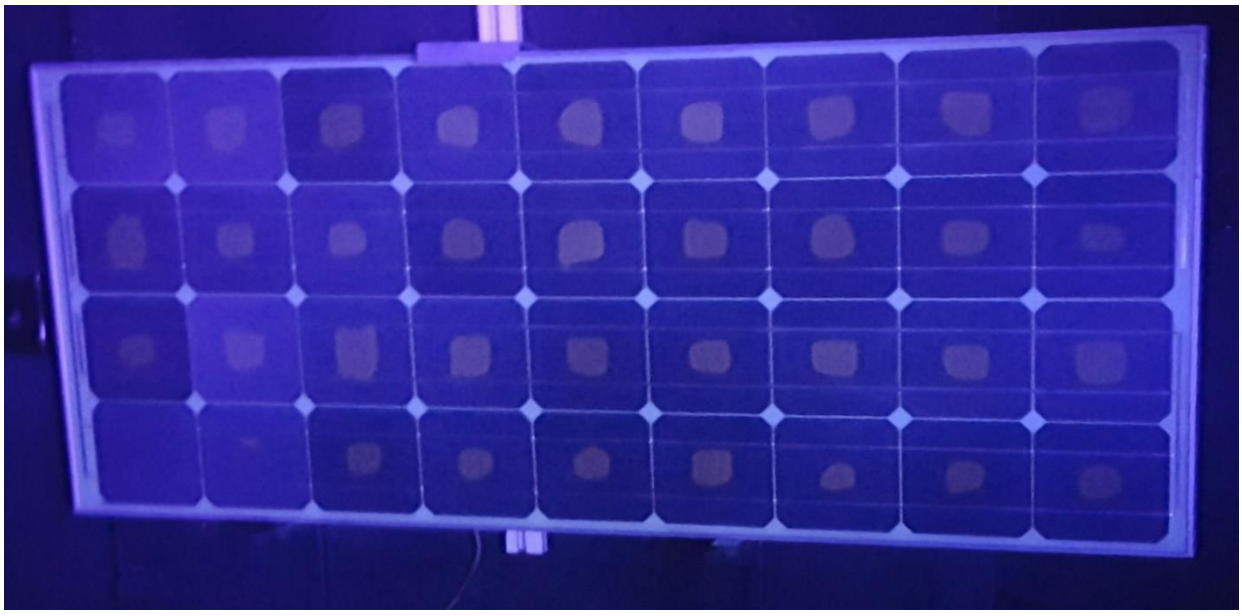

Figure 76: Module from Manufacturer A

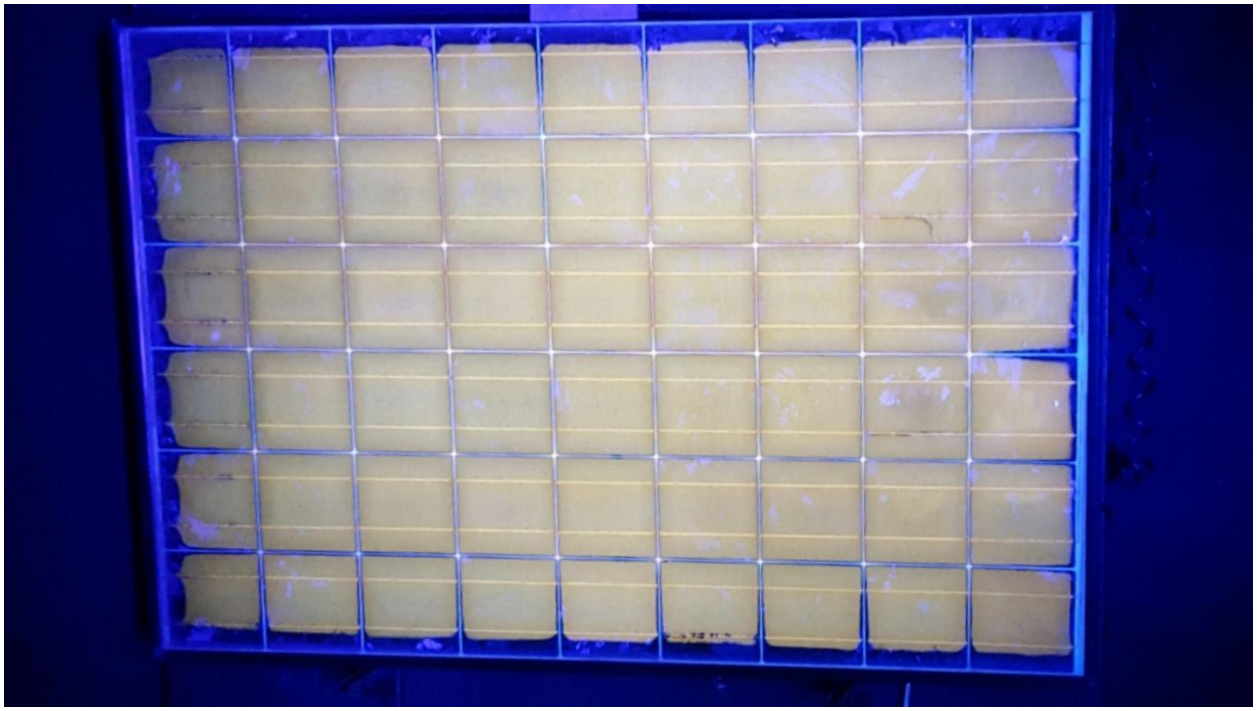

Figure 77: Module from manufacturer C

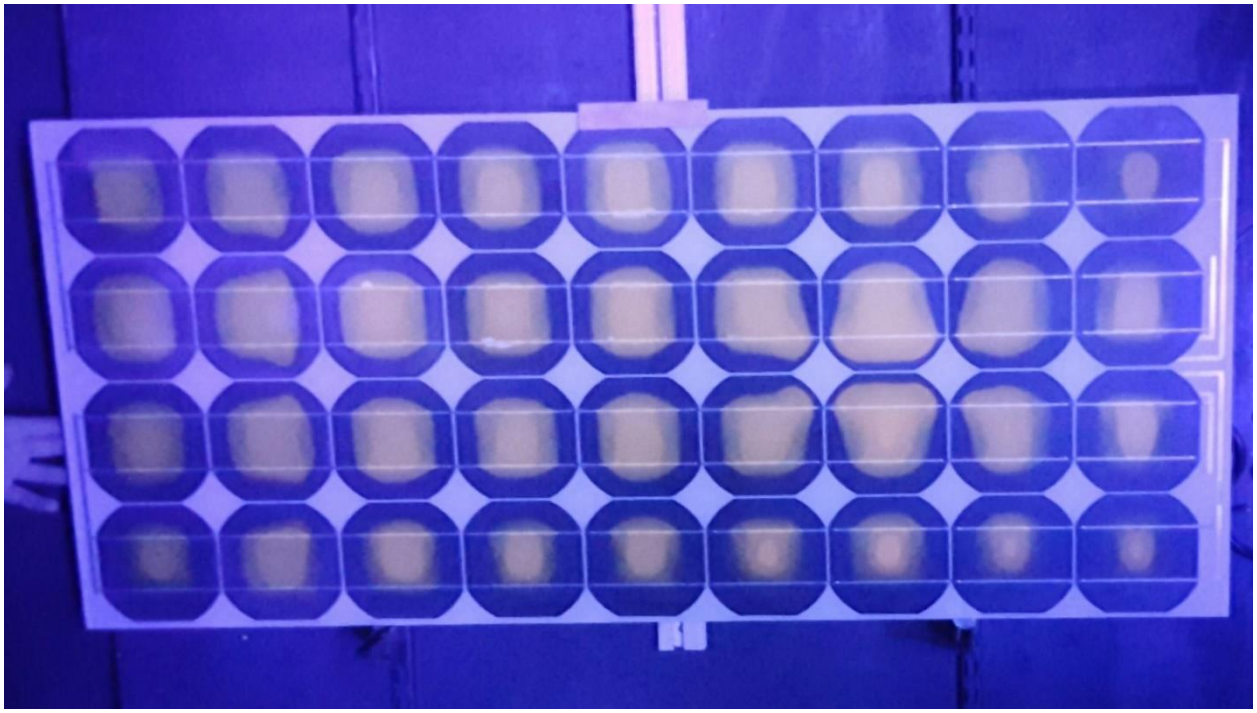

Figure 78: Module from manufacturer D

CHAPTER 7
CONCLUSION AND RECOMMENDATIONS

The chapter summarizes the research and presents recommendations for future work

7.1 Conclusion: ANN Based MPPT for Solar PV

The adaptation of ANNs in every field begs to ask the question whether it is also applicable in any way in the field of energy or not. The research justifies the simple and easy implementation of ANNs for the purpose of MPPT in a novel way. The results not only prove that the proposed ANN based technique is superior to the two age old conventional techniques but it even shows that without the usage of a properly trained and sophisticated MPPT system, huge economic losses can be incurred. For the last condition used in testing, the two conventional techniques lagged behind the MPP by 1kW. This can make or break a major energy project. The debate against the usage of ANNs for this purpose often goes in vain due to the complexity and longer time durations needed to implement it. However, the study shows that the proposed technique trained the ANN in less than 5 seconds. The results can be obtained using module manufacturer's data sheet and data set created to train the ANN. This entire process is very robust and is even worth the extra effort for long time savings.

7.1.1 Recommendation

Following steps can be taken for future studies to make the study even better

- Design consideration for shading conditions
- Obtaining data set from multiple module manufacturers
- Testing the system under dynamic loads
- Comparison between FLC and ANN based techniques

7.2 Conclusion: Performance of Field Aged Modules

The increase in series resistance and decrease in FF results in an increase in temperature coefficient for P_{MAX}. This change in temperature coefficient is of significance as performance ratios are calculated using coefficient of fresh modules. The performance tests such as EL, UV, IR give justifications for the decrease in performance over time by highlighting defects such as cracks, hotspots and browning. Further study about how the imaging techniques correspond quantitatively to defects can be carried out using the already existing results. This research aims to break the stereotypical assumption made during calculating performance ratio that that coefficient of P_{MAX} remains constant. For this purpose modules from different manufacturers were subjected to different performance tests and the results were used to find series, shunt resistance, all the performance parameters and the temperature coefficient for P_{MAX} and open circuit voltage. The results clearly suggest that the industrial assumption is wrong and hence can lead to incorrect performance ratio values. The imaging techniques used can help to understand why the modules exhibit low performance now in a future study.

References

[1] How do I read the solar panel specifications? (2016, April 28). Retrieved December 16, 2017, from https://www.altestore.com/blog/2016/04/how-do-i-read-specifications-of-my-solar-panel/

[2] Electroluminescence. (n.d.). Retrieved December 16, 2017, from http://www.pveducation.org/pvcdrom/characterisation/electroluminescence

[3] Lord, K., Walters, M., & Woodyard, J. (n.d.). Investigation of light and dark I-V characteristics of a-Si:H alloy solar cells, irradiated with 1.0 MeV protons. *Conference Record of the Twenty Third IEEE Photovoltaic Specialists Conference - 1993 (Cat. No.93CH3283-9)*. doi:10.1109/pvsc.1993.346903

[4] Danner, M., & Bucher, K. (n.d.). Reverse characteristics of commercial silicon solar cells-impact on hot spot temperatures and module integrity. *Conference Record of the Twenty Sixth IEEE Photovoltaic Specialists Conference - 1997*. doi:10.1109/pvsc.1997.654289

[5] Morlier, A., Siebert, M., Kunze, I., Mathiak, G., & Kontges, M. (2017). Detecting Photovoltaic Module Failures in the Field During Daytime With Ultraviolet Fluorescence Module Inspection. *IEEE Journal of Photovoltaics, 7*(6), 1710-1716. doi:10.1109/jphotov.2017.2756452

[6] Measuring the temperature coefficient of a PV module. (2016, February 12). Retrieved December 16, 2017, from http://sinovoltaics.com/solar-basics/measuring-the-temperature-coefficients-of-a-pv-module/